NASA Technical Memorandum 85917

Flutter Clearance of the Schweizer 1-36 Deep-Stall Sailplane

Michael W. Kehoe and Joseph F. Ellison

August 1985

National Aeronautics and Space Administration

NASA Technical Memorandum 85917

Flutter Clearance of the Schweizer 1-36 Deep-Stall Sailplane

Michael W. Kehoe and Joseph F. Ellison
Ames Research Center, Dryden Flight Research Facility, Edwards, California

1985

National Aeronautics and
Space Administration
Ames Research Center
Dryden Flight Research Facility
Edwards, California 93523

SYMBOLS AND ABBREVIATIONS

ADFRF	Ames Dryden Flight Research Facility
f_0	half power analysis center frequency
f_1	half power analysis lower frequency
f_2	half power analysis upper frequency
$\bar{g}$	structural damping coefficient
$\bar{g}'$	total structural damping coefficient
GVT	ground vibration test
Hz	Hertz, 1 cycle/sec
KCAS	knots calibrated airspeed
KEAS	knots equivalent airspeed
sec	second

SUMMARY

A Schweizer 1-36 sailplane was modified for a controlled, deep-stall flight program. This modification allowed the horizontal stabilizer to pivot as much as 70° leading edge down. Ground vibration and flutter testing were accomplished on the sailplane with the horizontal stabilizer in the normal flight and deep-stall flight positions. Test results indicated satisfactory damping levels and trends for the structural modes of the sailplane. The modified sailplane was demonstrated to be free of aeroelastic instabilities to 83 KEAS with the horizontal stabilizer in the normal flight position and to 39 KEAS with the horizontal stabilizer in the deep-stall flight position. This flight envelope was adequate for the controlled, deep-stall flight experiments.

INTRODUCTION

A Schweizer 1-36 sailplane was modified for the National Aeronautics and Space Administration's (NASA) controlled, deep-stall flight program. Aircraft controllability research in the deep-stall region above an angle of attack of 30° was conducted during the program.

The horizontal stabilizer (T-tail configuration) was modified by the Schweizer Aircraft Corporation so that it could pivot as much as 70° leading edge down. This modification included mass-balancing the horizontal stabilizer for flutter considerations. A ground vibration test (GVT) (ref. 1) and a flight flutter test (ref. 1) were conducted by Schweizer at Elmira, N.Y., on the sailplane with the horizontal stabilizer in the normal flight position.

Upon delivery of the sailplane to the Ames Dryden Flight Research Facility (ADFRF), the pitch-control mechanization of the horizontal stabilizer was determined to be unacceptable. The stretching of the cables used to rotate the horizontal stabilizer under load did not provide an acceptable means of controlling the horizontal stabilizer.

The pitch-control mechanism was further modified for ADFRF by Irv Prue of Prue Sailplanes, Pearblossom, Calif. This modification included the installation of bellcranks, push-pull rods, and cables to control the horizontal stabilizer.

The fuselage of the sailplane was modified, at ADFRF, to include a flight test instrumentation system. This modification included

1. The installation of 18.16-kg (40-lb) instrumentation pallet just aft of the cockpit.

2. The installation of an 18.16-kg (40-lb) battery for the cockpit radio and instrumentation just forward of the cockpit.

3. The addition of a nose boom.

These modifications made it necessary to again clear the flutter envelope of the sailplane's horizontal stabilizer in the normal and deep stall positions. Since no flutter analysis was accomplished for the sailplane, it was decided that the prudent method of clearing the envelope would be to remove the wings, mount the fuselage on a truck, and expose the empennage to the maximum airspeed needed for the flight test program, and then conduct a flight flutter test program.

Upon completion of the ground (truck) and flight flutter test program, it was necessary to conduct a GVT on the sailplane. The GVT was conducted because of the discrepancies in frequency between the flight test data and the GVT data obtained from Schweizer. The GVT conducted at Ames Dryden was done in a soft system using single-point random excitation.

OBJECTIVES

The objective of the truck test was to provide a quick assessment of the dynamic/aeroelastic stability of the modified empennage with the horizontal stabilizer in the normal and deep stall positions.

The objective of the flight flutter test was to verify the lack of flutter within the flight envelope of the modified Schweizer 1-36 sailplane with the horizontal stabilizer in the normal and deep stall positions.

The objective of the GVT was to measure the frequencies and mode shapes below 50 Hz.

VEHICLE DESCRIPTION

The Schweizer 1-36 sailplane (fig. 1) is a single-place, all-aluminum sailplane, except for the rudder, which is covered with fabric. The wing has a span of approximately 14 m (46 ft) and the fuselage length is approximately 6.4 m (21 ft). The horizontal stabilizer is a T-tail configuration with a span of 2.4 m (7.9 ft). The elevator is connected to the stick through a cable and pulley arrangement. The horizontal stabilizer in its normal flight position is shown in figure 2.

The horizontal stabilizer in the deep stall flight position is shown in figure 3. The horizontal stabilizer is rotated leading edge down by a handle

mounted on the left side of the cockpit. The control linkage to the horizontal stabilizer consists of bellcranks, push-pull rods, and cables.

Instrumentation

Ground vibration test- Piezoelectric accelerometers were attached to the sailplane to measure the response of the structure. A force link was used to measure the input force to the structure from the electrodynamic shaker. A minicomputer-based structural analysis system (fig. 4) was used to acquire, filter, and display/record four channels of data (one input force and three response).

Truck and flight test- Six accelerometers were installed and oriented on the empennage as shown in figure 5. In addition, position transducers were installed on the horizontal stabilizer, elevator, and rudder. Airspeed and altitude were also measured. For the truck test, a pitot static tube was mounted on the front of the truck and connected by a plastic tube to an airspeed indicator.

TEST PROCEDURE

Ground Vibration Test

Test setup- The sailplane was suspended from an overhead suspension system mounted on a crane in the Flight Loads Research Facility. This system consisted of a self-regulating airbag attached to the sailplane's center-of-gravity hook on top of the fuselage. The airbag attached to the hoist is shown in figure 6. The overall test setups for the sailplane with the horizontal stabilizer in the deep stall and normal flight positions are shown in figures 7 and 8, respectively.

The control stick was fixed in the cockpit by an arrangement of sheet metal and C-clamps as shown in figure 9. The rudder was fixed by clamping the rudder cables with C-clamps in the cockpit (fig. 10).

A dummy was placed in the cockpit (fig. 11) to simulate the pilot's weight. The weight of the dummy was 90.8 kg (200 lb).

The speed brakes on each wing were taped along the edges to eliminate rattling of the brakes.

There was noticeable freeplay in the horizontal stabilizer and in the elevators. The components were preloaded to enhance the frequency response. The horizontal stabilizer was preloaded with 0.95-cm (0.375-in.) diameter bungee chord (two strands) attached at the tip of the stabilizer and the tail wheel (fig. 12). The elevators were preloaded with 0.95-cm (0.375-in.) diameter bungee chord attached to cans each containing 4.54 kg (10-lb) of lead shot (fig. 13). The resonant frequency of each can/bungee system was approximately 1 Hz.

A single strand of 0.95-cm (0.375-in.) bungee chord was attached to the nose boom and to the left wing tip wheel to stabilize the rigid body motion of the sailplane. Figures 7 and 8 show the location of these bungee chords.

Excitation- The minicomputer system was capable of generating a sinusoidal or a random forcing function of a bandwidth and amplitude specified by the user. After computer generation of the random forcing spectrum, a tape recorder was used to record the input force time history. This signal was then played back through an electrodynamic shaker attached to the sailplane. A schematic of the setup is shown in figure 14.

A single shaker was placed at three different locations: vertically on the left aft wing tip (fig. 15), laterally on the vertical fin (fig. 16), and vertically on the aft fuselage (fig. 17). Each shaker was attached to the sailplane by means of a metal rod, a mechanical fuse, and a force link. The force link attached to a locking ball nut joint, which was mounted to the structure by a threaded stud. These components are shown in figure 15. The total weight of the shaker armature, attachment linkage, and force transducer was 0.4 kg (0.88-lb).

Data acquisition- Data were acquired with the structural analysis system for each location shown in figure 18. Transfer and coherence functions were then calculated. The coherence function was used as a measurement of the quality of the data before they were stored on the system disk. The base-band data were sampled at 128 samples/sec using a data block size of 1024 samples (8 sec required to fill the block). The anti-aliasing filters were set at 50 Hz. The total number of averages used to calculate each transfer function was 300. This total included an overlap factor of four. Overlap processing is a procedure by which a time history includes a certain amount of previously processed data and a certain amount of new data. This technique is useful when a Hanning window is used. A Hanning window was applied to the data to reduce leakage errors.

Once data acquisition was completed for the sailplane, frequency, damping, phase, and amplitude were estimated for each mode by fitting a multi-degree-of-freedom curve to a selected transfer function that exhibited a good response for the structural modes of interest. The estimated modal parameters, particularly phase, for each mode were examined to determine whether the curve fit was acceptable. It was necessary to examine several different transfer functions to ensure a good curve fit for all of the structural modes below 50 Hz.

Once a good fit was obtained to estimate the modal parameters (frequency, damping, amplitude, and phase), the modal coefficients for each mode shape were calculated by using the amplitude and phase of the measured response at the selected resonance frequency. Animated mode shapes were then displayed to identify each mode. A more detailed example of this procedure can be found in reference 2.

Truck Test

The sailplane, without wings, was mounted high on a flatbed truck. The fuselage was mounted in two different positions. The first position was for flight with the horizontal stabilizer in its normal position (fig. 19) and the second position was with the horizontal stabilizer in the deep stall position (fig. 20).

The truck was driven across the Rogers dry lake bed at airspeeds of 35, 60, and 78 KCAS with the horizontal stabilizer in the normal flight position. The maximum truck ground speed was 57 KCAS with a 21-KCAS head wind. The accelerometer data were telemetered to a telemetry van capable of recording and displaying the accelerometer, airspeed, and control position transducer data on stripcharts. A line was attached to the horizontal stabilizer and routed to the cab of the truck to provide a means of impulse excitation to the horizontal stabilizer.

The horizontal stabilizer in the deep stall position was tested at 39 KCAS in a manner similar to the testing of the stabilizer in the normal flight position.

Frequency and damping data for the empennage modes were calculated after the truck test. A detailed explanation of this analysis is presented in appendix A.

Flight Test

The sailplane was towed to an altitude of 3,657 m (12,000 ft) MSL. Upon release from the tow plane, the sailplane was stabilized at the initial test point. Random atmospheric turbulence was used to excite the structural modes. Typically, 20 sec of random data were collected at each test point. The empennage was also excited by pilot-induced elevator and rudder pulses at each test point. The test points flown were 57, 65, 74, and 83 KCAS at an altitude of 3,352 m ±305 m (11,000 ft ±1,000 ft). These points were accomplished in one flight.

A second flight was required to test the sailplane with the horizontal stabilizer in the deep stall position. The speed at which this test was flown was 39 KCAS at an altitude of 3,352 m ±305 m (11,000 ±1,000 ft).

The accelerometer, airspeed, and position transducer data were telemetered to a ground receiving station where the data were displayed on stripcharts. The sailplane was cleared to the next test point after a review of the time history data indicated satisfactory damping.

Frequency and damping information was calculated after the flight. A detailed explanation of the data analysis is presented in Appendix A.

RESULTS

Ground Vibration Test

Rigid body modes- The rigid body modes of the sailplane suspended in the soft support system were measured. Pure (uncoupled) modes were not obtained for the pitch, yaw, and roll modes. Each of these modes coupled with one another. This was most likely due to the suspension single point attachment. The frequency and damping of each mode measured is presented in table 1. These modes were measured with the horizontal stabilizer in the normal flight position.

Modal frequencies and damping- Table 2 lists the measured modal frequencies and damping for each mode identified with the horizontal stabilizer in the normal and deep stall positions. The modal frequencies identified by Schweizer are also presented.

The rotation of the horizontal stabilizer from the normal flight position to the deep stall position resulted in a frequency decrease of the horizontal stabilizer roll and bending modes. The elevator rotation frequency increased slightly.

Mode shapes- Appendix B contains the normalized mode shape plots for each mode measured. Each plot was labeled to aid in the identification of each mode. This appendix contains data for the sailplane with the horizontal stabilizer in the normal and deep stall positions.

An "oil canning" (figs. B1 and B2) of the wing outboard of the aileron was measured for the first two symmetric modes. This was present on both the normal and deep stall stabilizer positions. The oil canning occurred in the area of the wing where the ribs did not extend from the leading to the trailing edge of the wing (fig. 21). In the area where the ribs extended from the leading to the trailing edge (inboard of the aileron), the oil canning was not observed. The oil canning was not reported in the Schweizer ground vibration test report (ref. 1).

Frequency response functions- Frequency response functions calculated from the accelerometer response at several different locations on the sailplane are presented in Appendix C.

Shaker location- Three different shaker locations were used to excite the sailplane. The left wing tip location was the best in terms of exciting the most modes. The excitation from the vertical fin and aft fuselage shaker locations did not excite any mode that was not excited from the wing tip location. Therefore, the modal coefficients and shapes for all of the structural modes were calculated using the wing tip shaker location.

Preload effects- The elevators were preloaded with 4.54 kg (10-lb) of lead shot suspended by a bungee chord. Since the natural frequency of this system was approximately 1 Hz, it was basically uncoupled from the sailplane structure. Preloading was not required for the ailerons or rudder.

The horizontal stabilizer was preloaded to remove free play by attaching a bungee chord between one tip of the stabilizer and the tail wheel (fig. 12). Preloading in this manner appears to have lowered the stabilizer symmetric bending mode from 27.5 Hz to 23.41 Hz for the normal flight position.

The horizontal stabilizer without preload was excited by impact excitation, and the symmetric bending mode was determined to be 27.5 Hz. Impact excitation deflected the stabilizer outside of the free-play band.

The preload on the horizontal stabilizer most likely affected the frequency of the stabilizer roll mode, also. However, since there was no vibration analysis and this mode was not excited during flight test, the size of the effect is unknown.

Truck and Flight Test Results

The results of the truck and flight tests are presented in figures 22-27. It was assumed that KEAS was equal to KCAS at these speeds and altitudes in figures 22-27. The modal data indicated good agreement between the two tests, although there are significant differences in the air densities tested. In general, the structure is heavily damped. The mode that exhibited the lightest damping was the elevator rotation mode (fig. 26).

The largest error in damping between the two tests is exhibited in figure 22 for the fuselage torsion mode. This error may be due to the way the fuselage was mounted to the bed of the truck.

There is no data comparison for the antisymmetric wing bending mode (fig. 23) because the wing was not attached to the fuselage of the sailplane for the truck test.

The rudder rotation frequency for the truck and flight test differed by approximately 5 Hz. This was most likely due to the rudder being free for the truck test and being loaded by the pilot through the rudder pedals for the flight test.

A comparison of the damping with the horizontal stabilizer in the deep stall position (fig. 22-27) revealed large errors between the truck and flight test results. A trend could not be determined from the data. This difference in damping results may be due to a difference in airflow over the stabilizer for the two tests.

Flutter testing with the sailplane mounted on the bed of a truck resulted in support modes of vibration appearing in the data (fig. 28). It was determined that the modes labeled support modes in figure 28 were not airplane modes by comparing the ground vibration, truck, and flutter test data.

The flight envelope cleared for the Schweizer 1-36 deep-stall airplane is shown in figure 29. More flutter testing would be required if a larger flight envelope were desired.

CONCLUSION

A ground vibration test and ground and flight flutter tests were conducted on the Schweizer 1-36 deep-stall sailplane to verify that no aeroelastic instabilities existed within the flight envelope required for the experiment. The results of these tests indicated that there were no instabilities within the tested envelope.

The ground vibration test was conducted with the horizontal stabilizer in the normal and deep-stall positions. The test was conducted to help interpret the modal data obtained from the flutter tests. Fourteen modes were identified from the ground vibration test. The first symmetric wing bending mode shape was unusual in that an oil canning deformation occurred on the wing tip area outboard of the aileron.

Flutter testing was accomplished with the horizontal stabilizer in the normal and deep-stall positions. Testing was conducted on the ground with the fuselage (without the wings) mounted on a truck. The maximum airspeed attained with the truck was 78 KCAS for the normal flight stabilizer position and 39 KCAS for the deep-stall stabilizer position.

Testing was also conducted at an altitude of 3,352 m (11,000 ft) ±305 m (±1,000 ft). The maximum airspeeds attained were 83 KCAS and 39 KCAS for the stabilizer in the normal and deep-stall positions, respectively.

The truck and flight test data comparison revealed good correlation for the frequency and damping data with the horizontal stabilizer in the normal flight position. However, for the stabilizer in the deep-stall flight position, the truck and flight test data did not compare well.

APPENDIX A

POST-FLIGHT DATA REDUCTION

Frequency and damping estimates were obtained from the ground and flight data by using autocorrelation/direct Fourier transform analysis methods (ref. 3). The autocorrelation function of each accelerometer response was calculated using the time lag products method. The autocorrelation was then multiplied by an exponential window (fig. A1) to smooth the data. The autocorrelation function was then transformed into the frequency domain by the direct Fourier transform (fig. A2). Total damping at each resonant frequency was calculated using the half-power technique. The damping added by the exponential window was then subtracted to obtain the true structural damping value.

Five hundred time lags were used for the data analysis. The number of time lags and the data sample rate determine the time length of the autocorrelation function. The data sampling rate was 400 samples/sec. The autocorrelation time is equal to 500/400 = 1.25 sec. Reference 3 states that the ratio of the total number of data points to the number of lags equal to 20 is preferred. The ratio in this analysis was 16.

APPENDIX B

MODE SHAPE DATA

The normalized mode shape data are presented as plots of the same mode with the horizontal stabilizer in both the normal flight and deep stall flight positions. These data are presented in figures B1-B11. The dashed line in each plot represents the undeformed shape and the solid line represents the deformed shape. The elevator balance weight lateral bending (15.35 Hz), nose boom lateral bending (20.0 Hz), and nose boom vertical bending (22.5 Hz) mode shapes are not shown because a detailed modal survey of these components was not accomplished. The frequencies of these modes were determined by impact excitation.

APPENDIX C

FREQUENCY RESPONSE FUNCTIONS

Frequency response functions obtained from single-point random excitation are shown for the right and left sides of the airplane. Each plot is identified by the location of the accelerometer used to record the function. These locations are shown in figure 18. Figures C1-C20 contain results with the horizontal stabilizer in the normal flight position. Figures C21-C40 contain the results with the horizontal stabilizer in the deep-stall position.

REFERENCES

1. Herber, G. A.: SGS 136 Vibration and Flutter Report 36-6. Schweizer Aircraft Corporation, Elmira, N.Y., 1980.

2. Modal-Plus User Manual, Structural Dynamics Research Corporation, San Diego, Calif., 1981.

3. Dobbs, S. K. and Hodson, C. H.: Evaluation of Methods For Determining Subcritical Flutter Response Frequency and Damping From Flight Test Data. NA-78-737, Los Angeles Division of Rockwell International Corporation, Los Angeles, Calif. 1978.

TABLE 1.- SCHWEIZER 1-36 RIGID BODY MODES

Mode	Frequency, Hz	Damping, $\tilde{g}$
Vertical translation	1.94	0.049
Lateral translation	----	-----
Pitch	0.26	0.09
Yaw	0.19	-----
Roll	0.25	0.073

TABLE 2.- SCHWEIZER 1-36 GROUND VIBRATION TEST RESULTS

Schweizer[1]	Normal flight position		Deep stall position		Mode
Frequency, Hz	Frequency, Hz	Damping, $\bar{g}$	Frequency, Hz	Damping, $\bar{g}$	
4.75	3.81	0.039	3.71	0.174	Sym. Wing Bend.
-----	4.43	.067	4.45	.091	Sym. Wing Bend./Fuse. Bend.
11.58	5.74	.047	5.67	.054	Fuselage Torsion
11.00	10.37	.019	10.40	.018	Antisym. Wing Bend.
16.33	14.97	.052	14.97	.049	2nd Sym. Wing Bend.
-----	15.35	.01	15.35	.01	Elevator Bal. Wt. Lateral Bend.
-----	17.45	.05	13.04	.05	H.T. Roll
22.17-22.83	19.49	.015	19.22	.016	Vt. Fin Bend./Fus. Lat. Bend.
-----	20.0	.06	20.0	.06	Nose Boom Lat. Bend.
-----	22.50	.076	22.50	.076	Nose Boom Vt. Bend.
25.17	23.47	.079	21.44	.024	H.T. Sym. Bend.
28.00	26.89	.048	26.8	.058	Aileron Rotation
33.33	34.38	.044	34.98	.054	3rd Sym. Wing Bend.
45.83	47.05	.046	48.21	.026	Elevator Rotation

NOTES:

1. Damping was not measured during the Schweizer test. The horizontal stabilizer was in the normal flight position for this test.

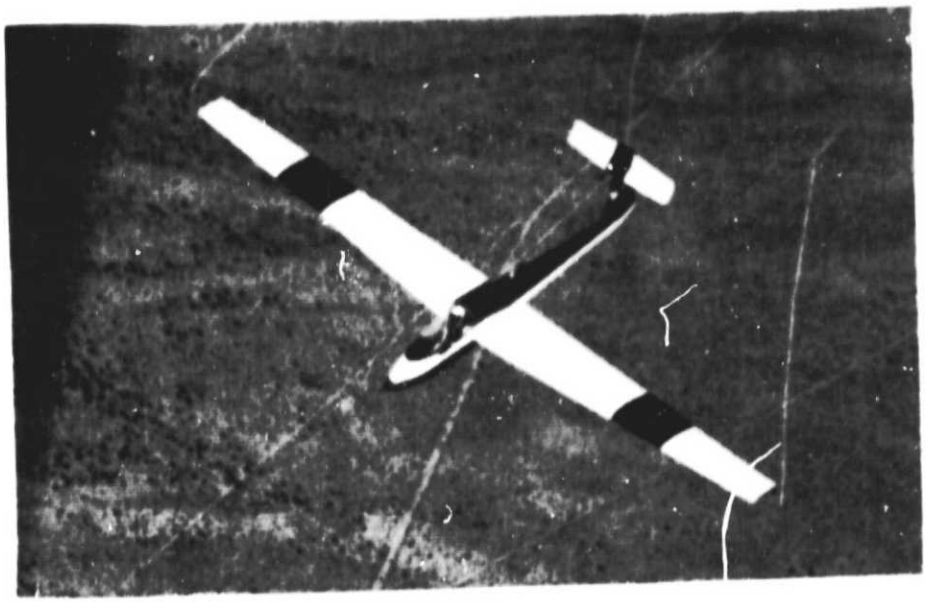

Figure 1.- Schweizer sailplane in flight.

Figure 2.- Horizontal stabilizer in the normal flight position.

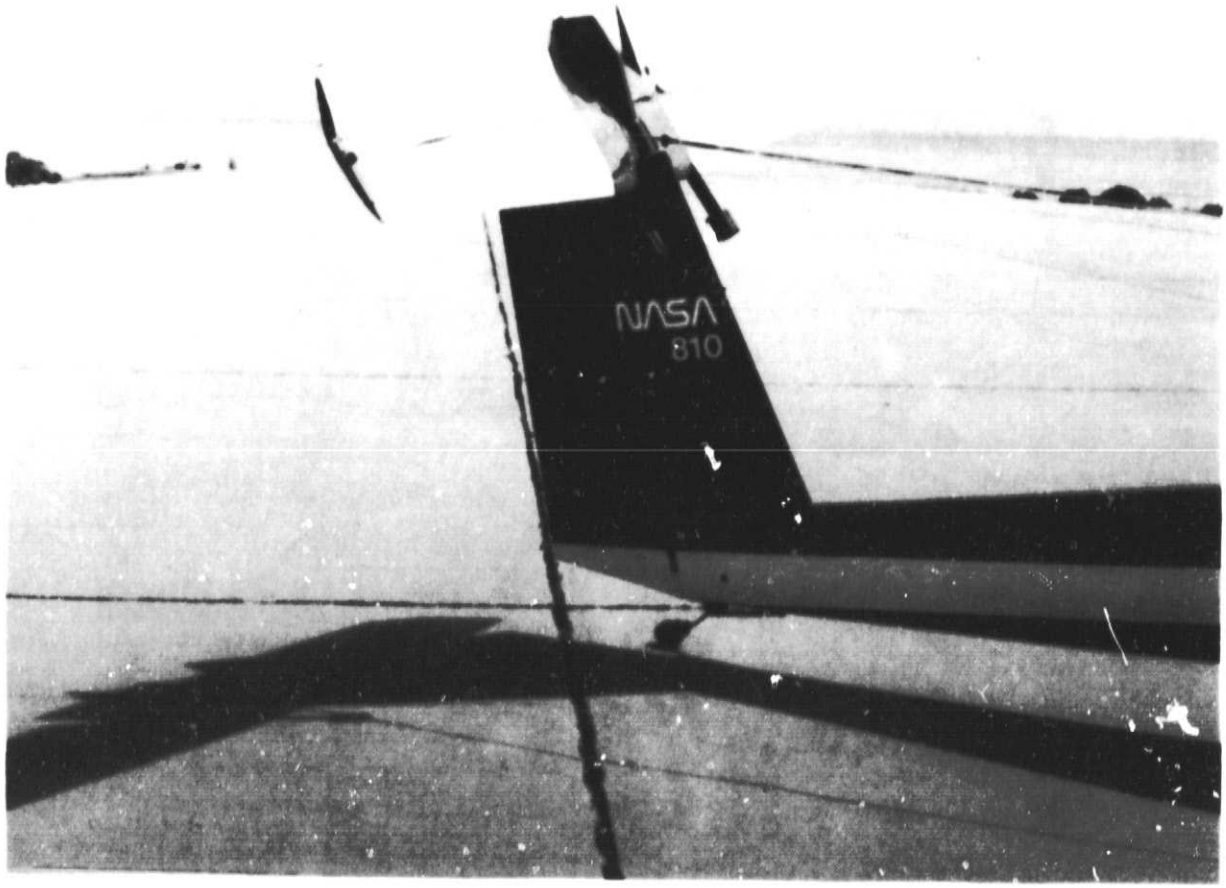

Figure 3.- Horizontal stabilizer in the deep stall position.

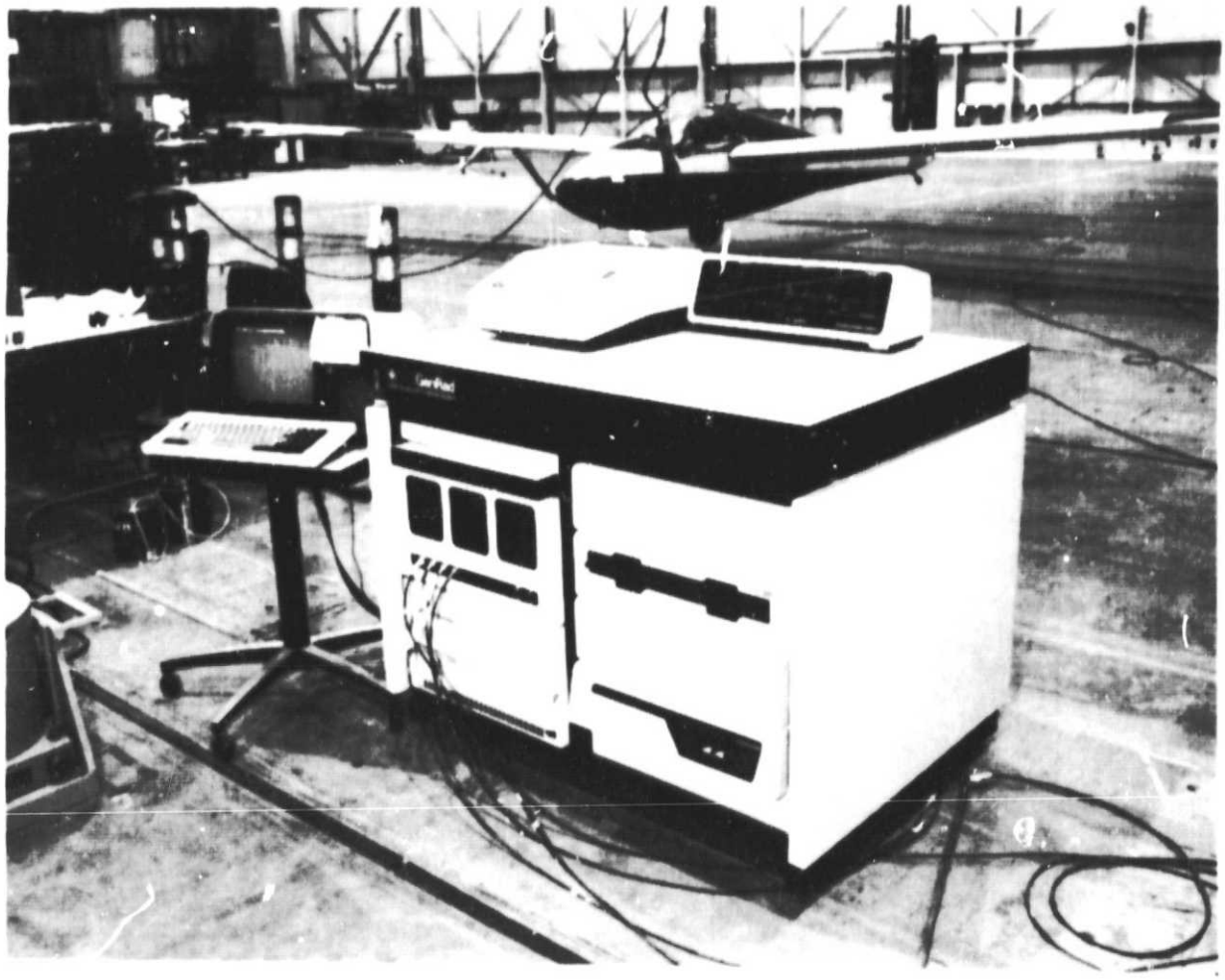

Figure 4.- Minicomputer structural analysis system.

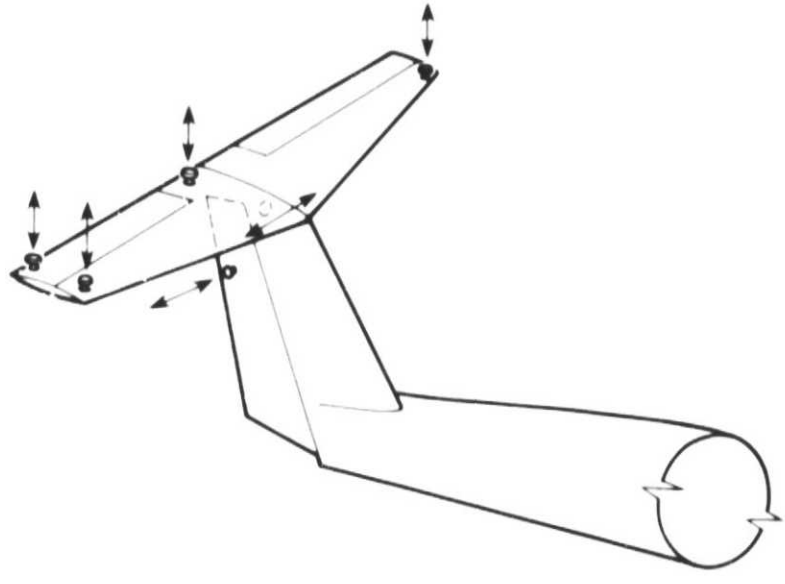

Figure 5.- Empennage accelerometer location.

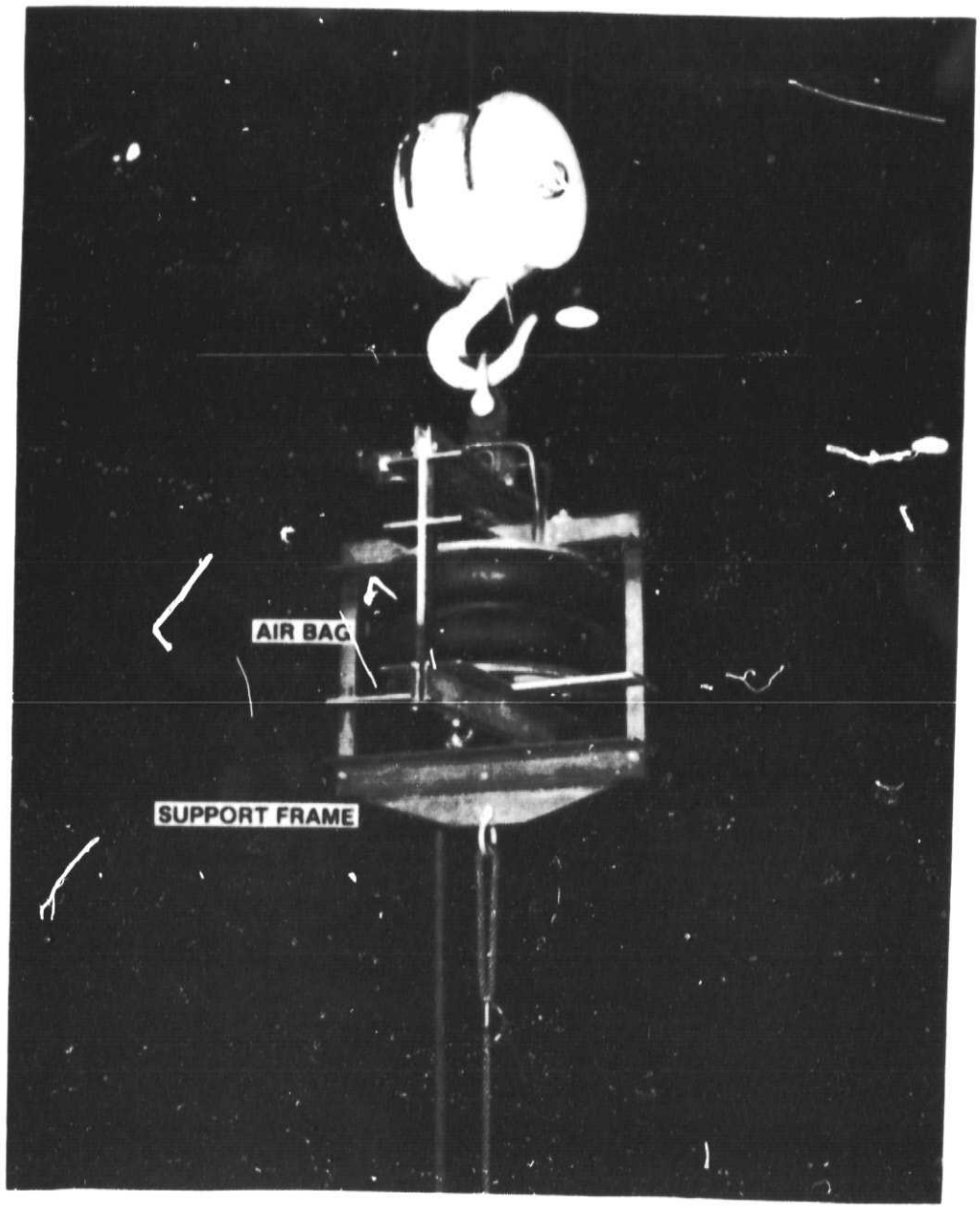

Figure 6.- Airbag suspension system.

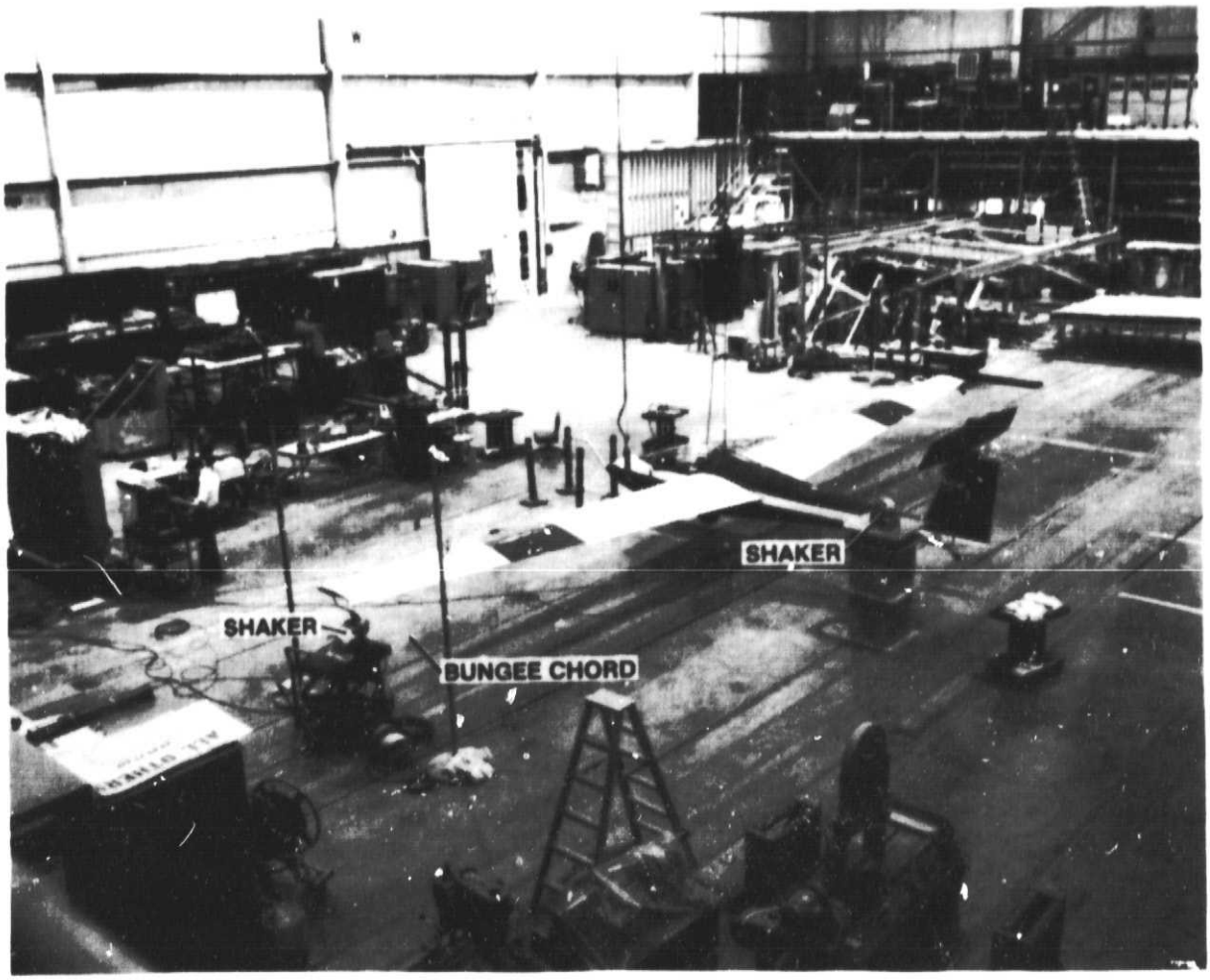

Figure 7.- Test setup with the horizontal stabilizer in the deep stall position.

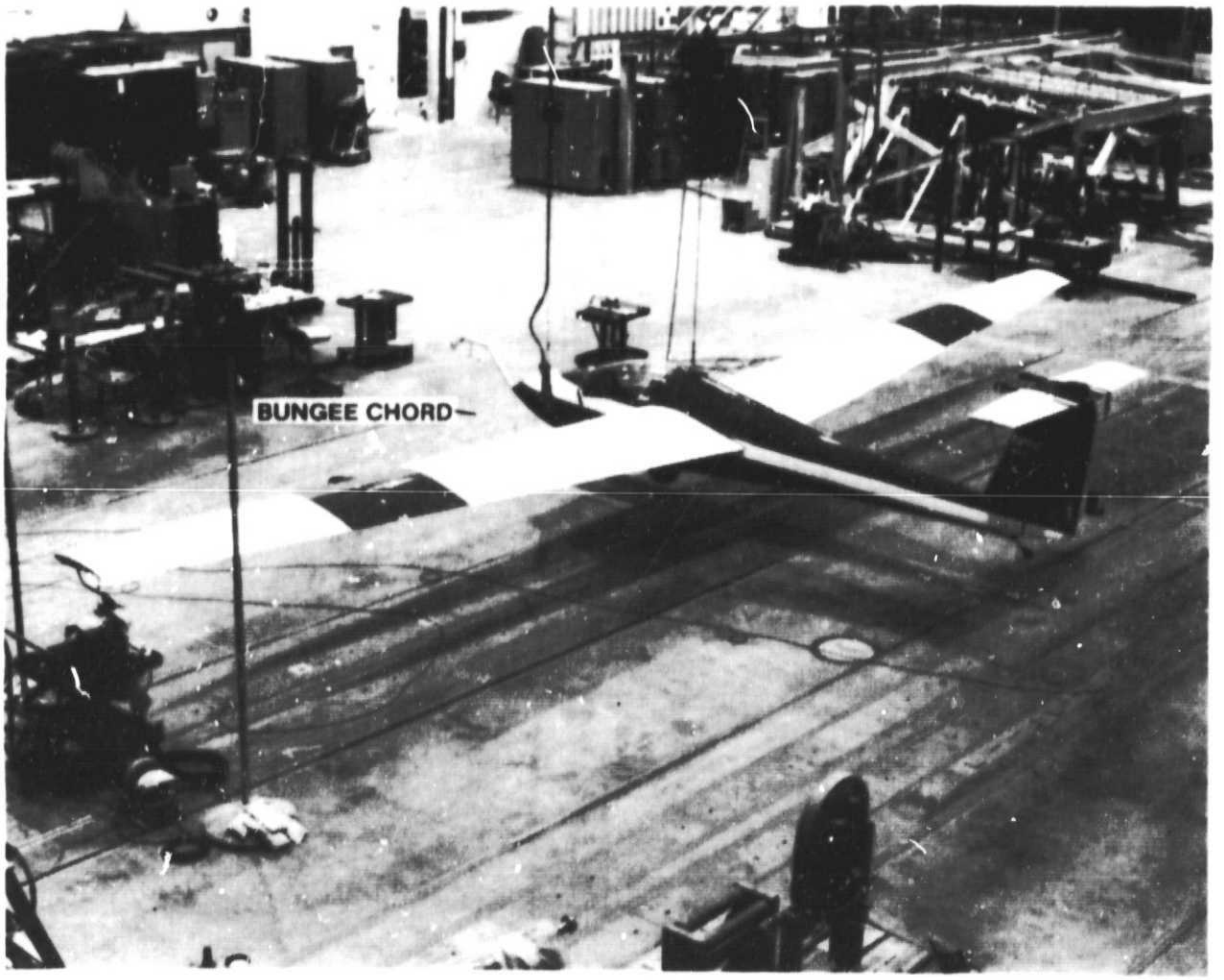

Figure 8.- Test setup with the horizontal stabilizer in the normal flight position.

Figure 9.- Control stick locking mechanism.

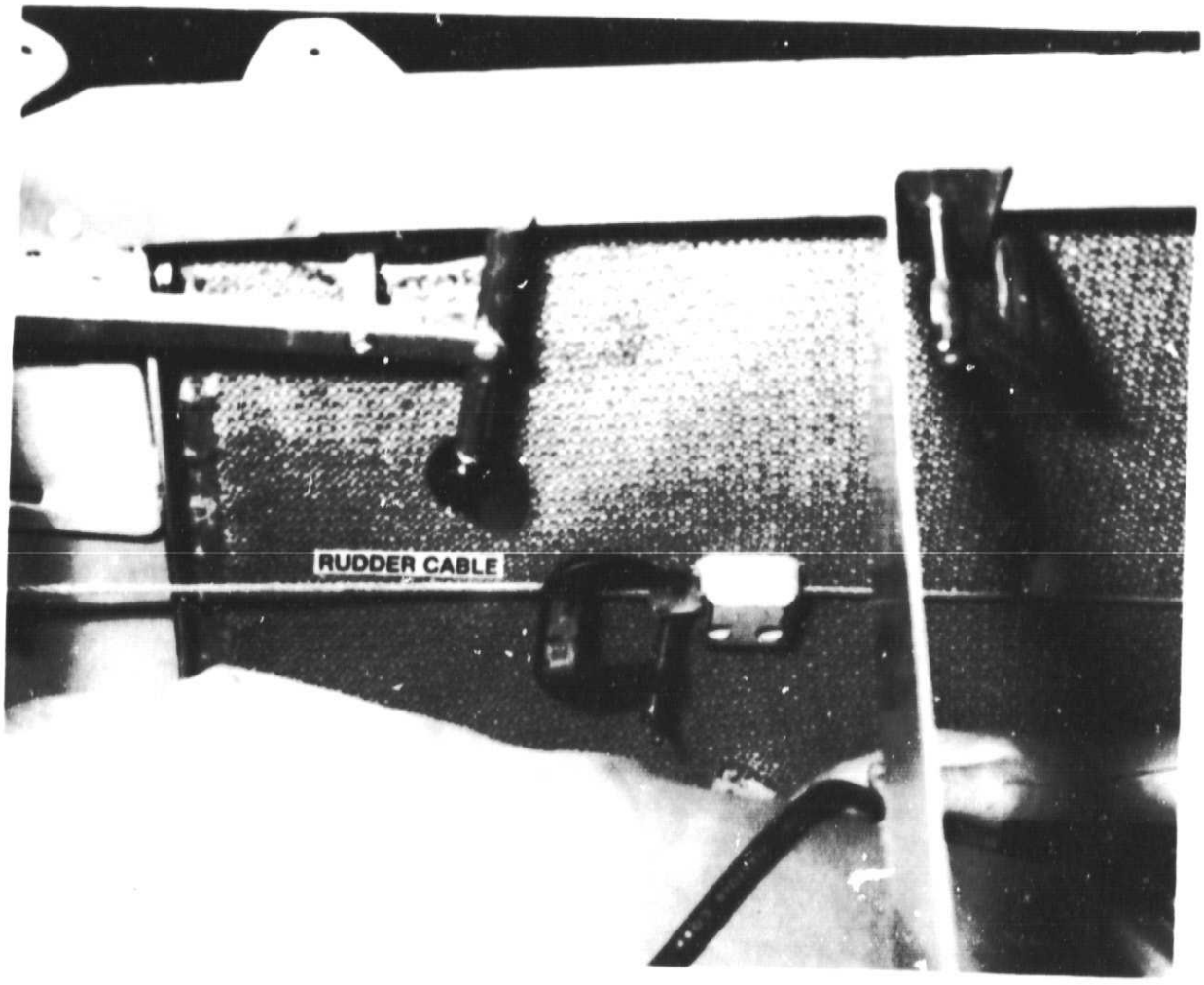

Figure 10.- Rudder locking mechanism.

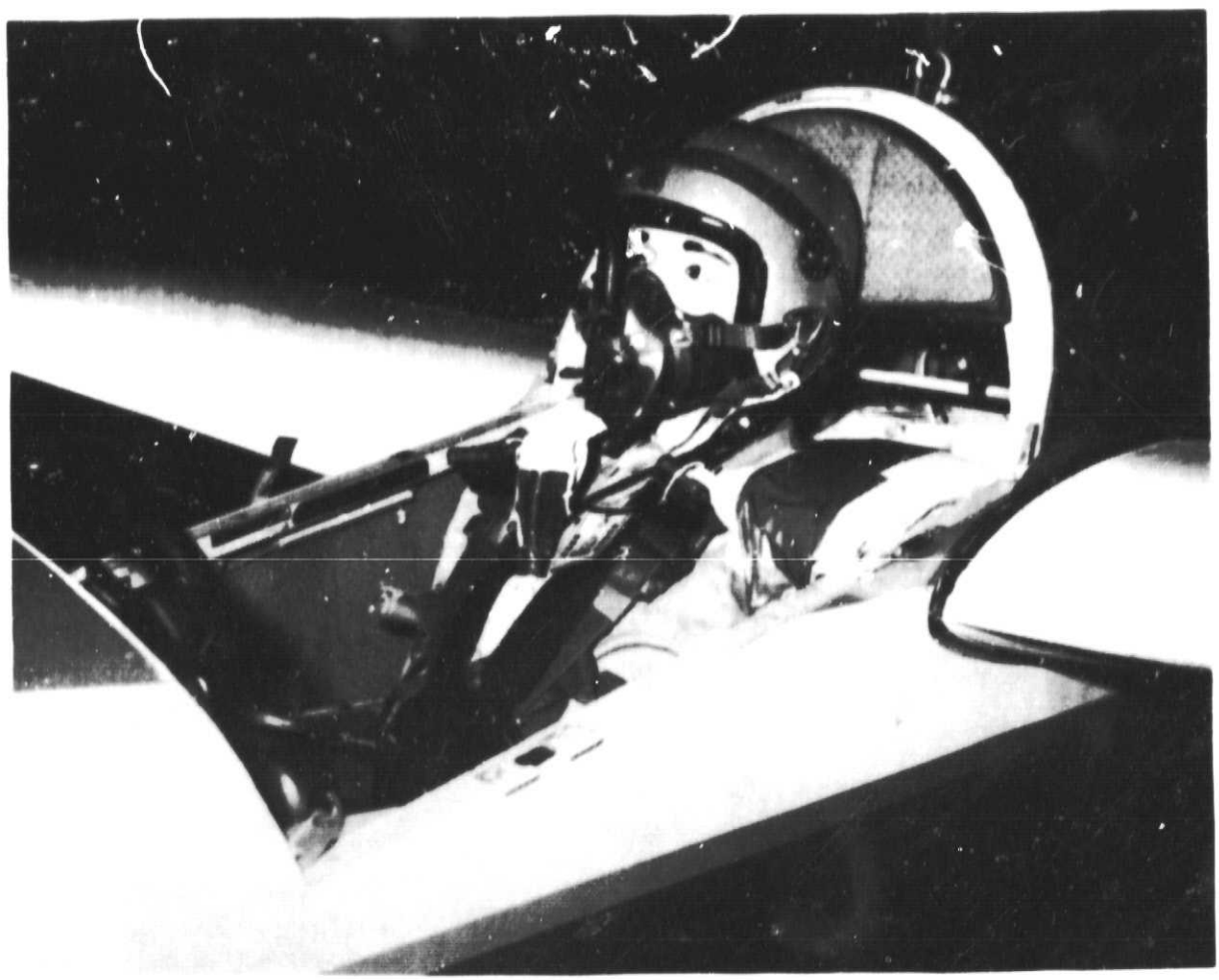

Figure 11.- Cockpit dummy to simulate the pilot's weight.

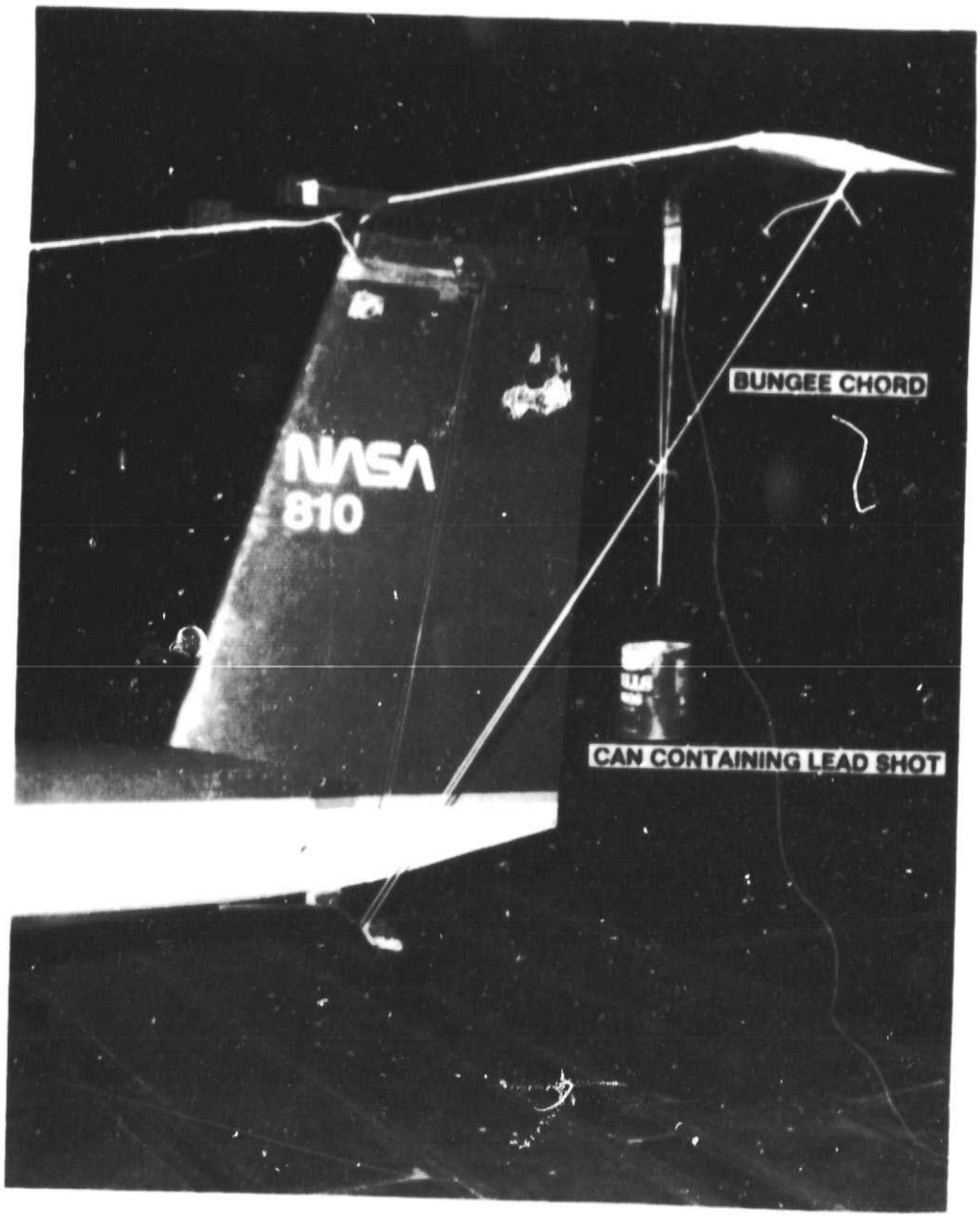

Figure 12.- Horizontal stabilizer preload.

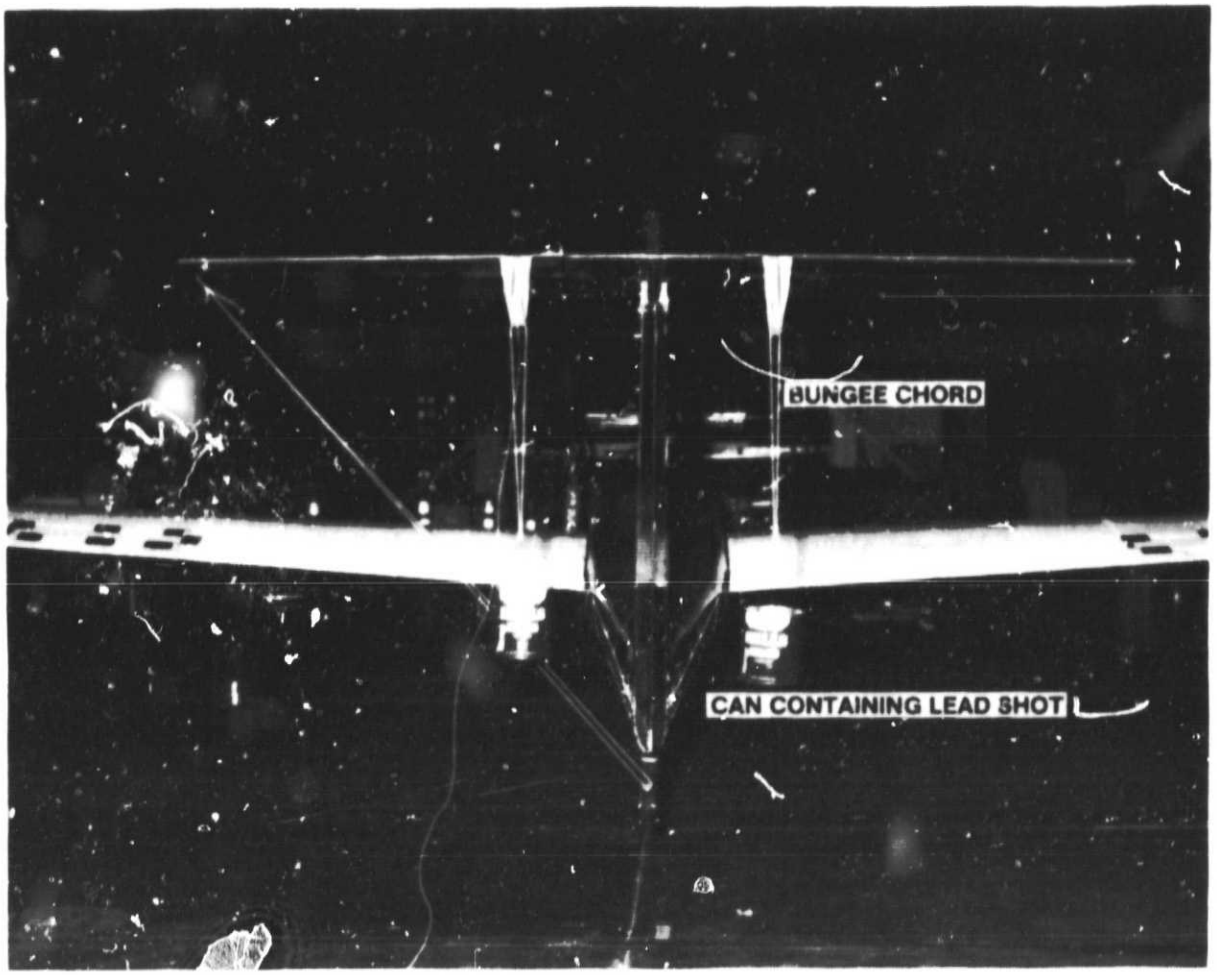

Figure 13.- Elevator preload.

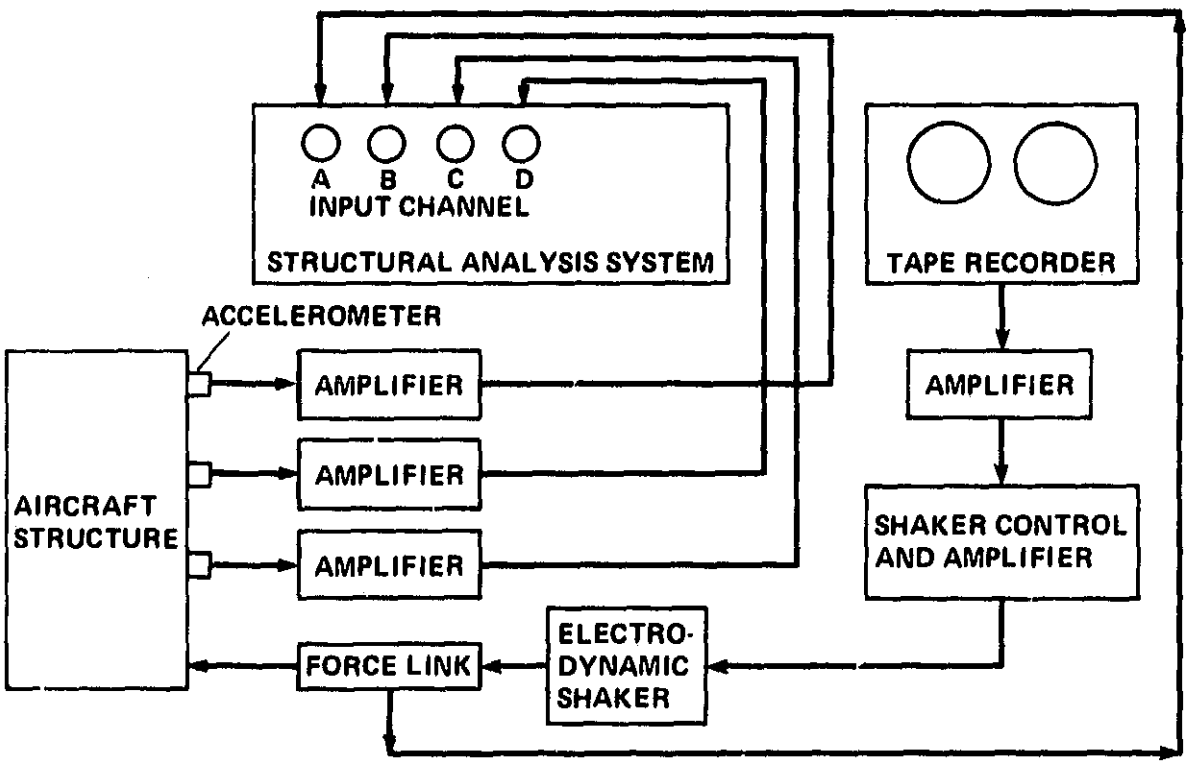

Figure 14.- Ground vibration test equipment diagram.

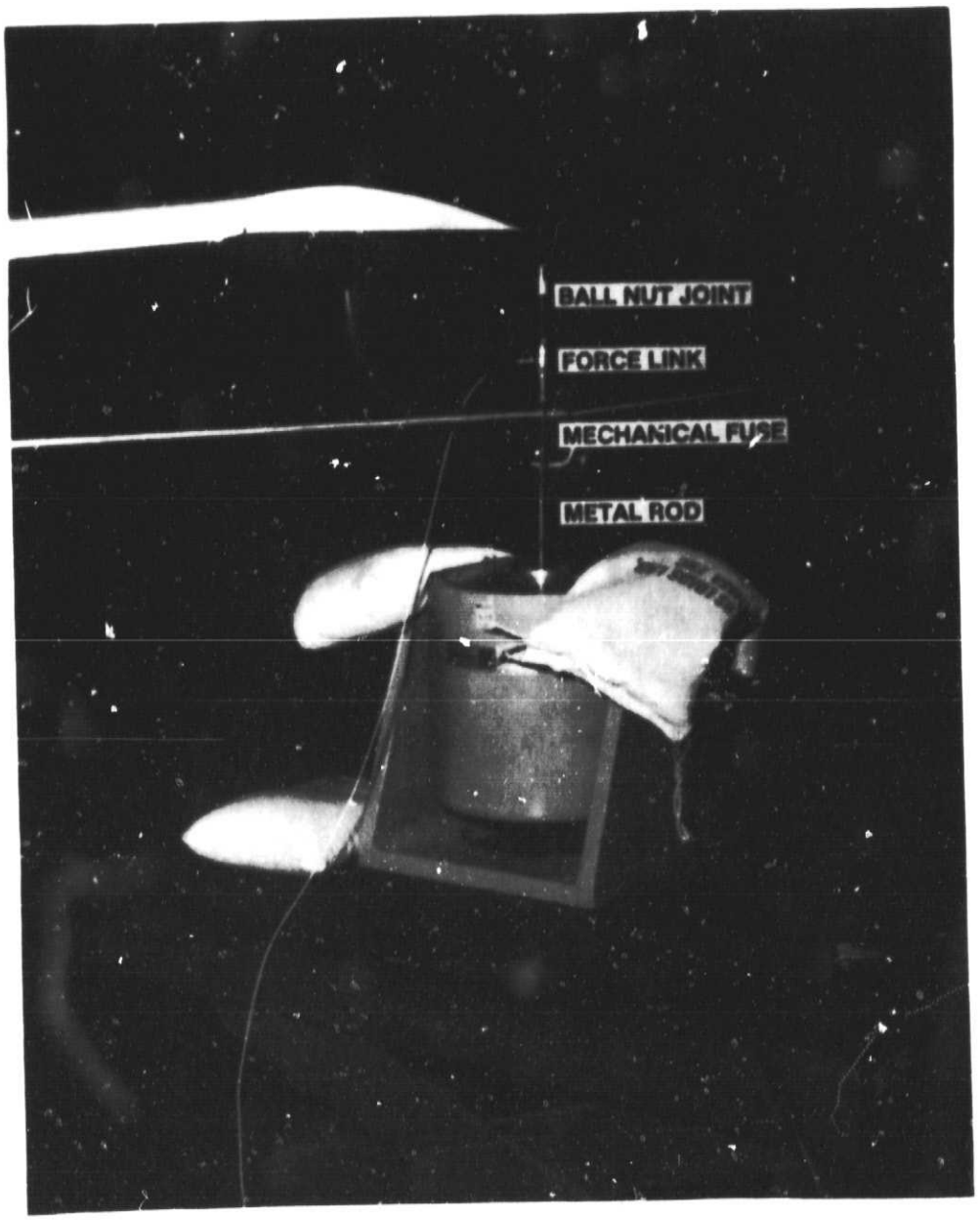

Figure 15.- Wingtip shaker location.

Figure 16.- Vertical fin shaker location.

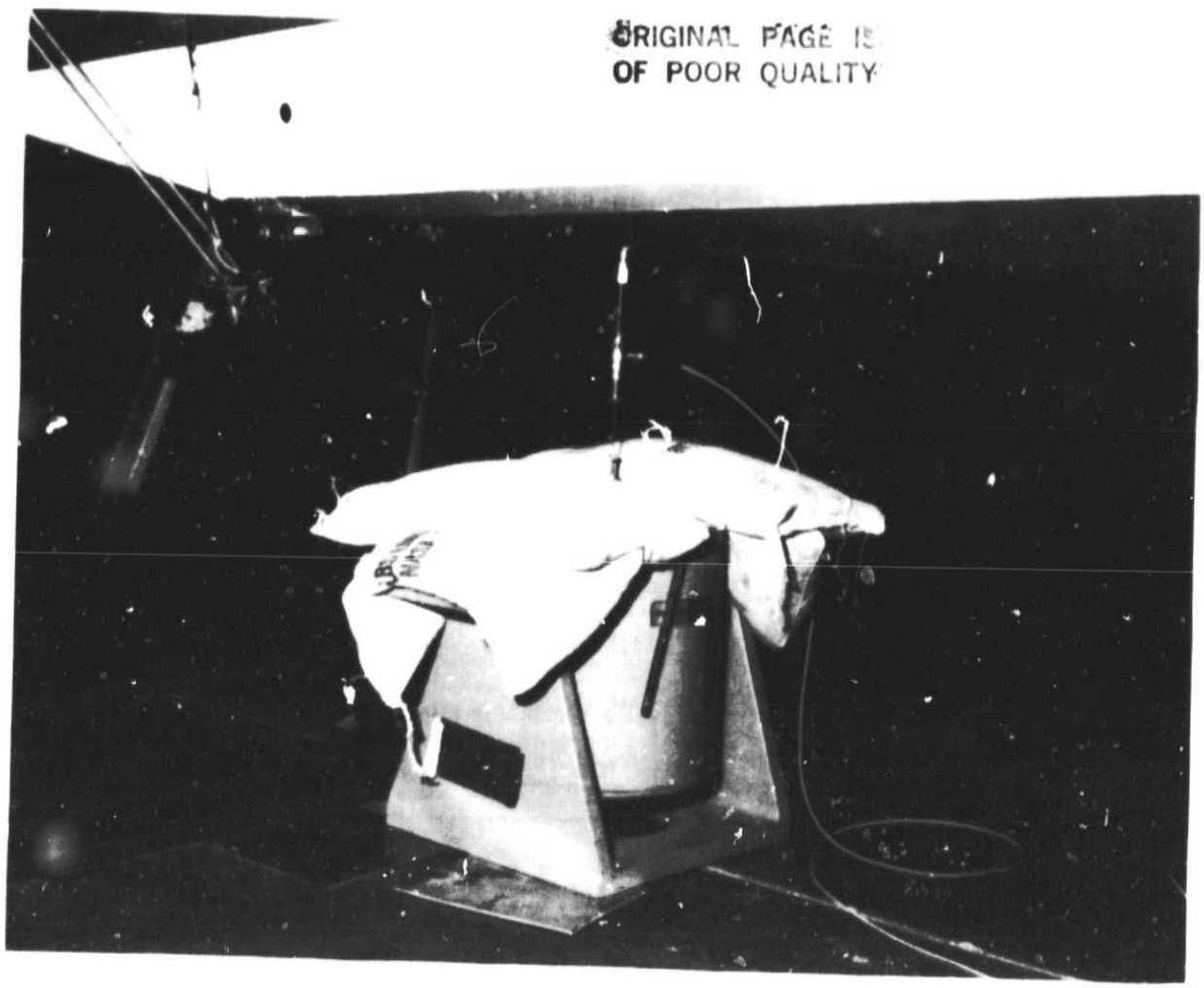

Figure 17.- Fuselage shaker location.

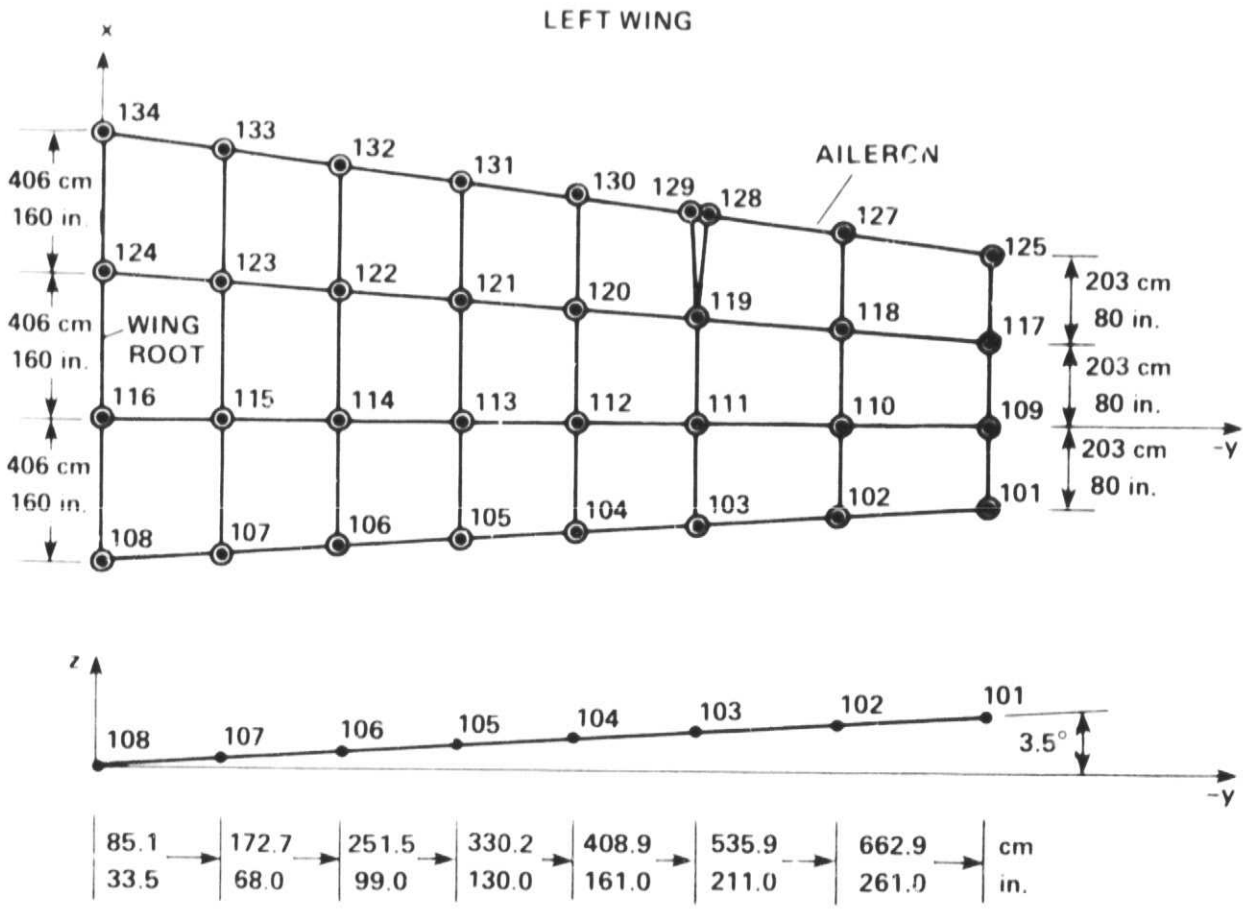

(a) Left wing.

Figure 18.- Modal survey points.

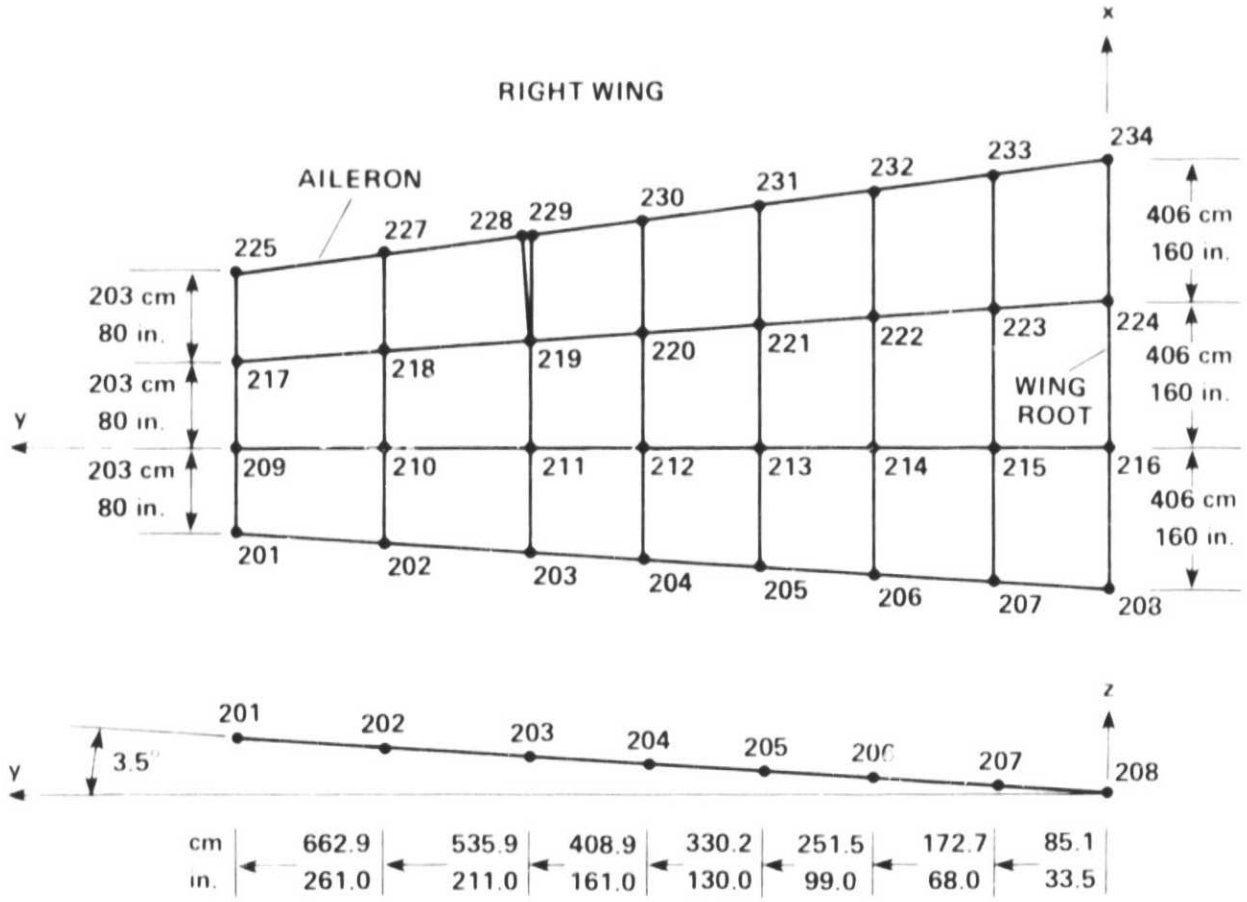

(b) Right wing.

Figure 18.- Continued.

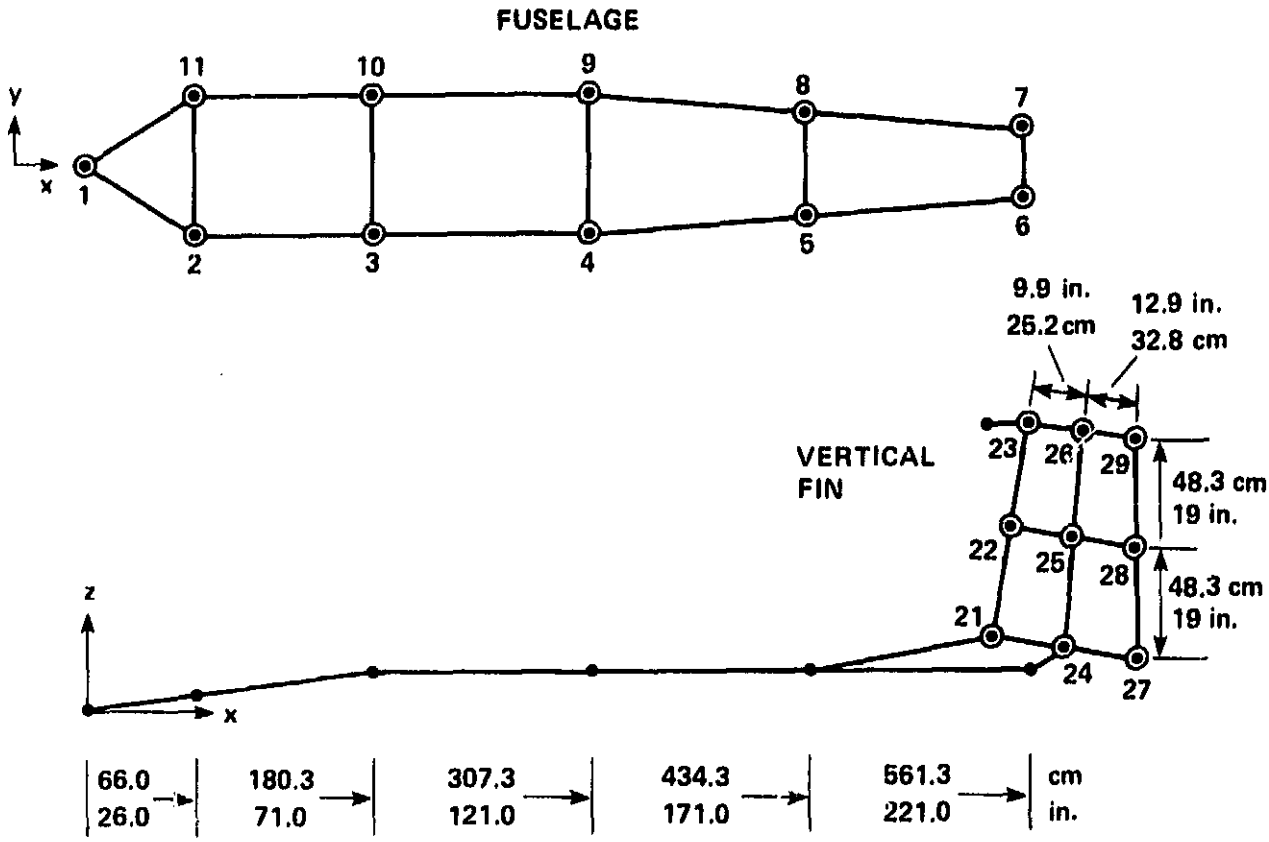

(c) Fuselage and vertical fin.

Figure 18.- Continued.

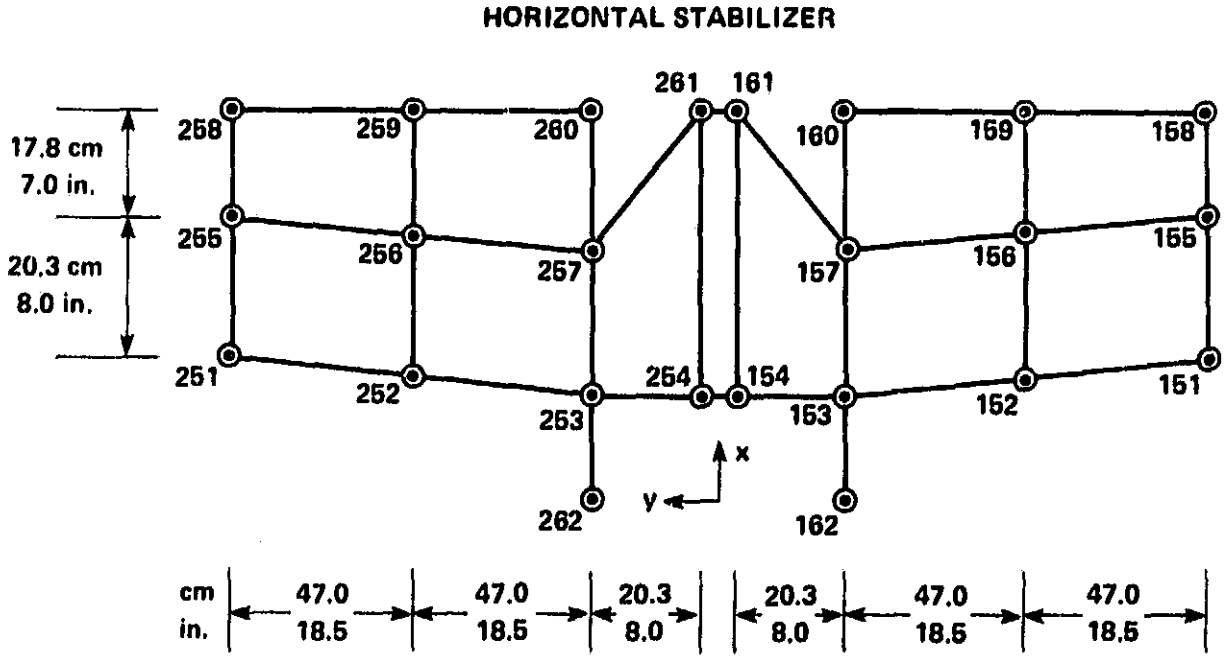

(d) Horizontal stabilizer.

Figure 18.- Concluded.

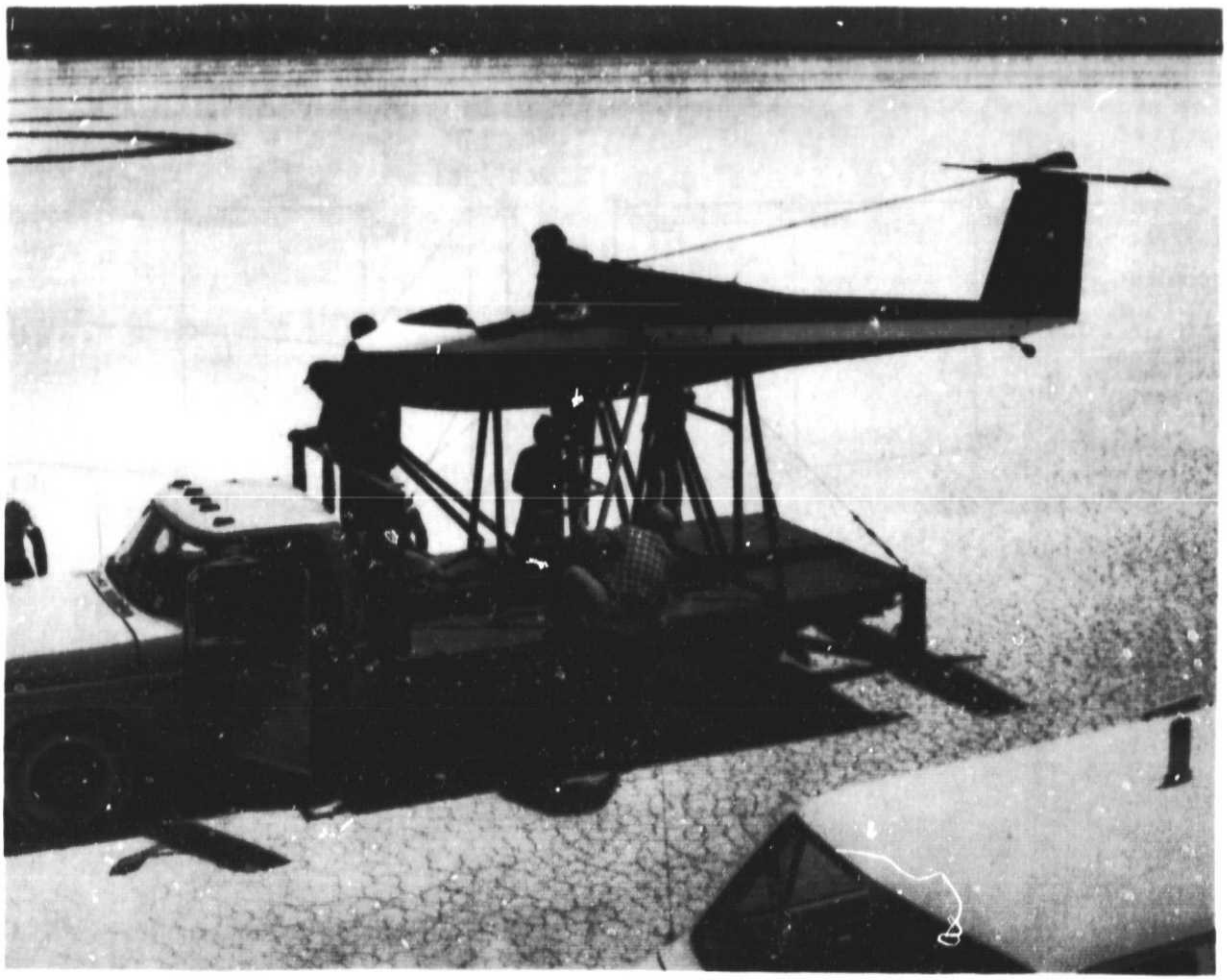

Figure 19.- Truck mounted sailplane with the horizontal stabilizer in the normal position.

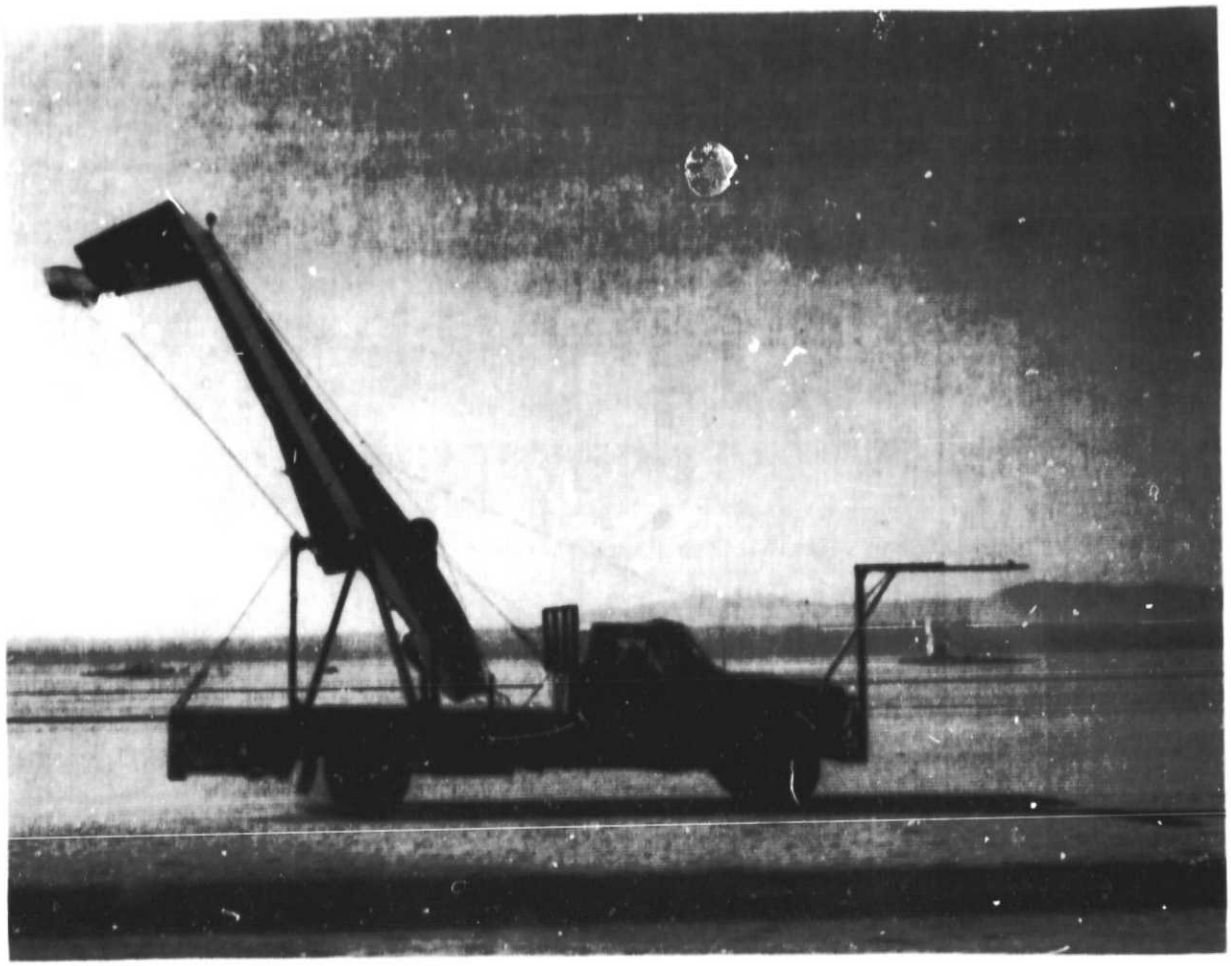

Figure 20.- Truck mounted sailplane with the horizontal stabilizer in the deep stall position.

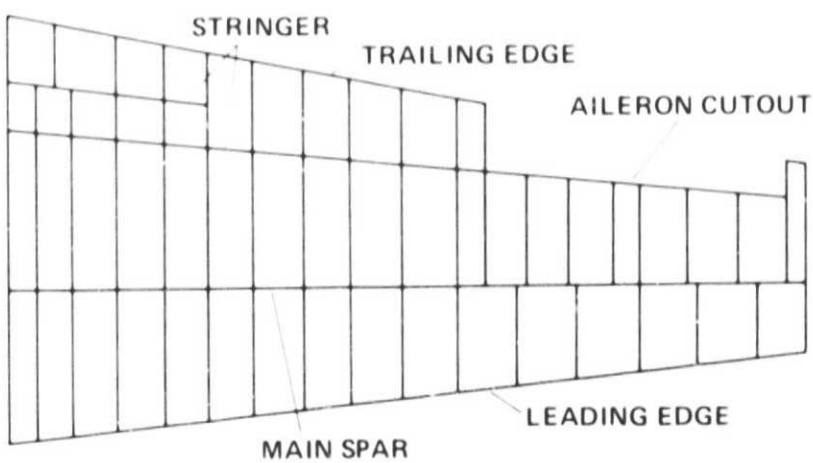

Figure 21.- Sailplane wing spar and rib locations.

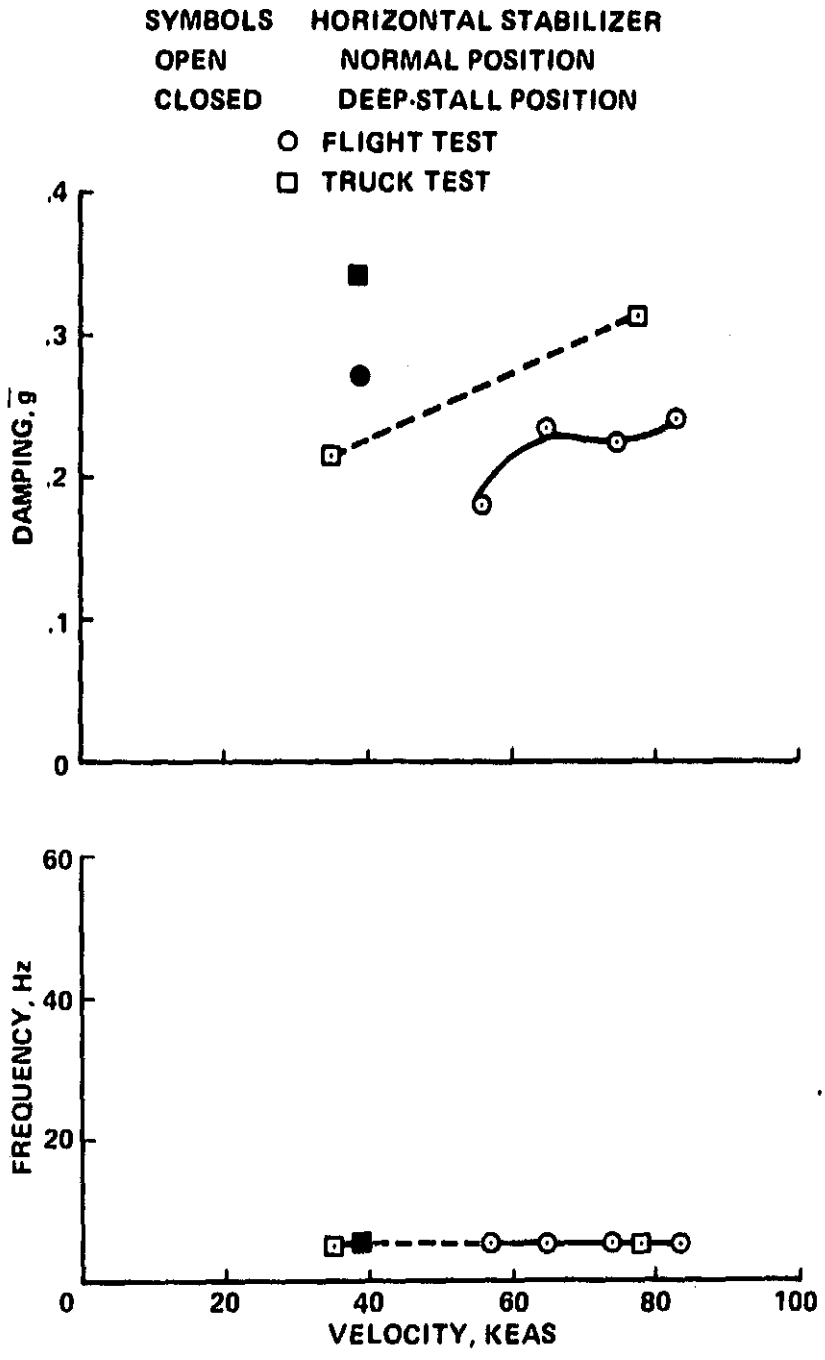

Figure 22.- Fuselage torsion modal data.

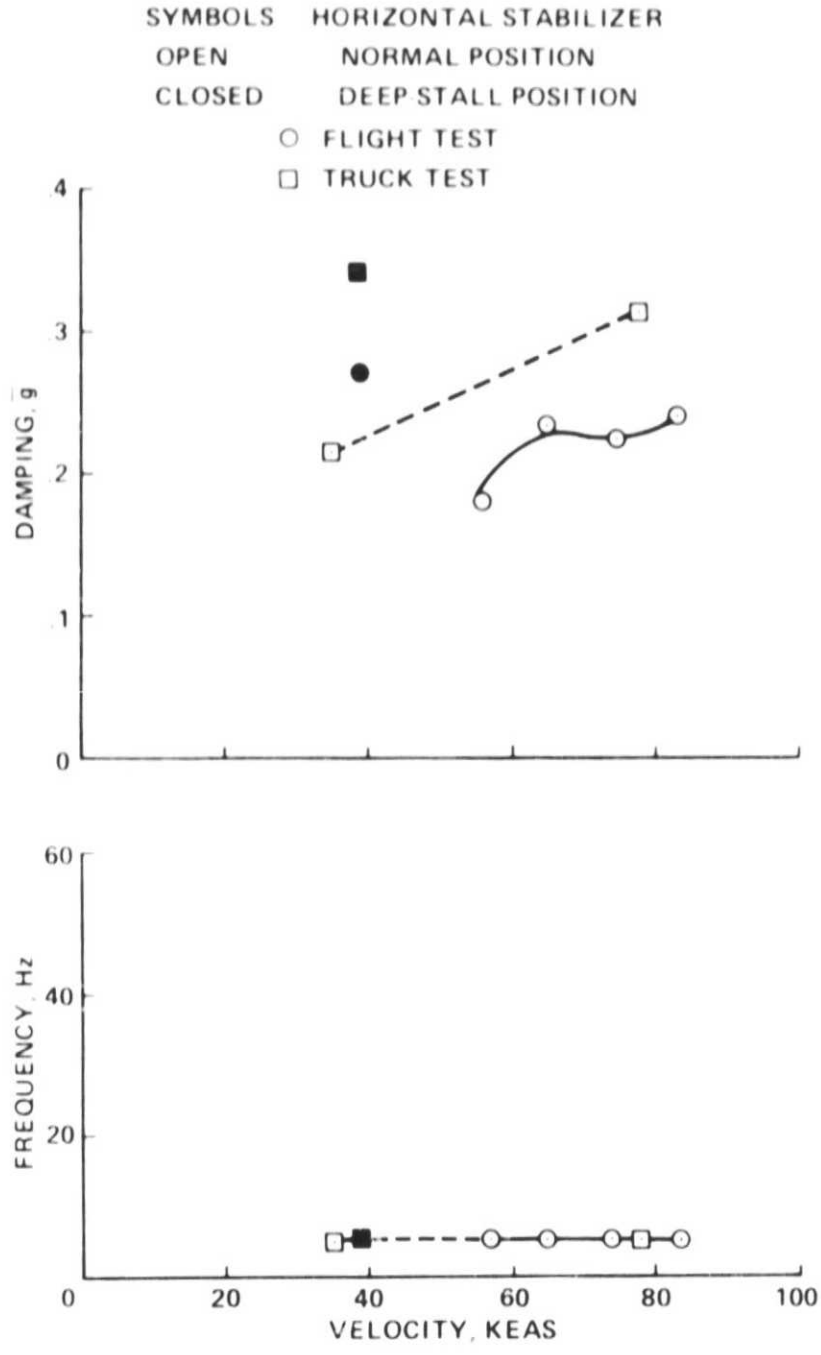

Figure 22.- Fuselage torsion modal data.

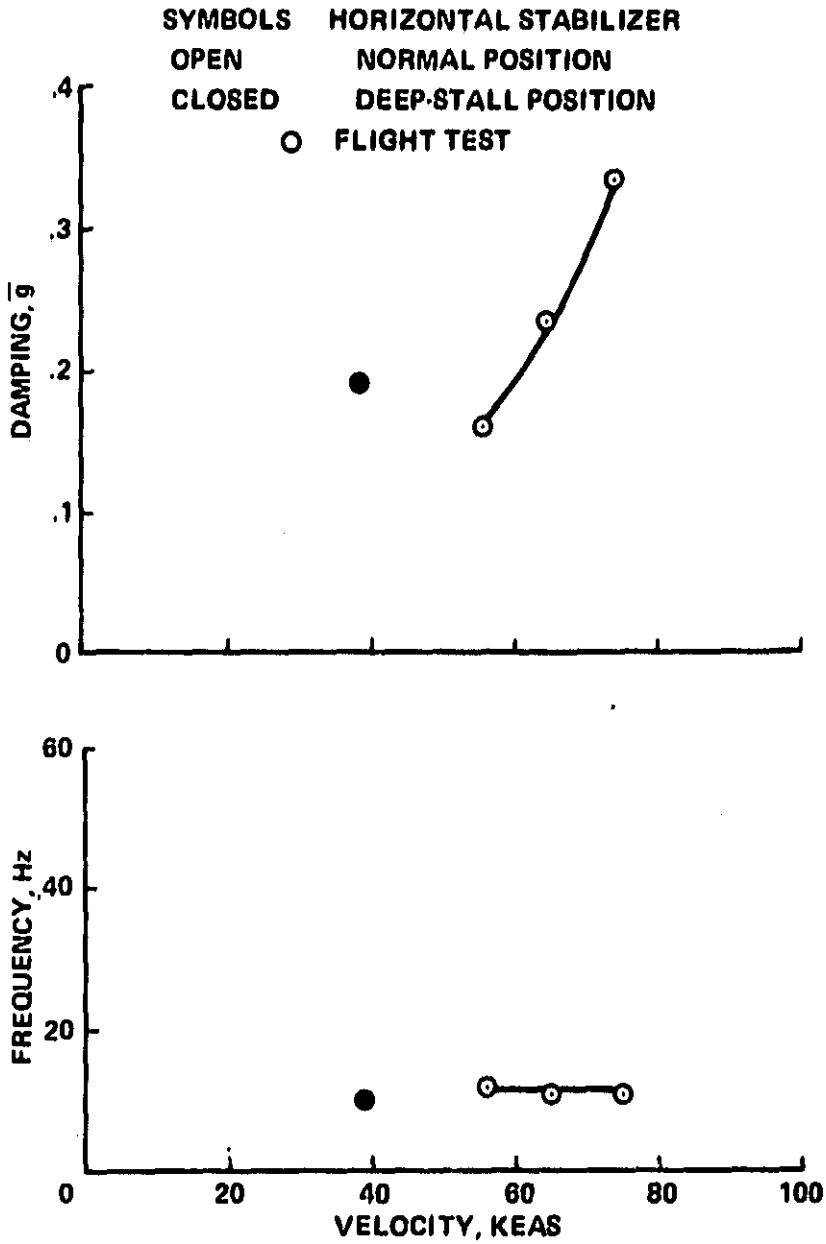

Figure 23.- Antisymmetric wing bending modal data.

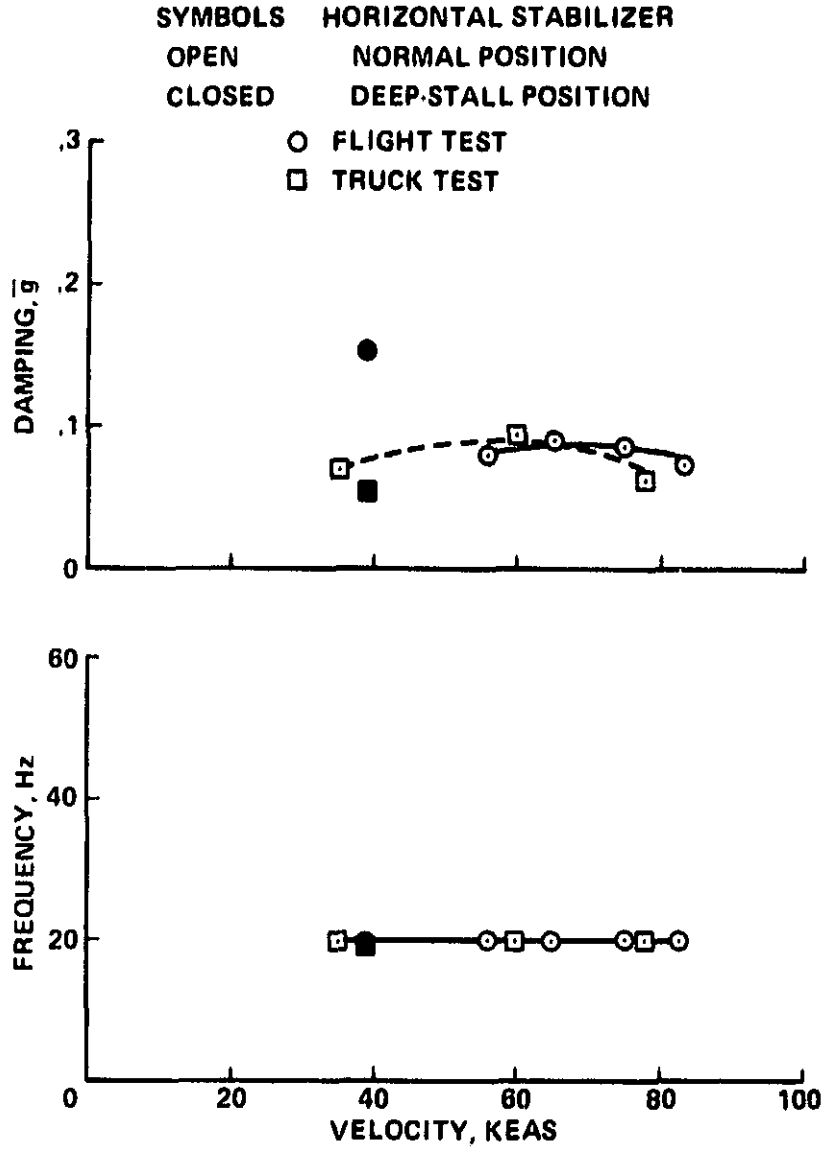

Figure 24.- Vertical fin bending modal data.

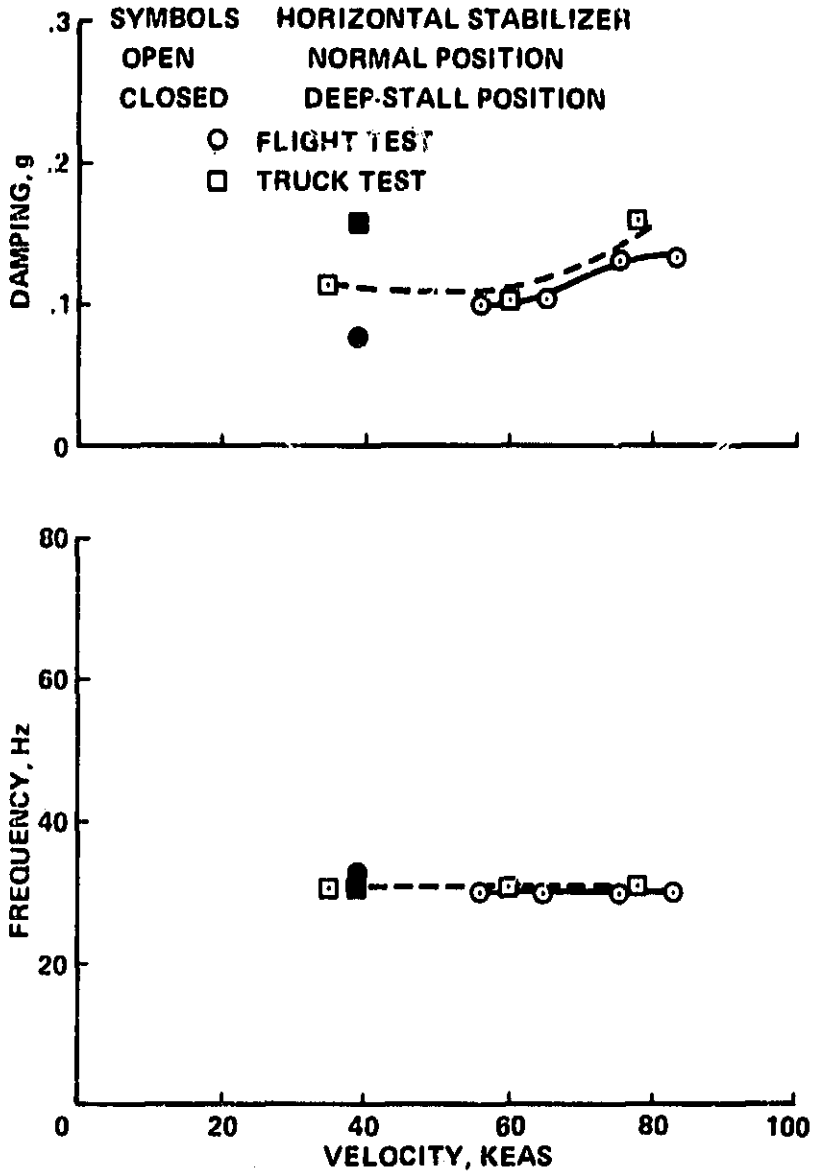

Figure 25.- Symmetric horizontal stabilizer bending modal data.

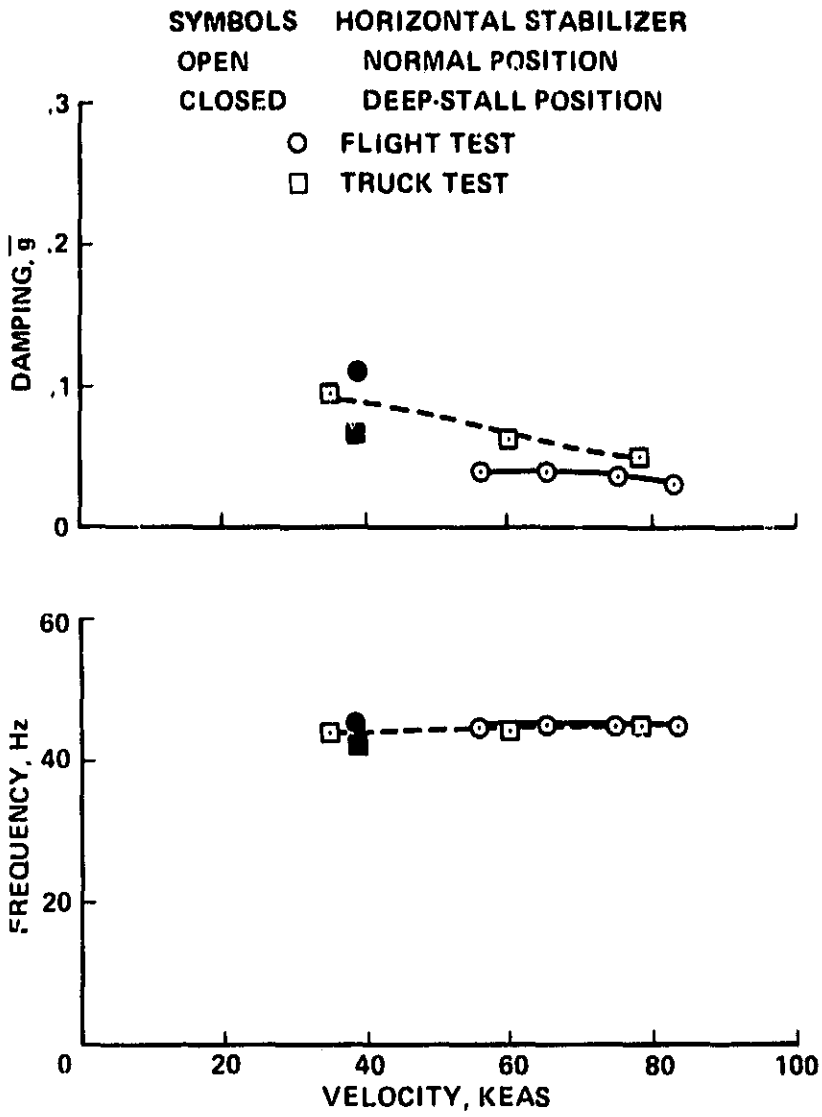

Figure 26.- Elevator rotation modal data.

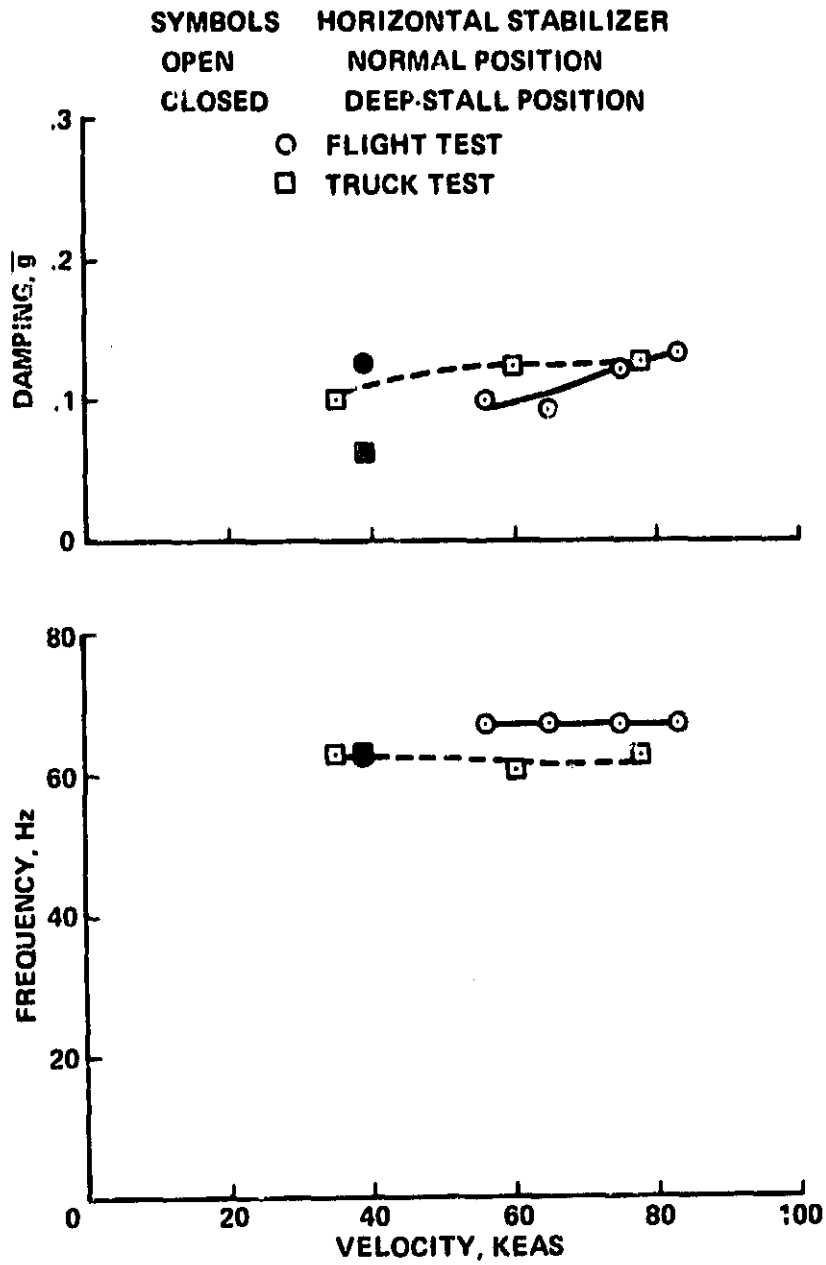

Figure 27.- Rudder rotation modal data.

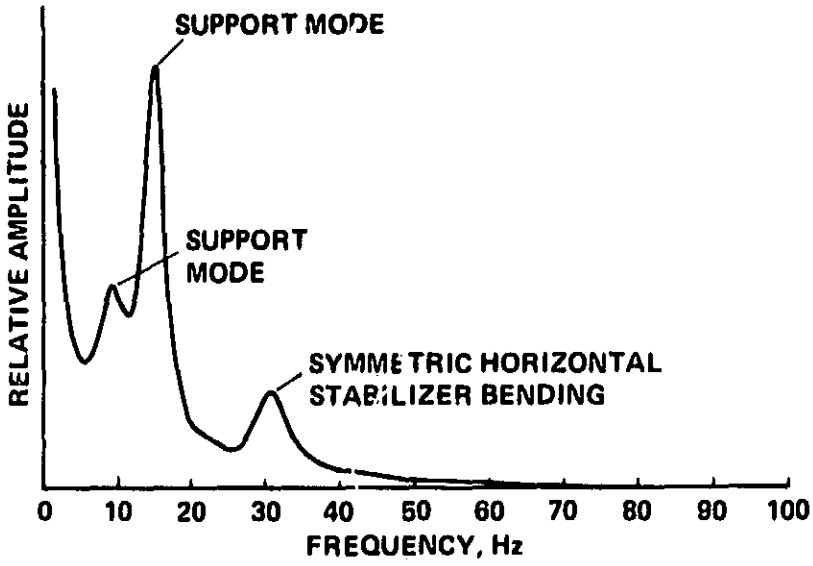

Figure 28.- Horizontal stabilizer response at 60 KEAS during truck testing.

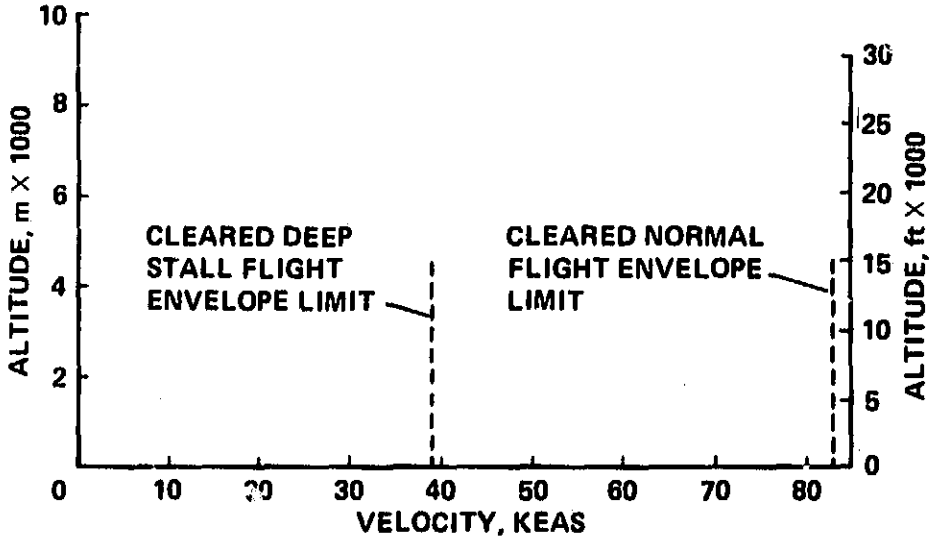

Figure 29.- Cleared flight envelope.

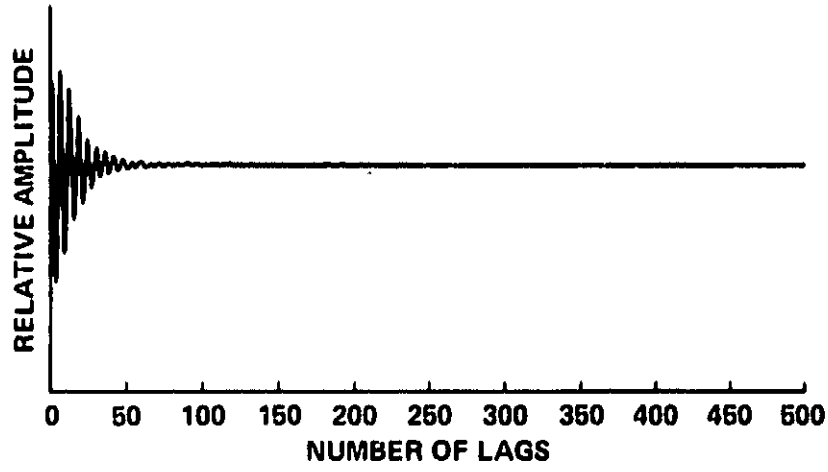

Figure A1.- Auto-correlation function multiplied by an exponential window.

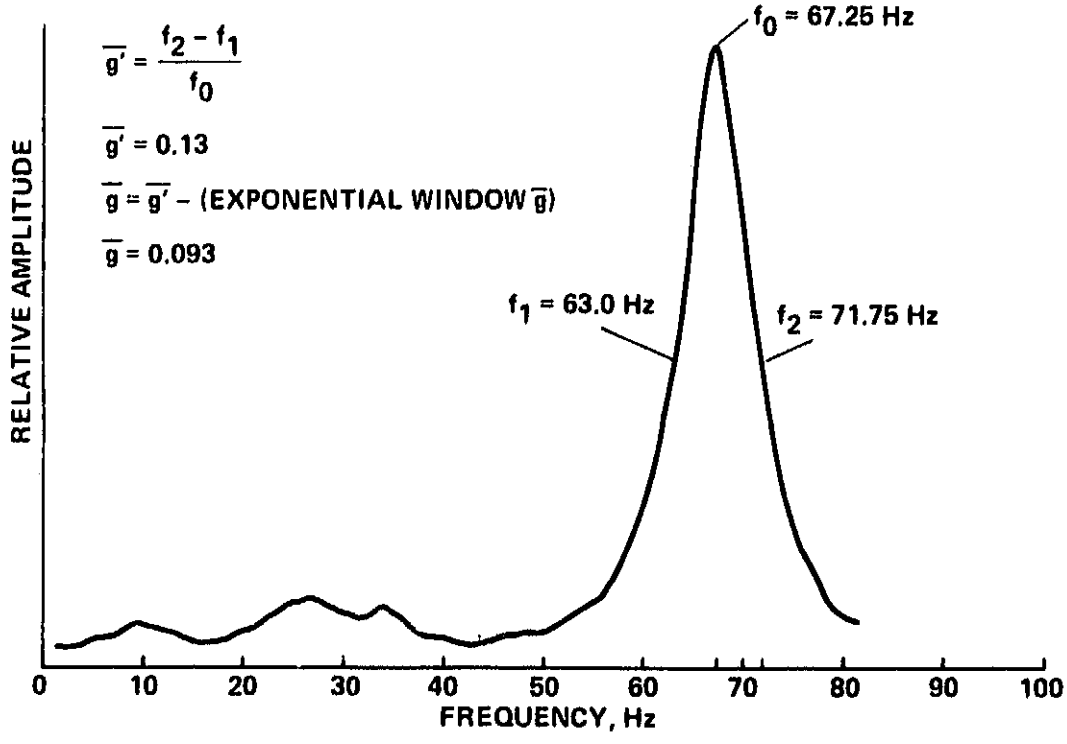

Figure A2.- Direct Fourier transform.

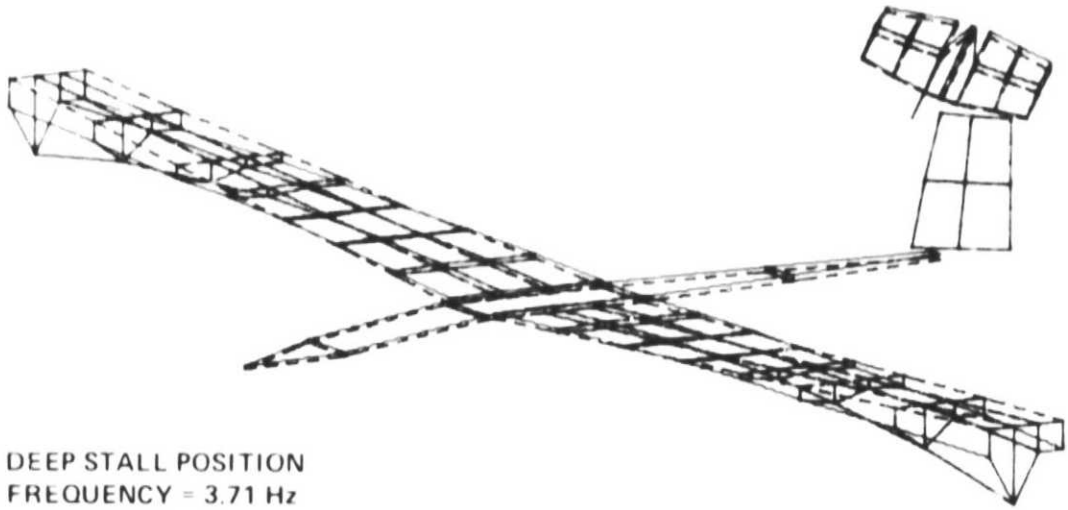

DEEP STALL POSITION
FREQUENCY = 3.71 Hz

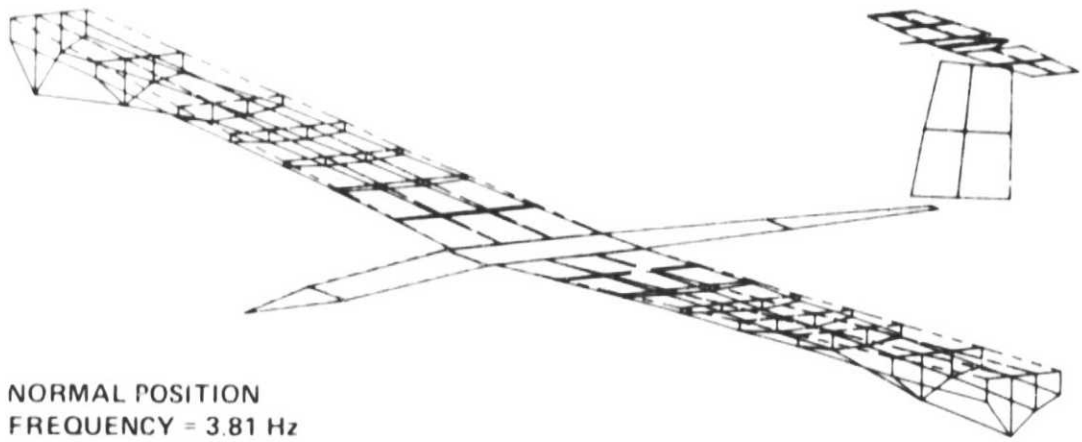

NORMAL POSITION
FREQUENCY = 3.81 Hz

Figure B1.- Symmetric wing bending mode shape comparison.

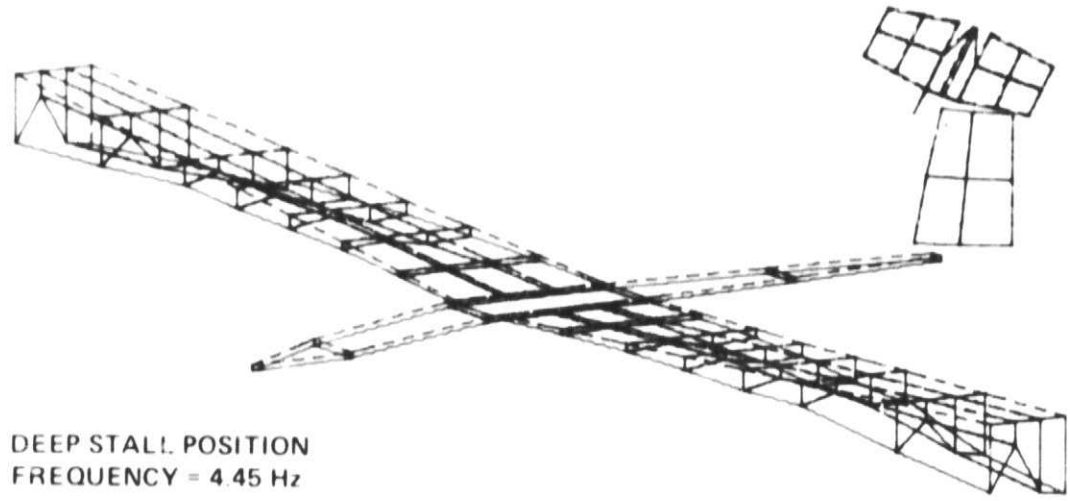

DEEP STALL POSITION
FREQUENCY = 4.45 Hz

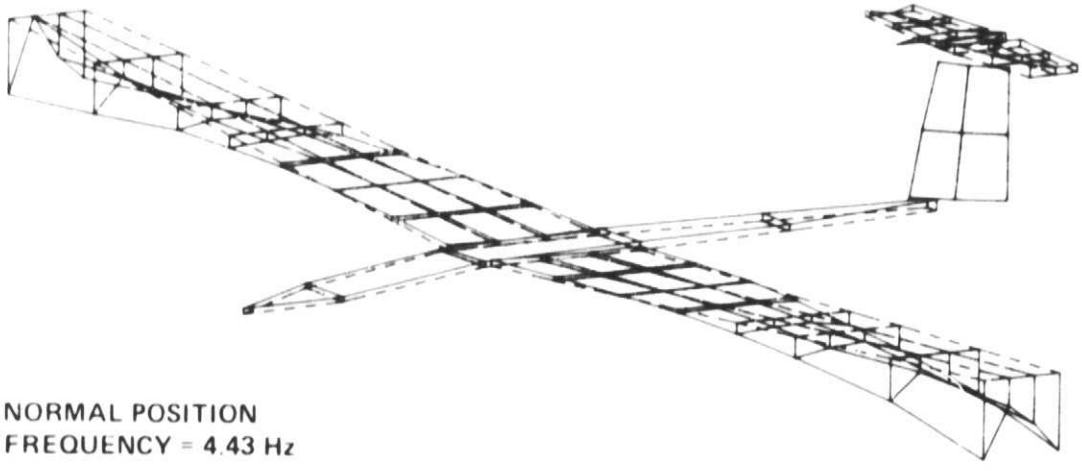

NORMAL POSITION
FREQUENCY = 4.43 Hz

Figure B2.- Symmetric wing bending/fuselage bending mode shape comparison.

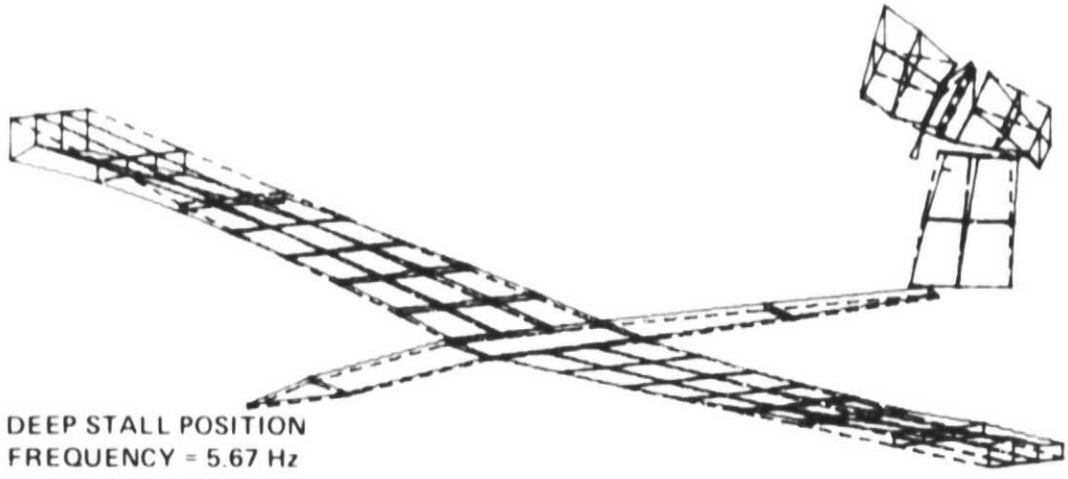

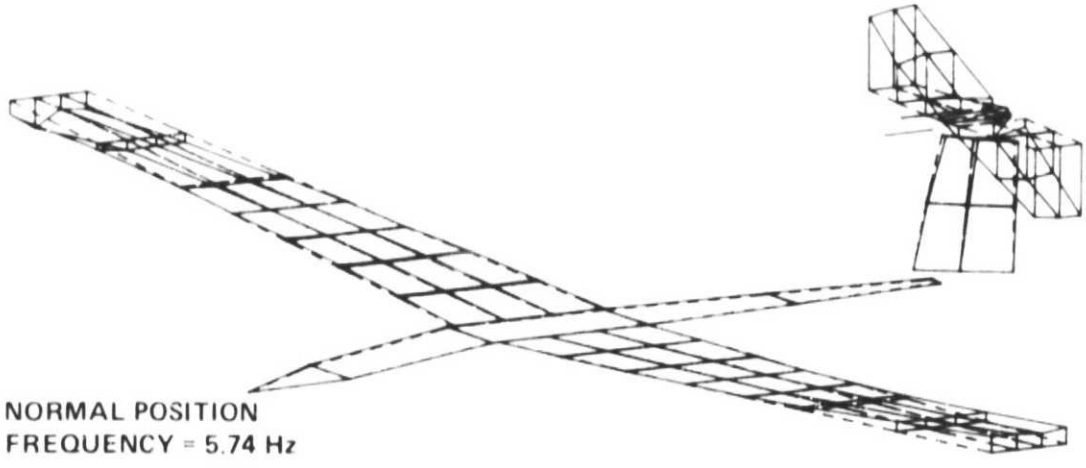

Figure B3.- Fuselage torsion mode shape comparison.

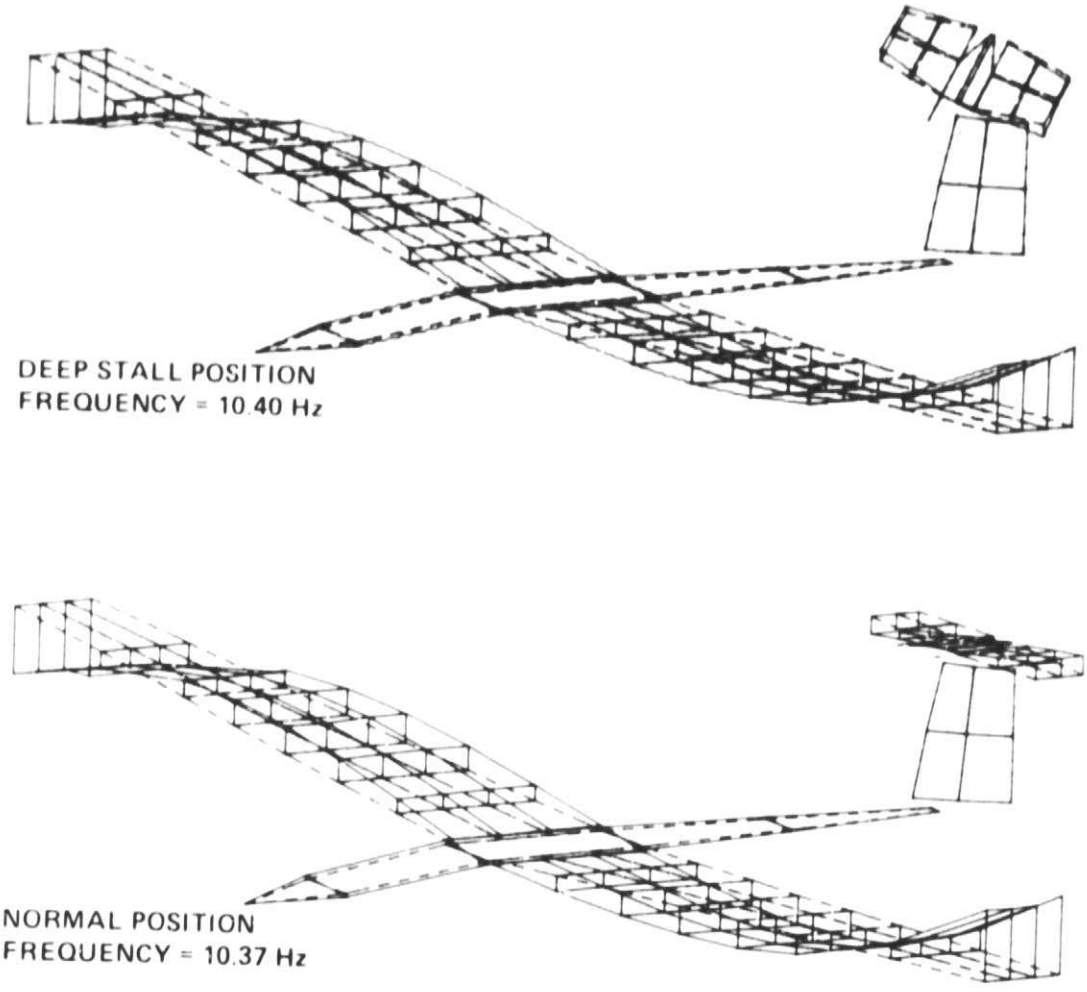

Figure B4.- Antisymmetric wing bending mode shape comparison.

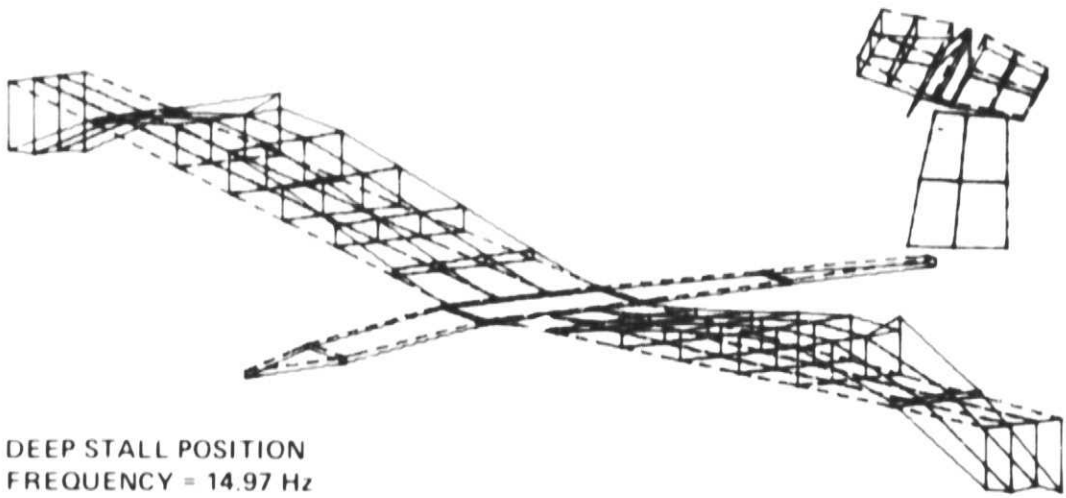

DEEP STALL POSITION
FREQUENCY = 14.97 Hz

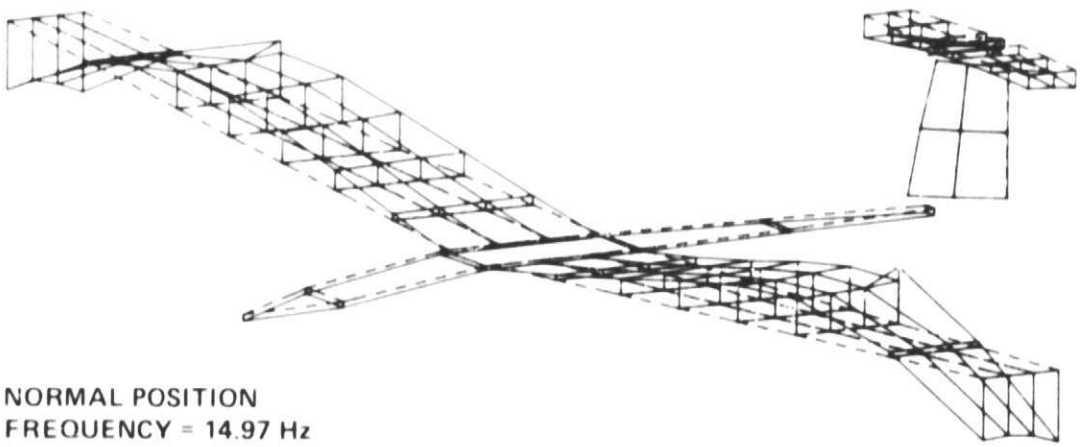

NORMAL POSITION
FREQUENCY = 14.97 Hz

Figure B5.- Second symmetric wing bending mode shape comparison.

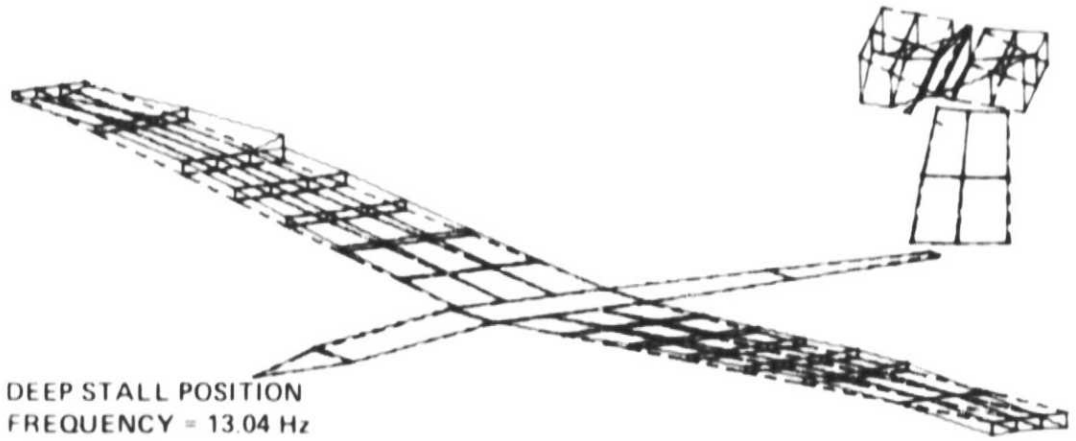

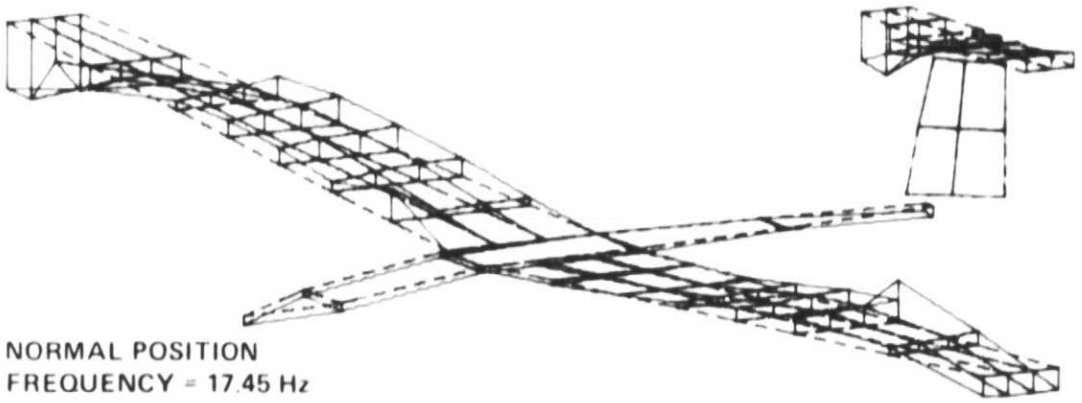

Figure B6.- Horizontal stabilizer roll mode shape comparison.

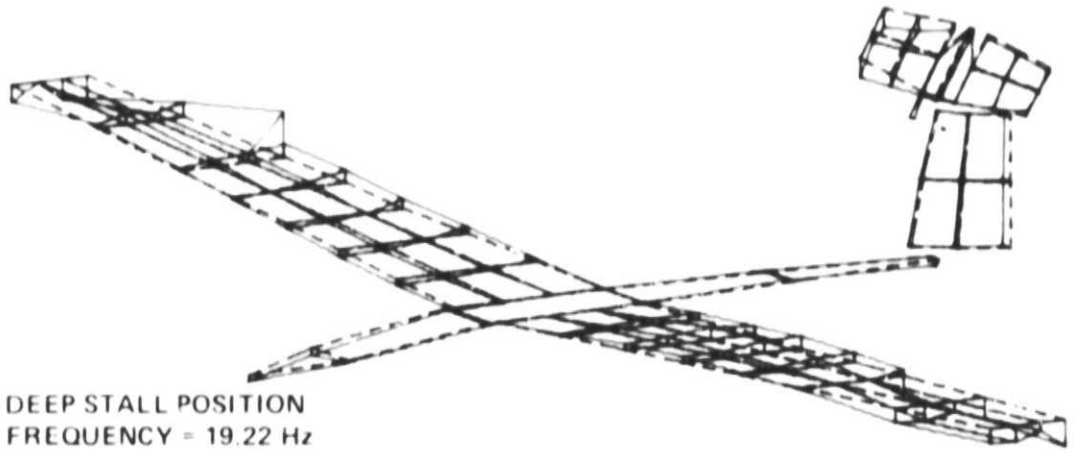

DEEP STALL POSITION
FREQUENCY = 19.22 Hz

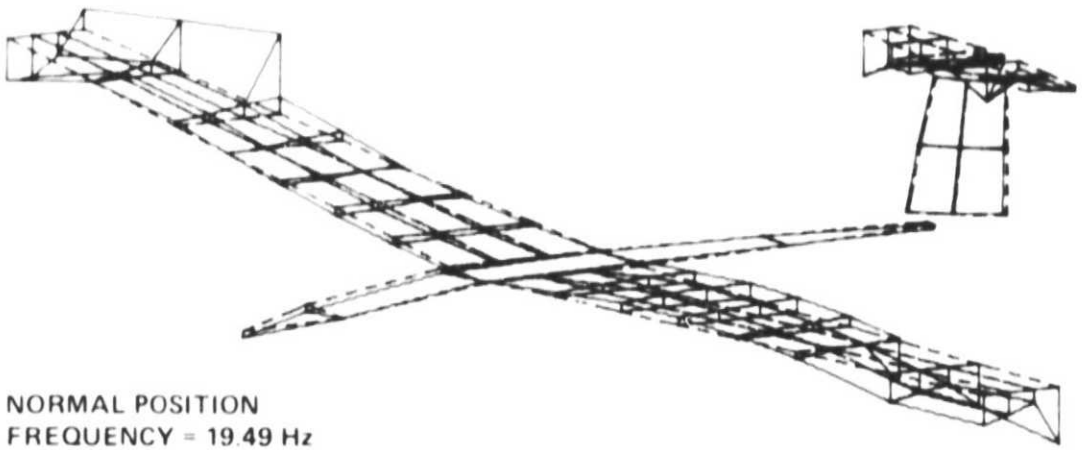

NORMAL POSITION
FREQUENCY = 19.49 Hz

Figure B7.- Vertical fin and fuselage lateral bending mode shape comparison.

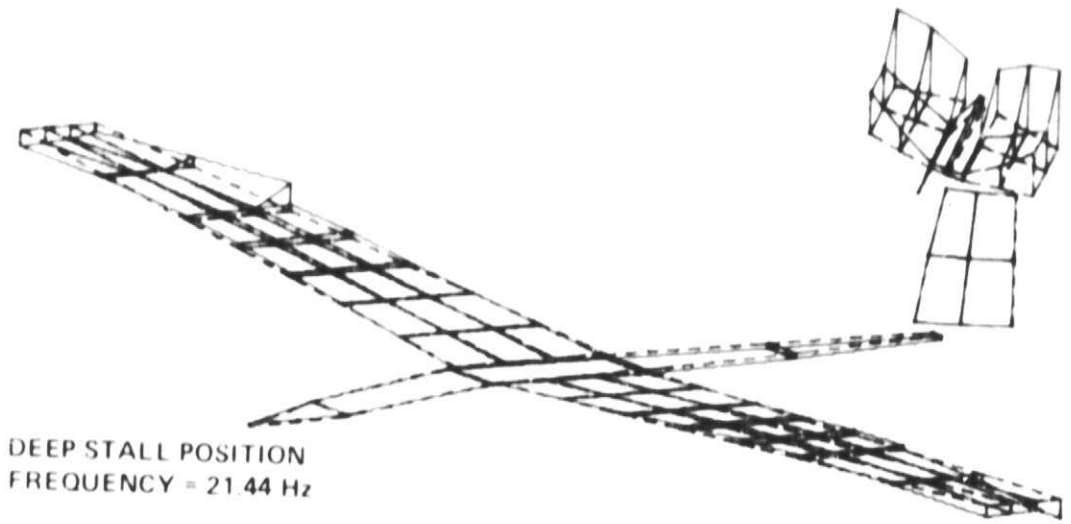

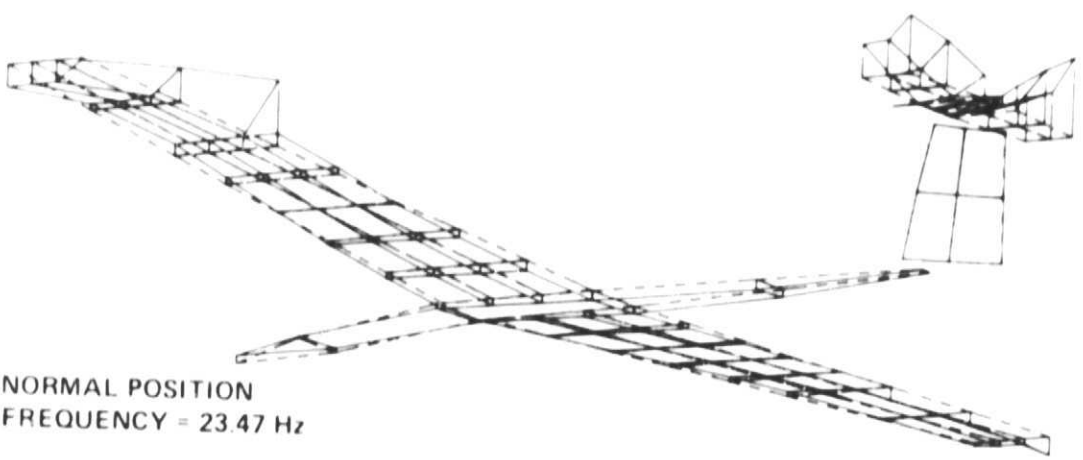

Figure B8.- Symmetric horizontal stabilizer bending mode shape comparison.

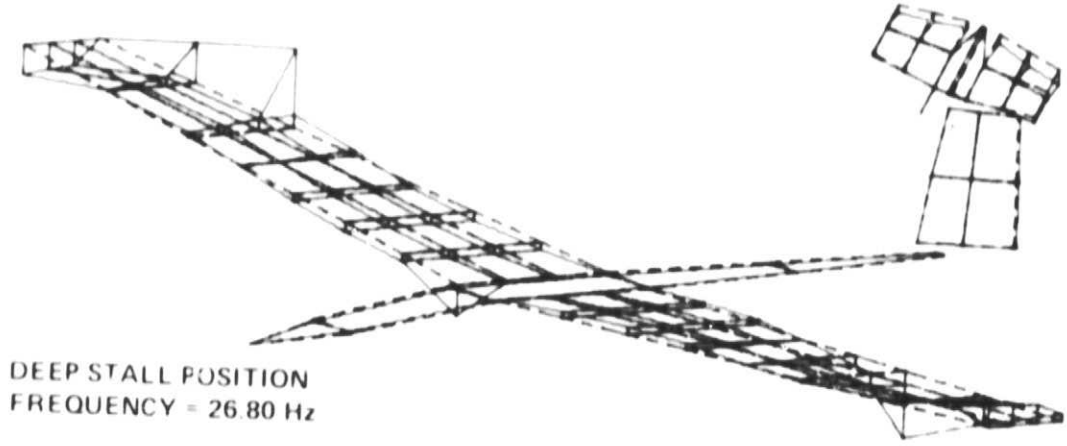

DEEP STALL POSITION
FREQUENCY = 26.80 Hz

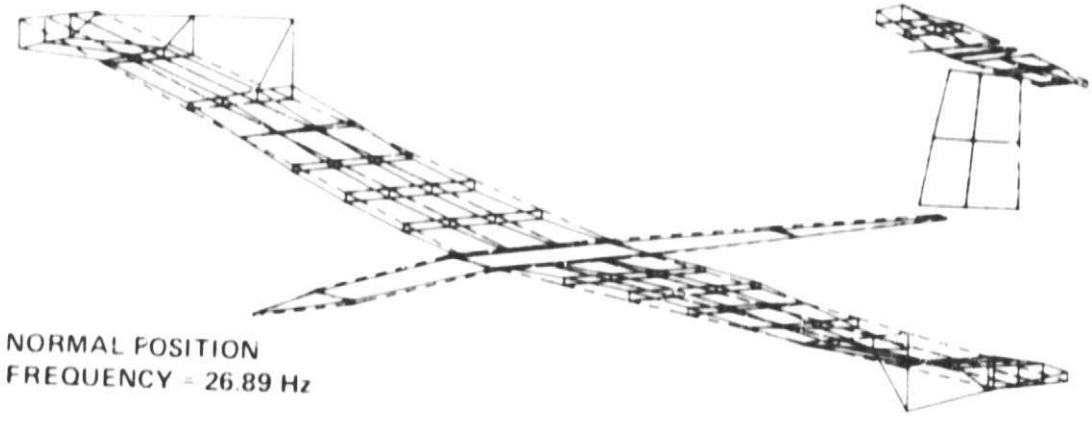

NORMAL POSITION
FREQUENCY = 26.89 Hz

Figure B9.- Aileron rotation mode shape comparison.

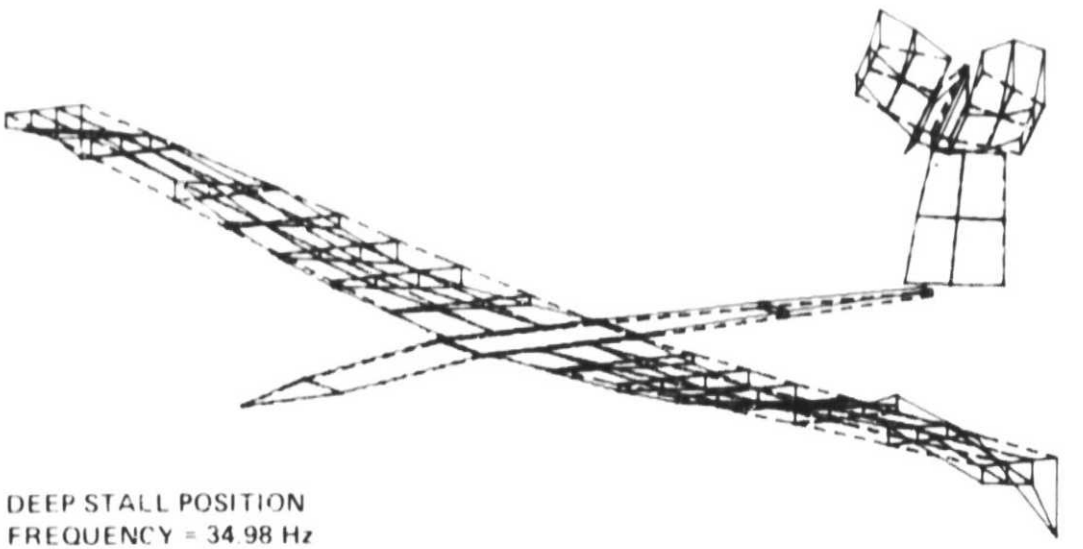

DEEP STALL POSITION
FREQUENCY = 34.98 Hz

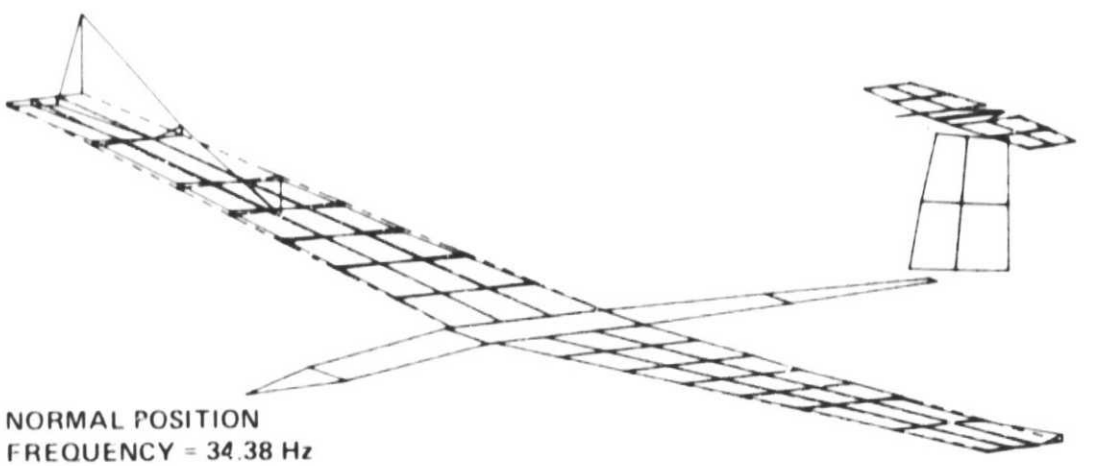

NORMAL POSITION
FREQUENCY = 34.38 Hz

Figure B10.- Third symmetric wing bending mode shape comparison.

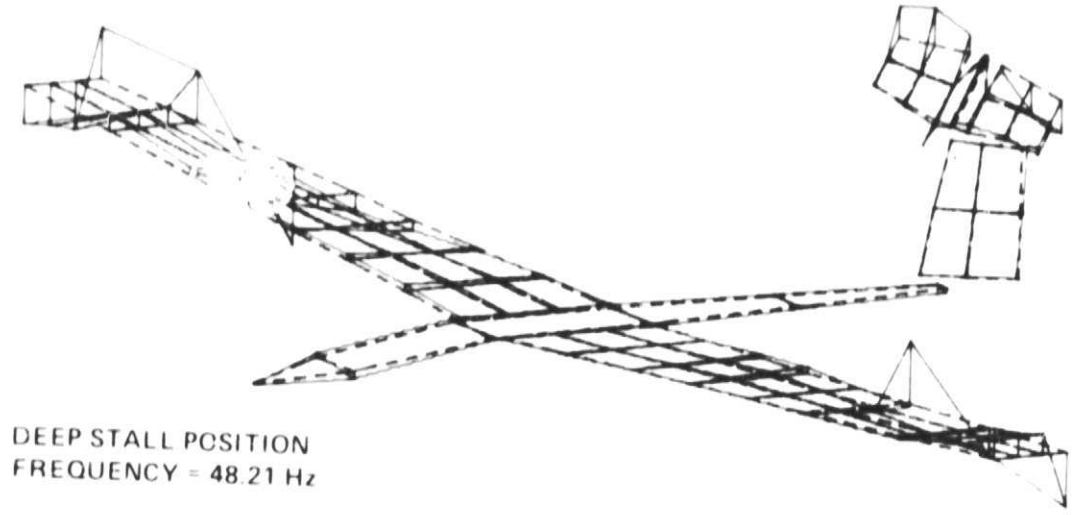

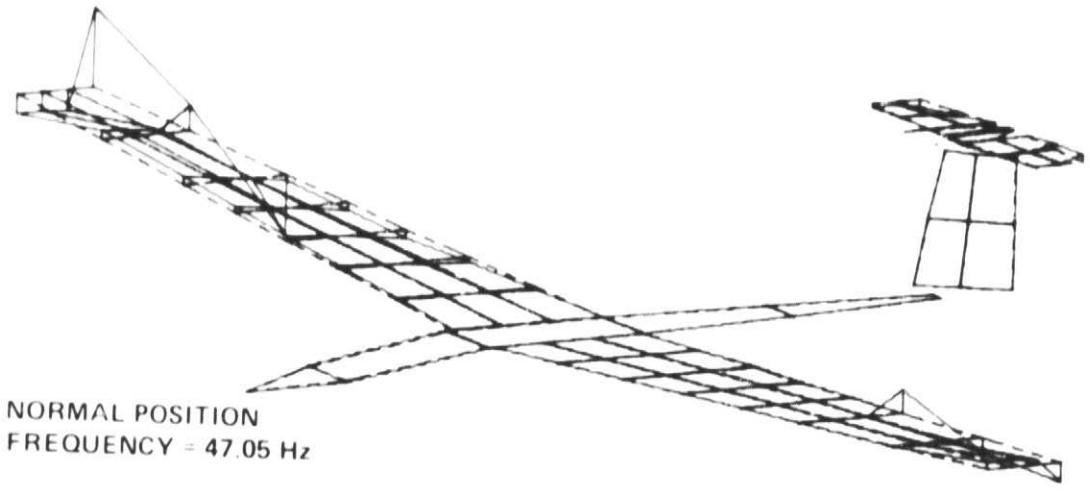

Figure B11.- Elevator rotation mode shape comparison.

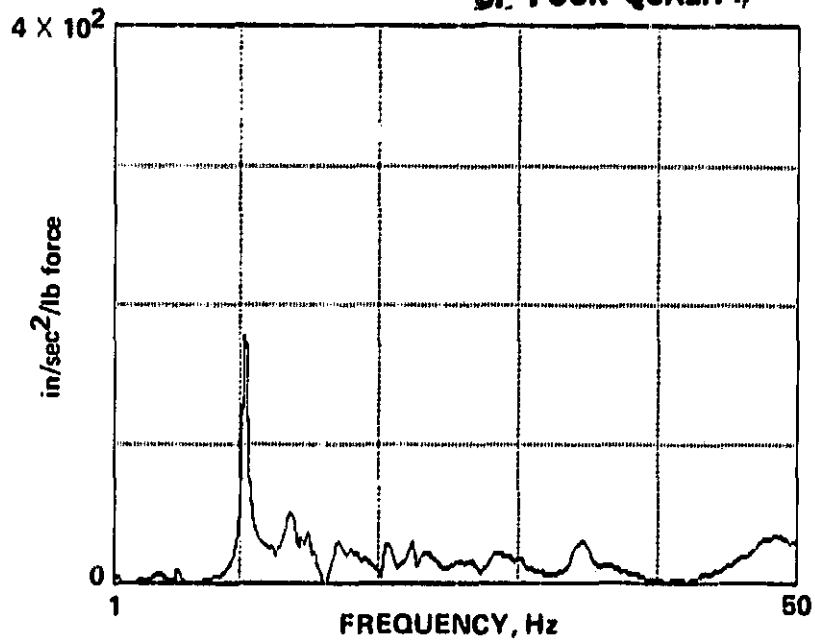

Figure C1.- Location 1 lateral frequency response function with the horizontal stabilizer in the normal flight position.

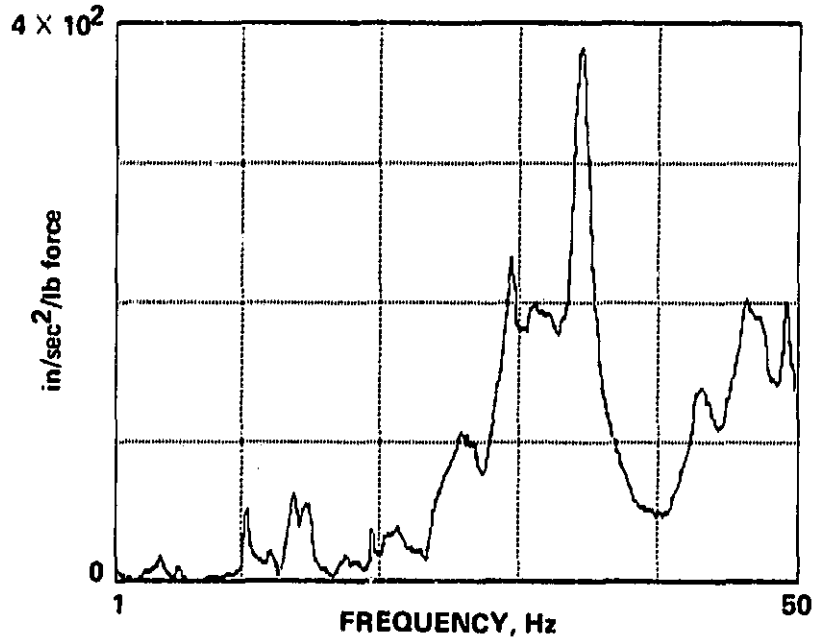

Figure C2.- Location 7 lateral frequency response function with the horizontal stabilizer in the normal flight position.

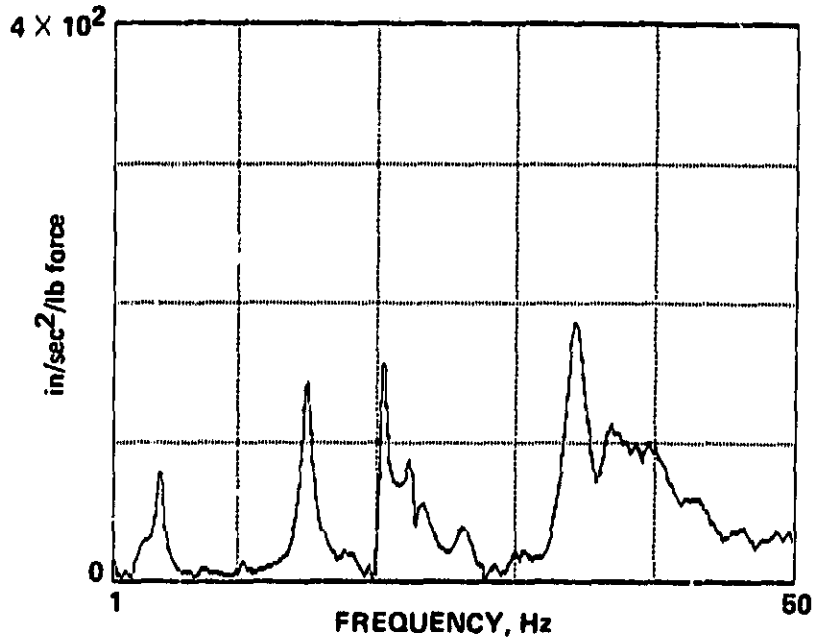

Figure C3.- Location 1 vertical frequency response function with the horizontal stabilizer in the normal flight position.

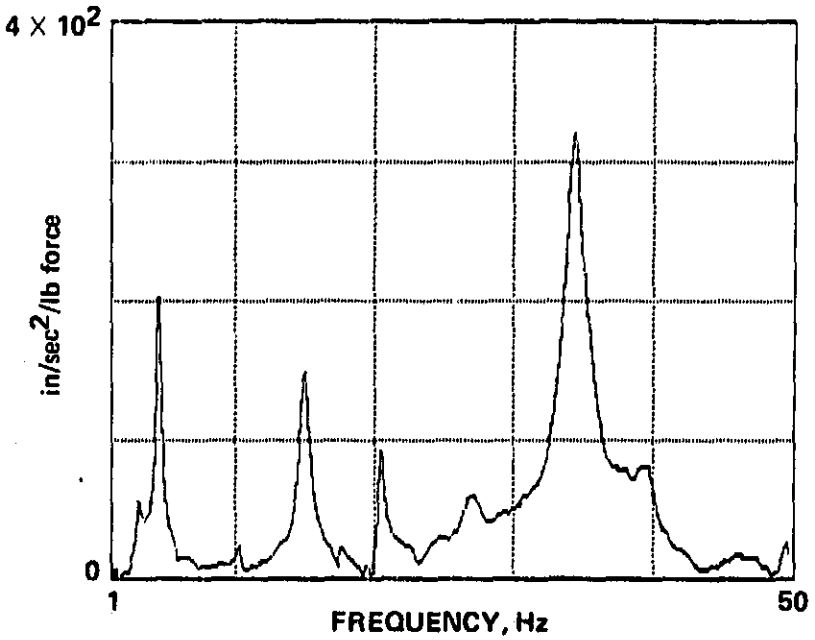

Figure C4.- Location 7 vertical frequency response function with the horizontal stabilizer in the normal flight position.

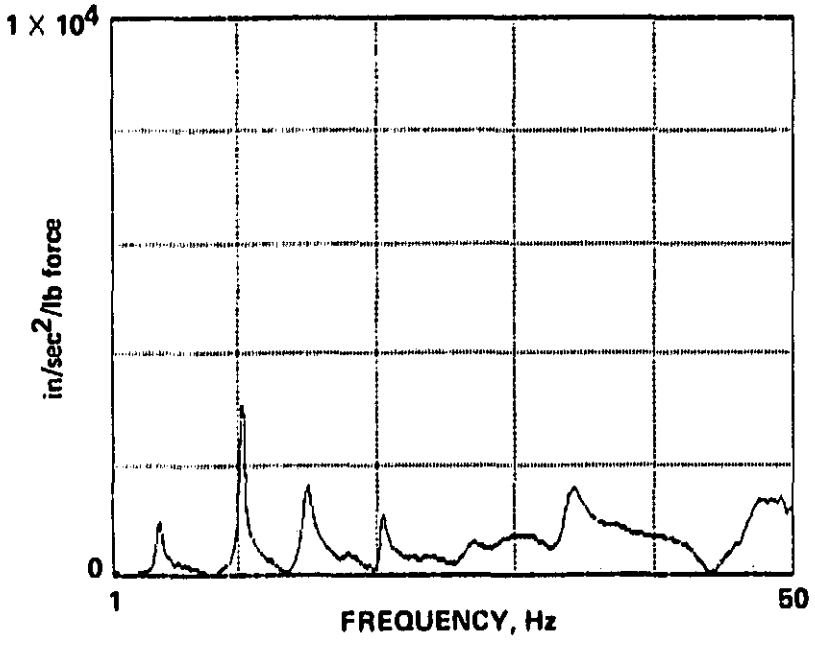

Figure C5.- Location 101 vertical frequency response function with the horizontal stabilizer in the normal flight position.

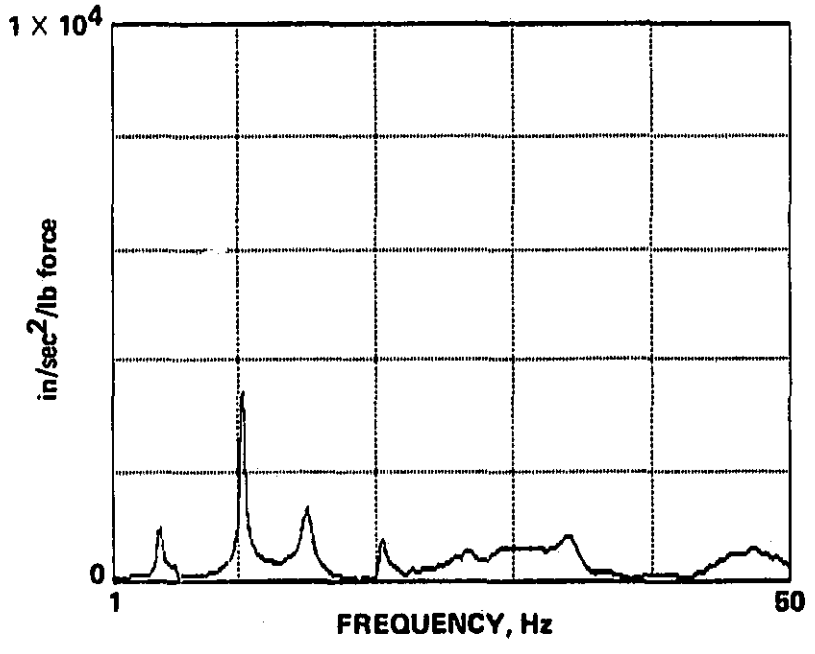

Figure C6.- Location 201 vertical frequency response function with the horizontal stabilizer in the normal flight position.

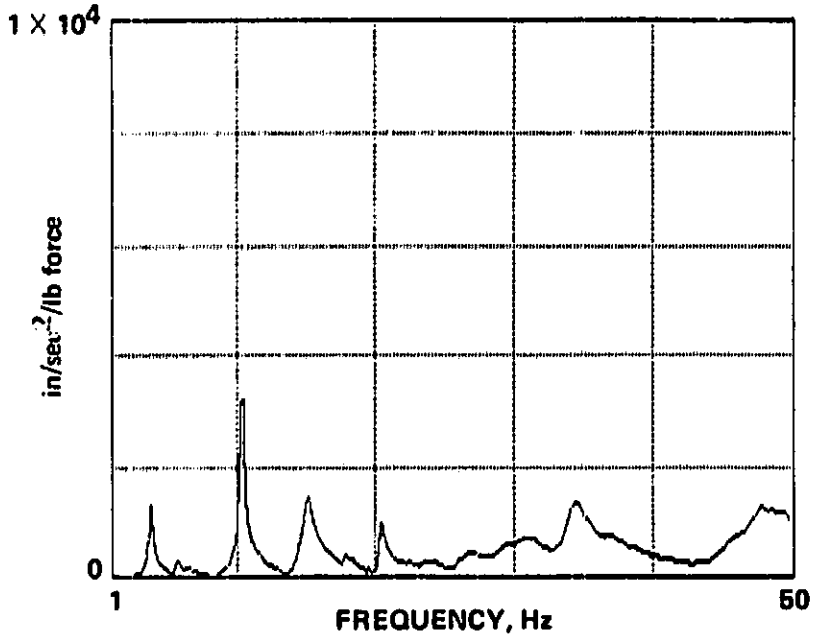

Figure C7.- Location 109 vertical frequency response function with the horizontal stabilizer in the normal flight position.

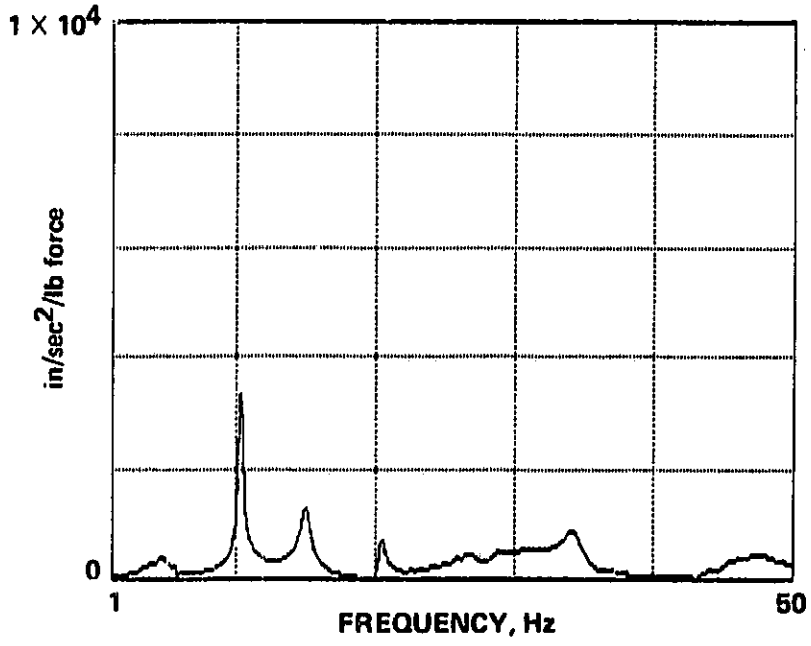

Figure C8.- Location 209 vertical frequency response function with the horizontal stabilizer in the normal flight position.

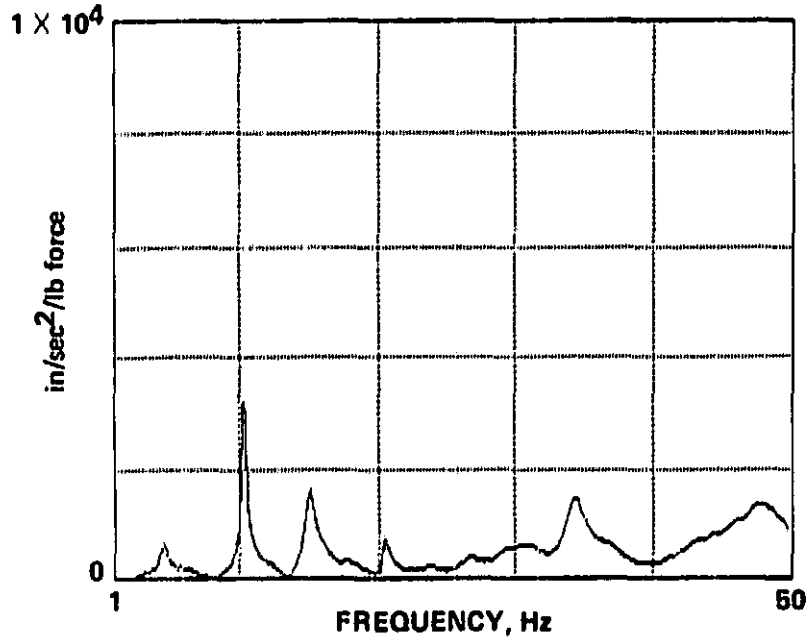

Figure C9.- Location 117 vertical frequency response function with the horizontal stabilizer in the normal flight position.

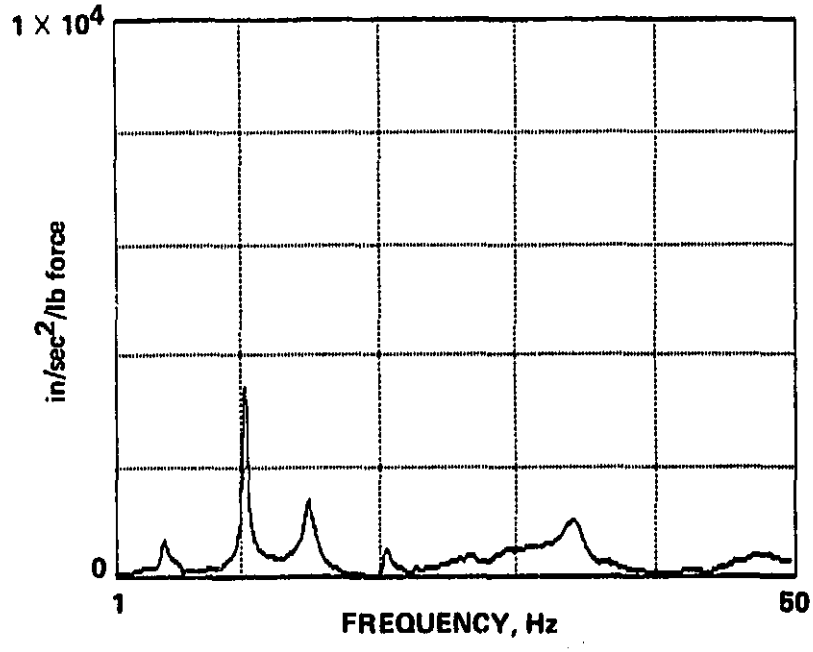

Figure C10.- Location 217 vertical frequency response function with the horizontal stabilizer in the normal flight position.

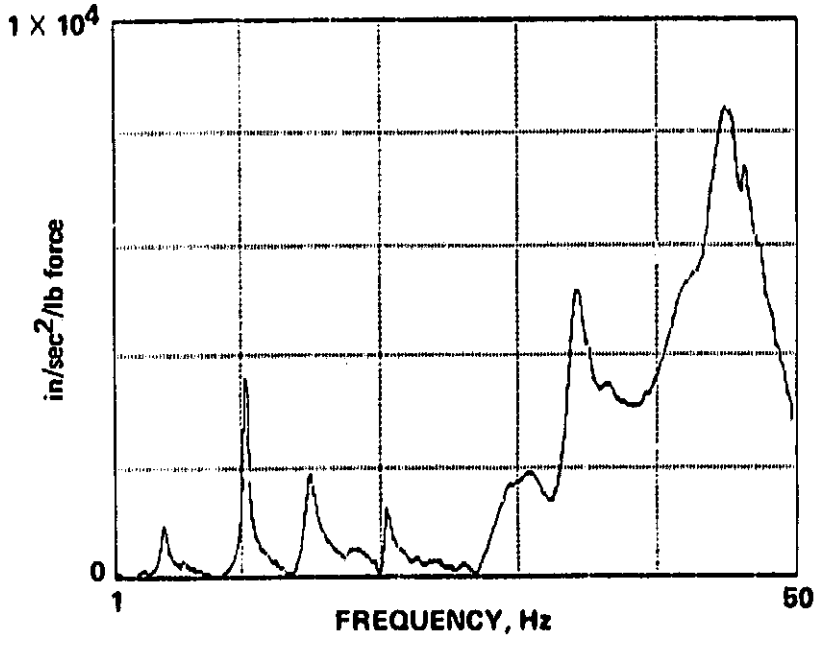

Figure C11.- Location 125 vertical frequency response function with the horizontal stabilizer in the normal flight position.

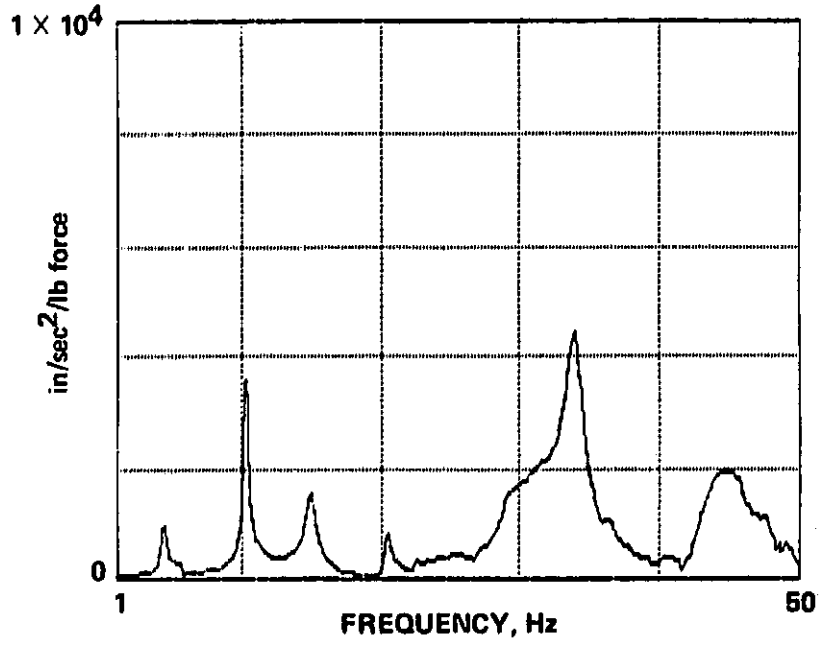

Figure C12.- Location 225 vertical frequency response function with the horizontal stabilizer in the normal flight position.

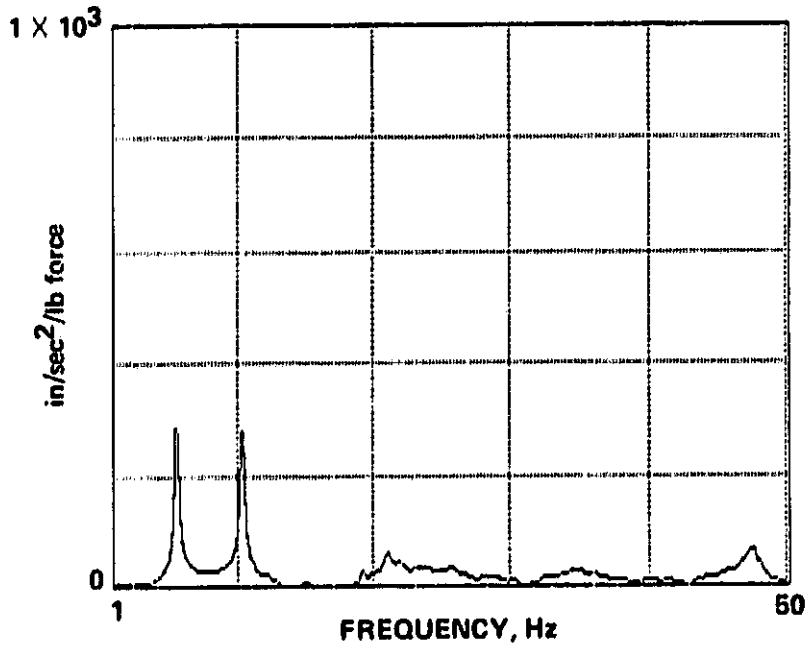

Figure C13.- Location 26 lateral frequency response function with the horizontal stabilizer in the normal flight position.

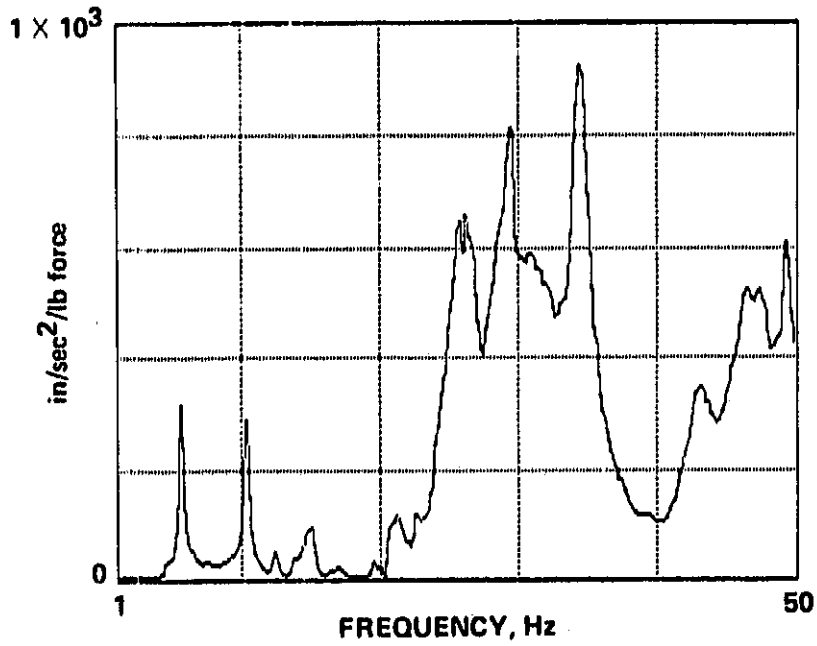

Figure C14.- Location 29 lateral frequency response function with the horizontal stabilizer in the normal flight position.

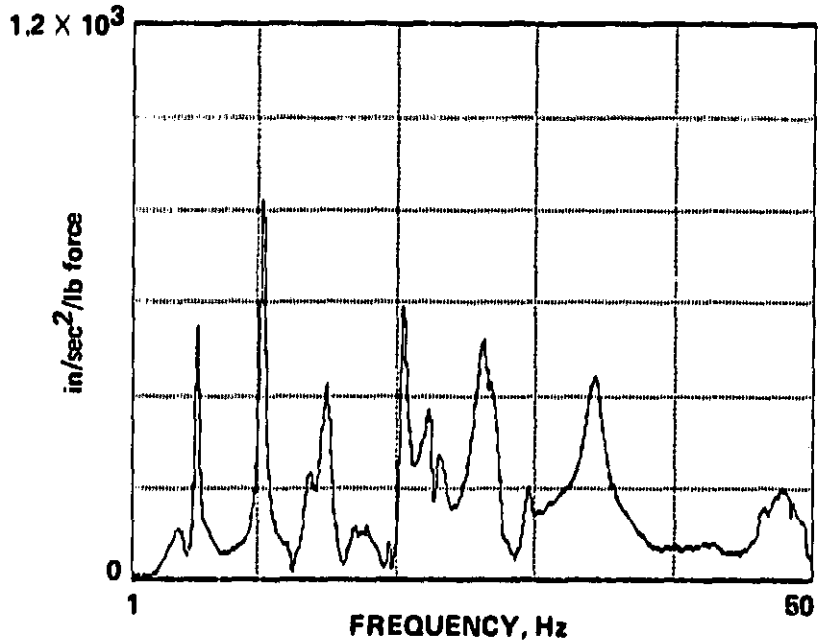

Figure C15.- Location 151 vertical frequency response function with the horizontal stabilizer in the normal flight position.

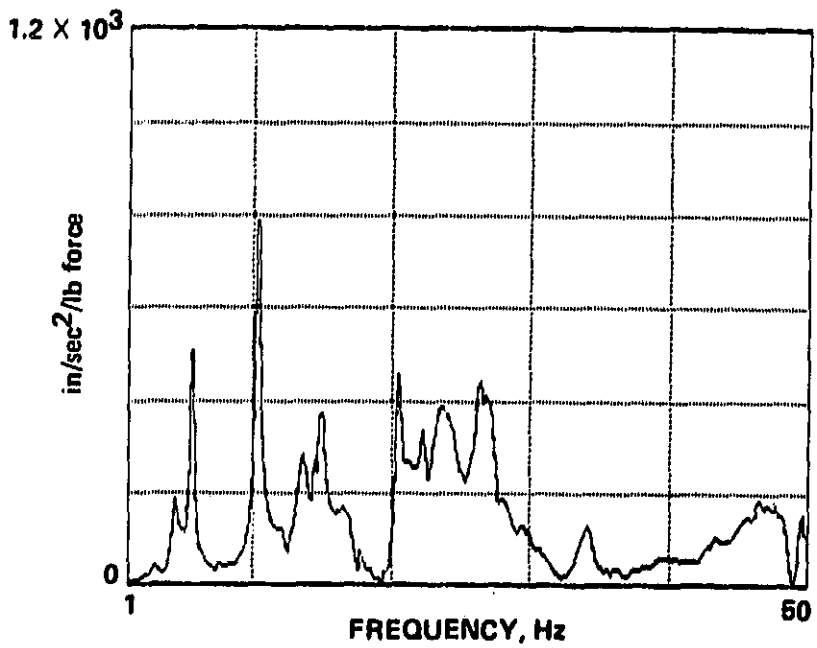

Figure C16.- Location 251 vertical frequency response function with the horizontal stabilizer in the normal flight position.

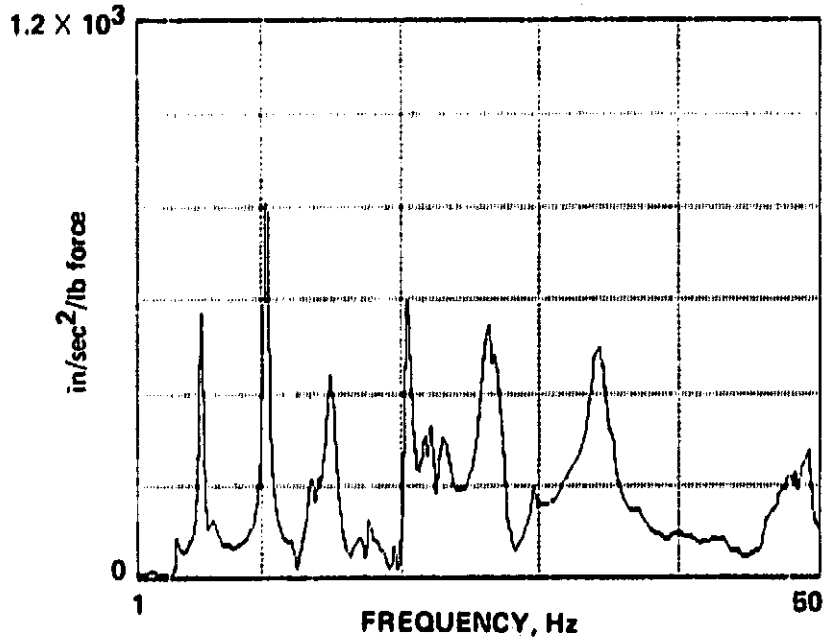

Figure C17.- Location 155 vertical frequency response function with the horizontal stabilizer in the normal flight position.

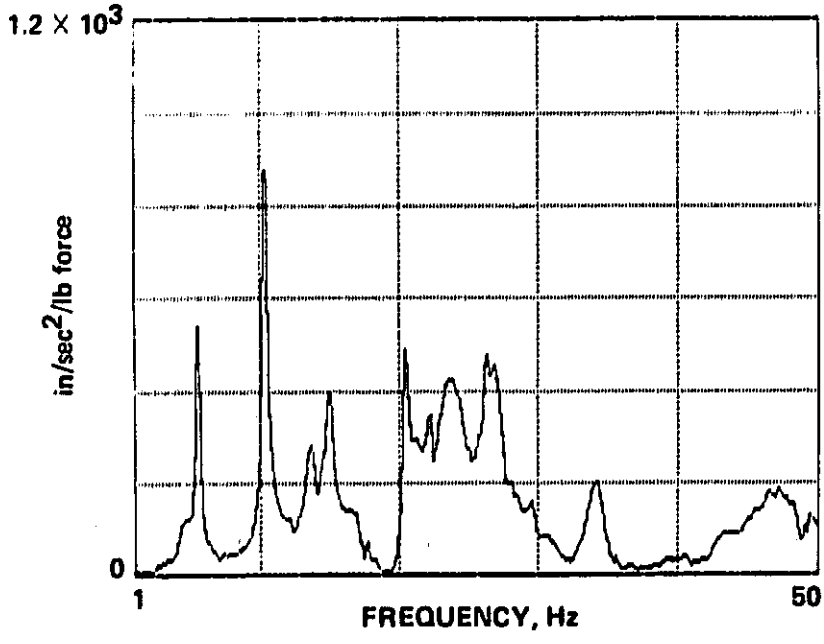

Figure C18.- Location 255 vertical frequency response function with the horizontal stabilizer in the normal flight position.

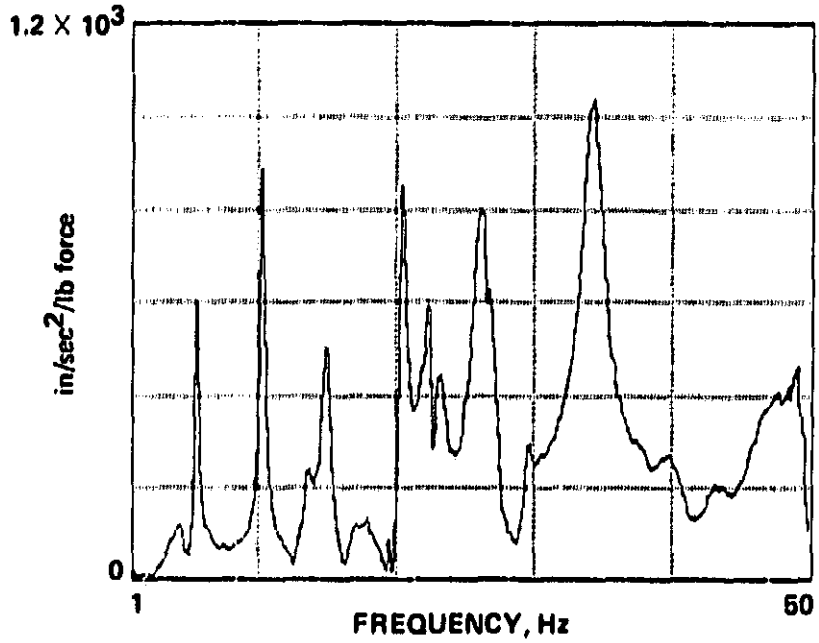

Figure C19.- Location 158 vertical frequency response function with the horizontal stabilizer in the normal flight position.

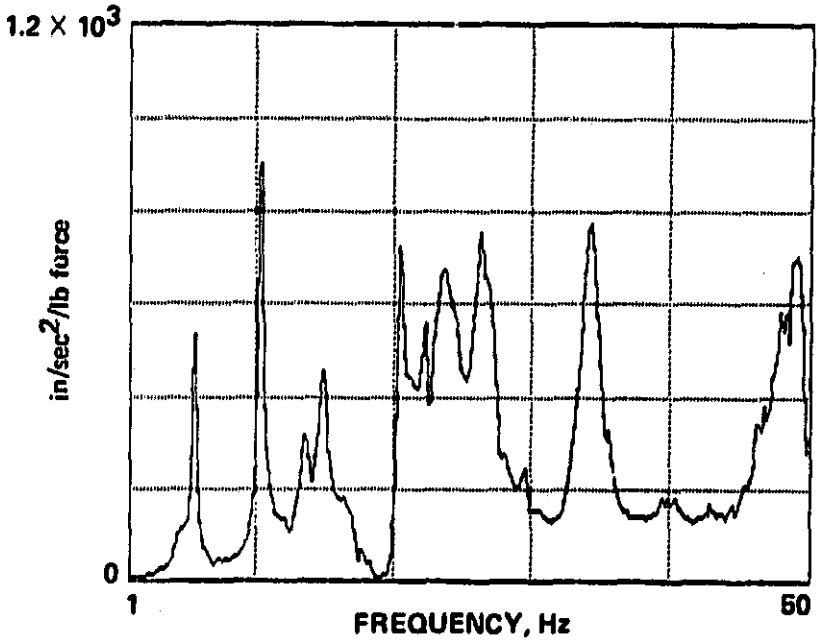

Figure C20.- Location 258 vertical frequency response function with the horizontal stabilizer in the normal flight position.

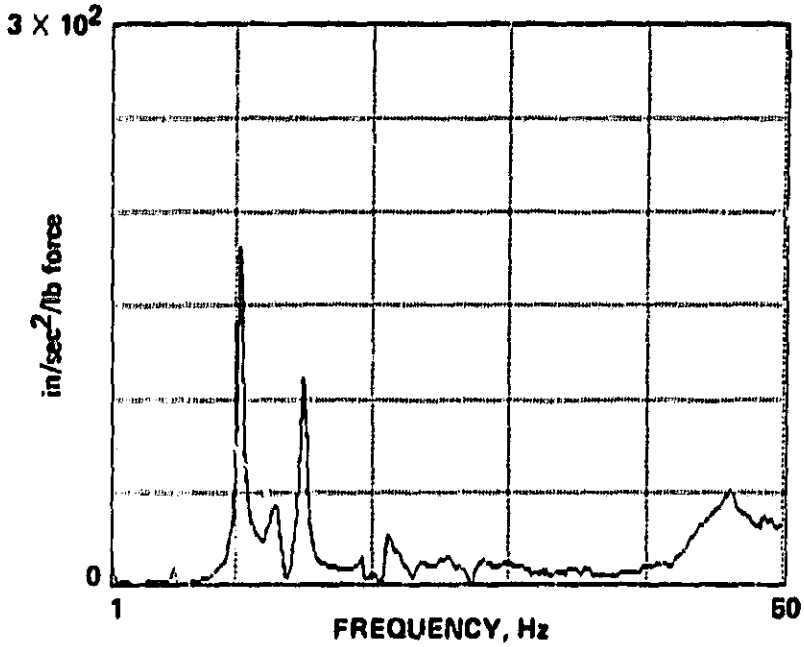

Figure C21.- Location 1 lateral frequency response function with the horizontal stabilizer in the deep stall position.

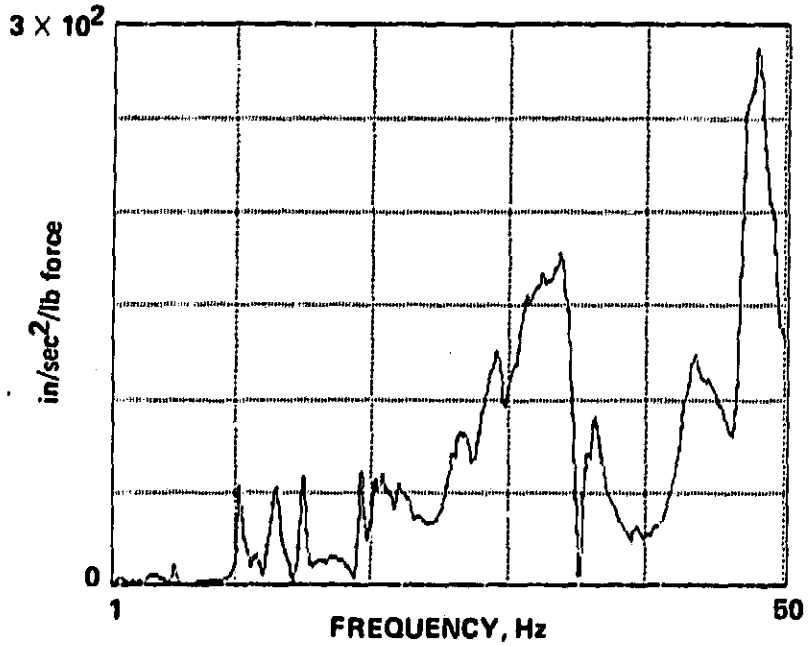

Figure C22.- Location 7 lateral frequency response function with the horizontal stabilizer in the deep stall position.

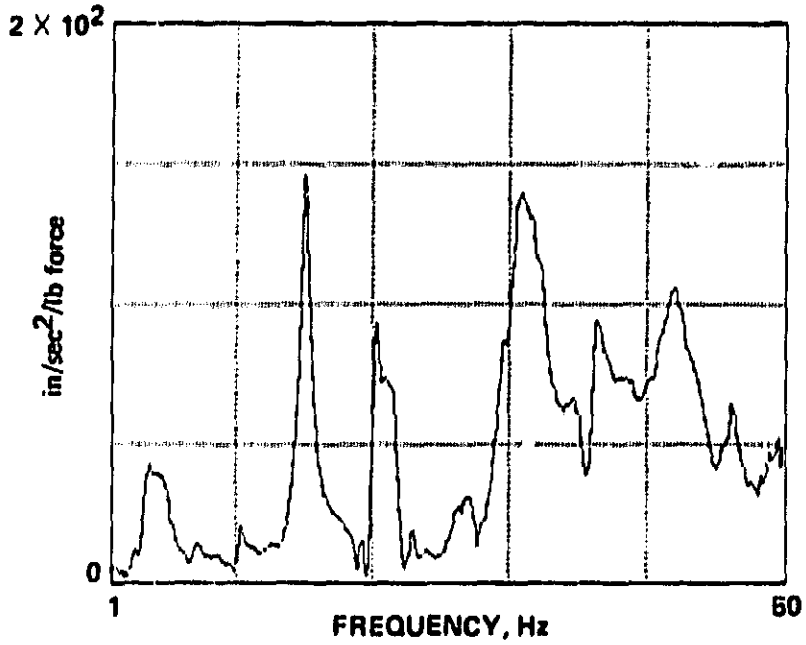

Figure C23.- Location 1 vertical frequency response function with the horizontal stabilizer in the deep stall position.

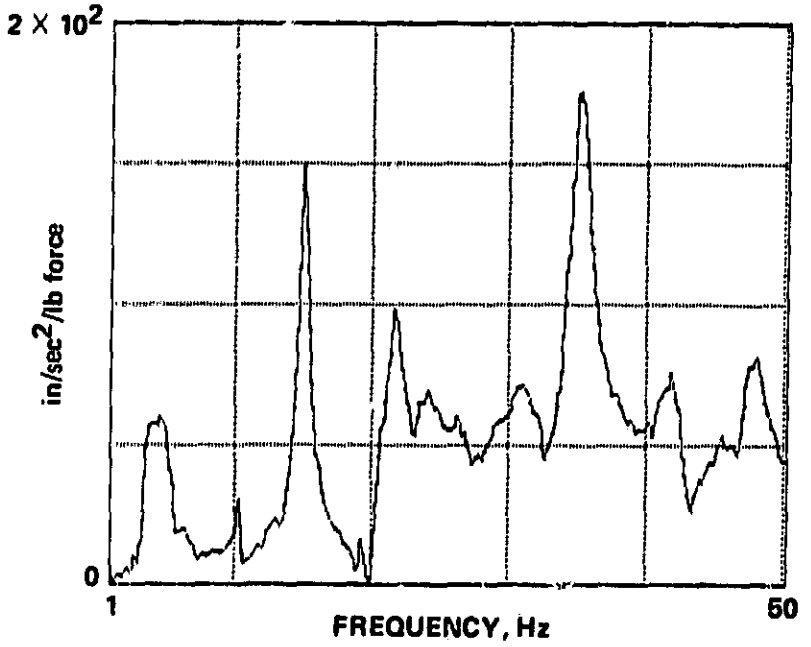

Figure C24.- Location 7 vertical frequency response function with the horizontal stabilizer in the deep stall position.

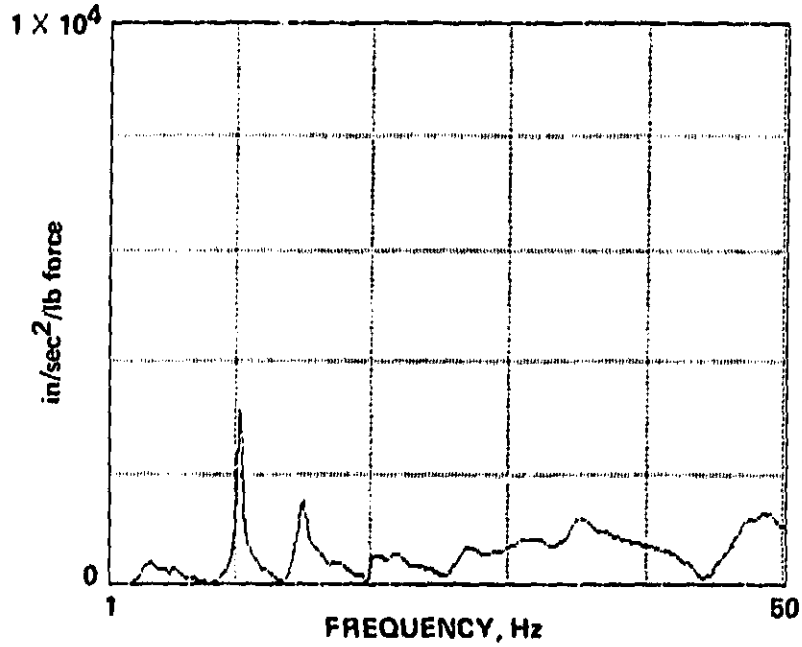

Figure C25.- Location 101 vertical frequency response function with the horizontal stabilizer in the deep stall position.

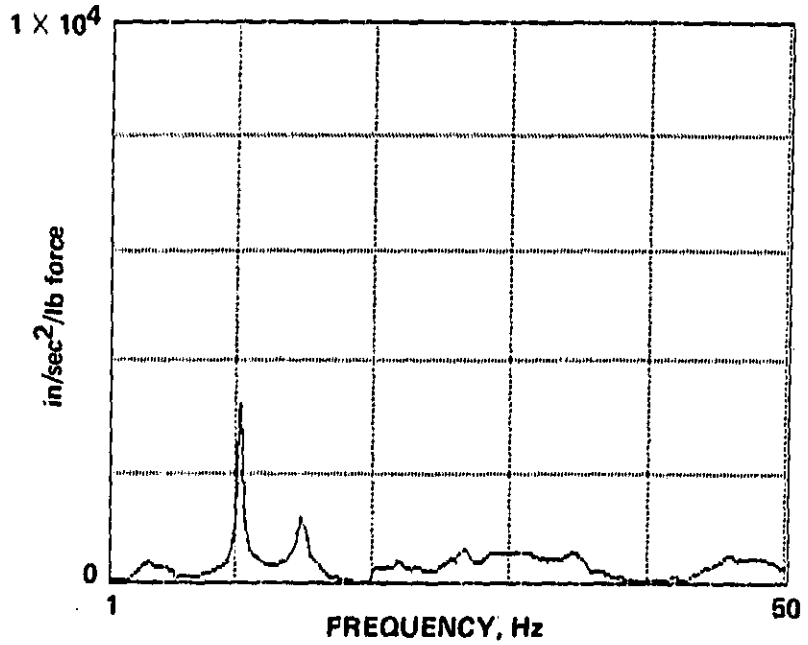

Figure C26.- Location 201 vertical frequency response function with the horizontal stabilizer in the deep stall position.

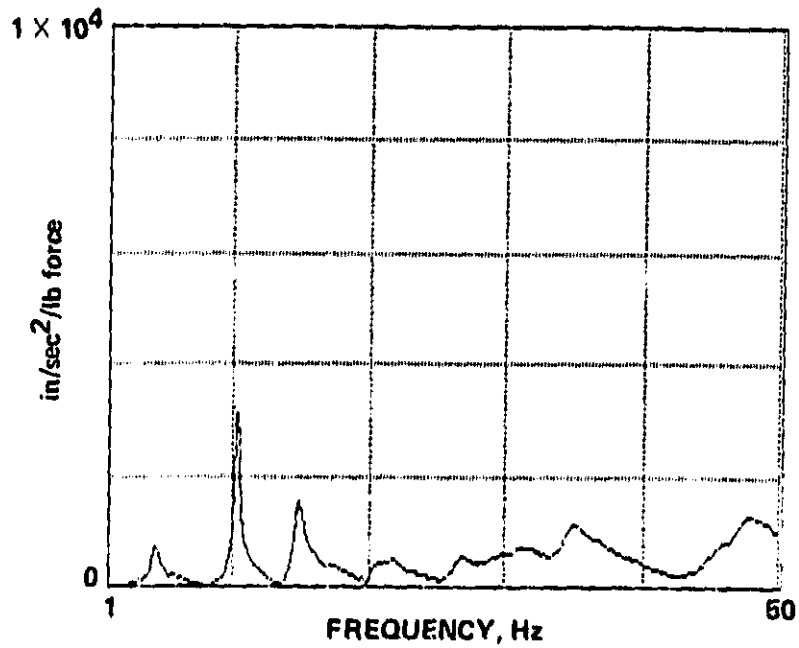

Figure C27.- Location 109 vertical frequency response function with the horizontal stabilizer in the deep stall position.

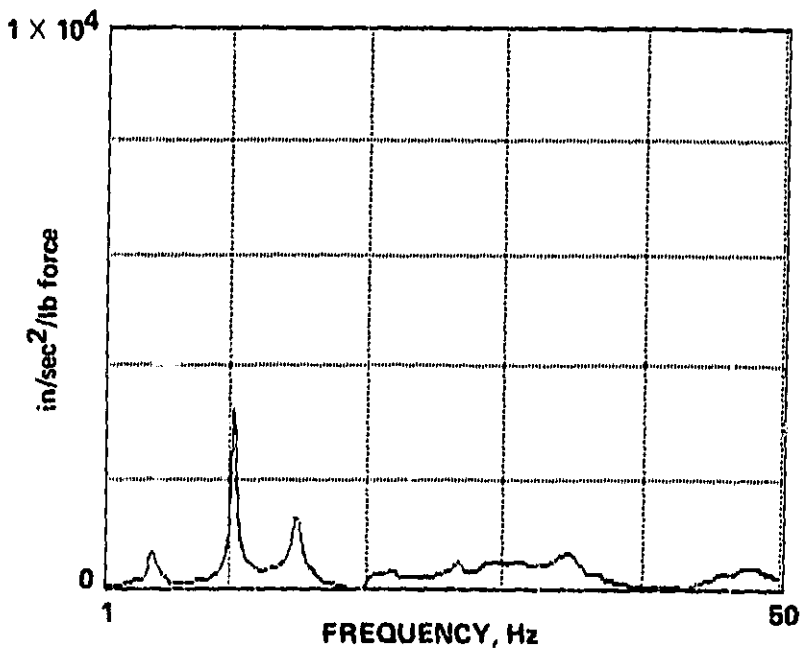

Figure C28.- Location 209 vertical frequency response function with the horizontal stabilizer in the deep stall position.

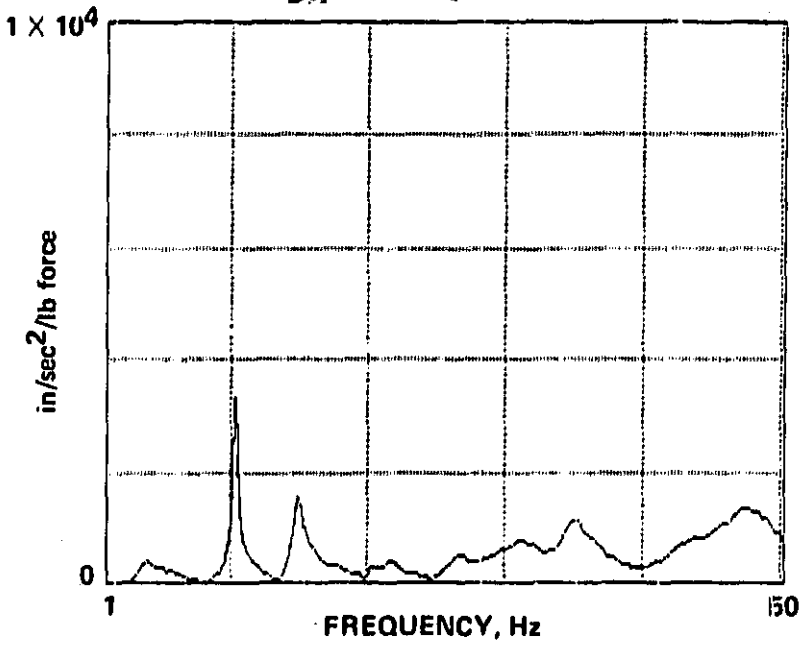

Figure C29.- Location 117 vertical frequency response function with the horizontal stabilizer in the deep stall position.

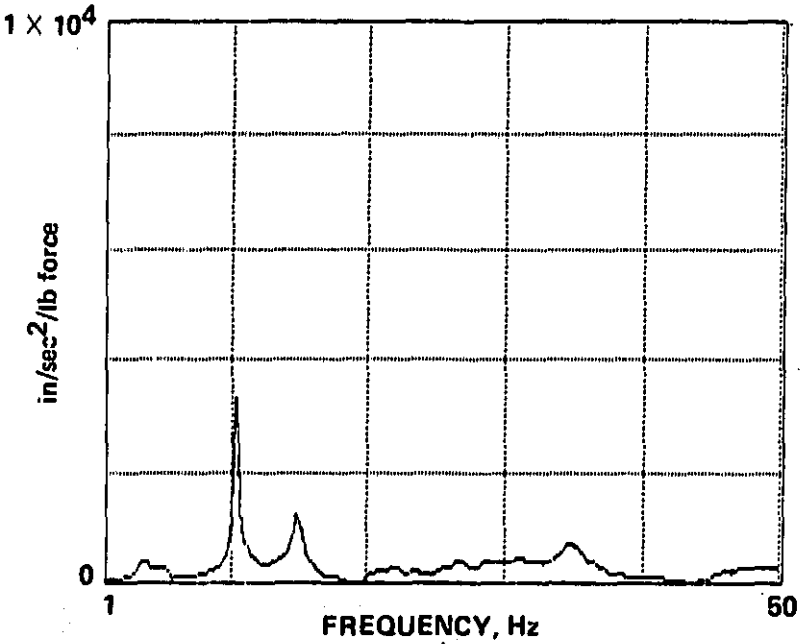

Figure C30.- Location 217 vertical frequency response function with the horizontal stabilizer in the deep stall position.

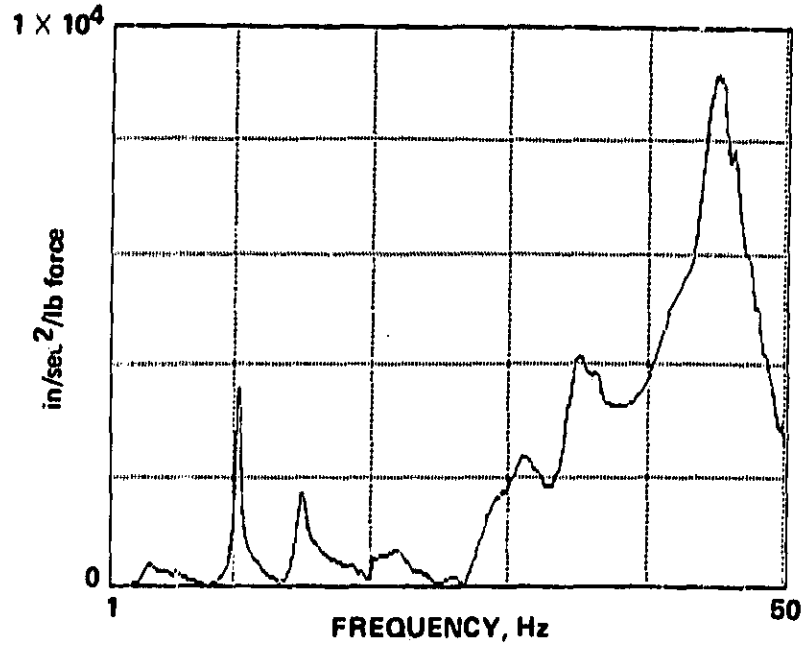

Figure C31.- Location 125 vertical frequency response function with the horizontal stabilizer in the deep stall position.

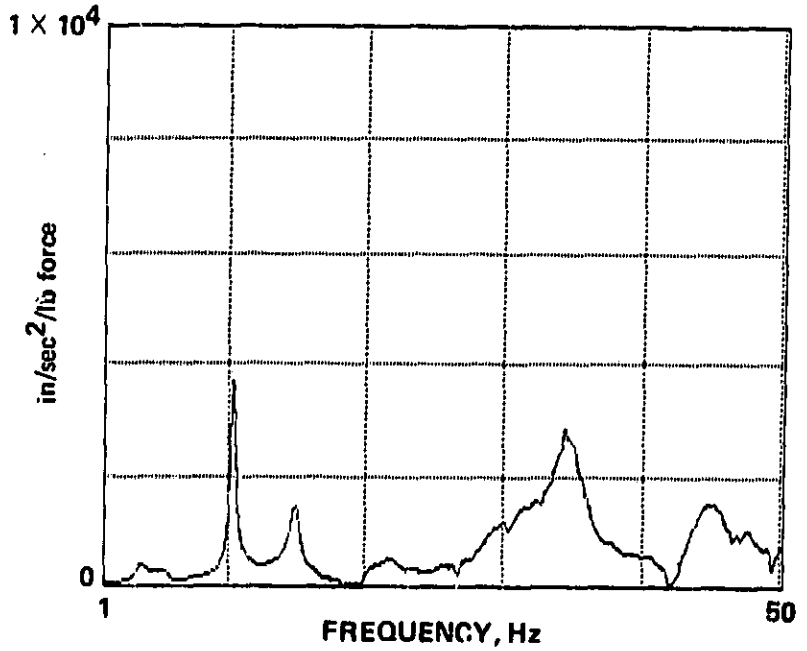

Figure C32.- Location 225 vertical frequency response function with the horizontal stabilizer in the deep stall position.

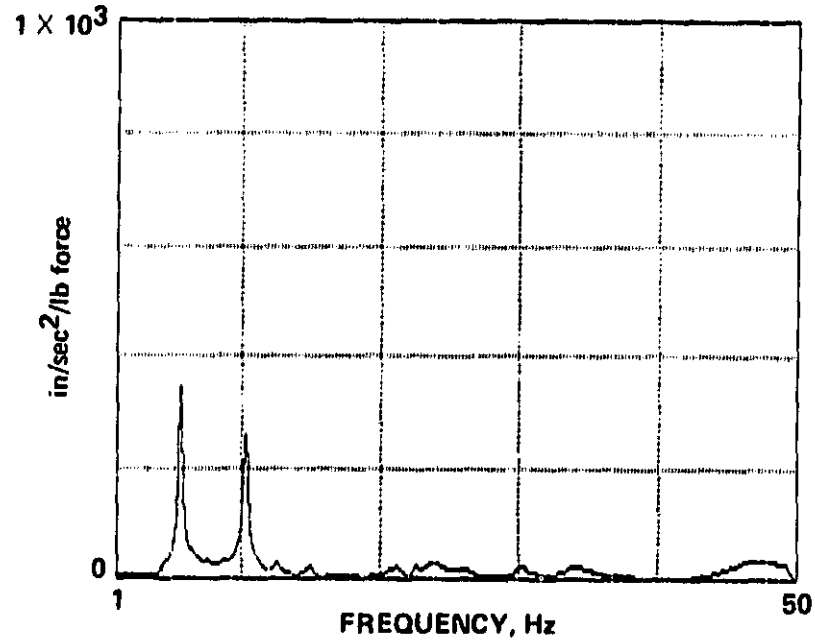

Figure C33.- Location 26 lateral frequency response function with the horizontal stabilizer in the deep stall position.

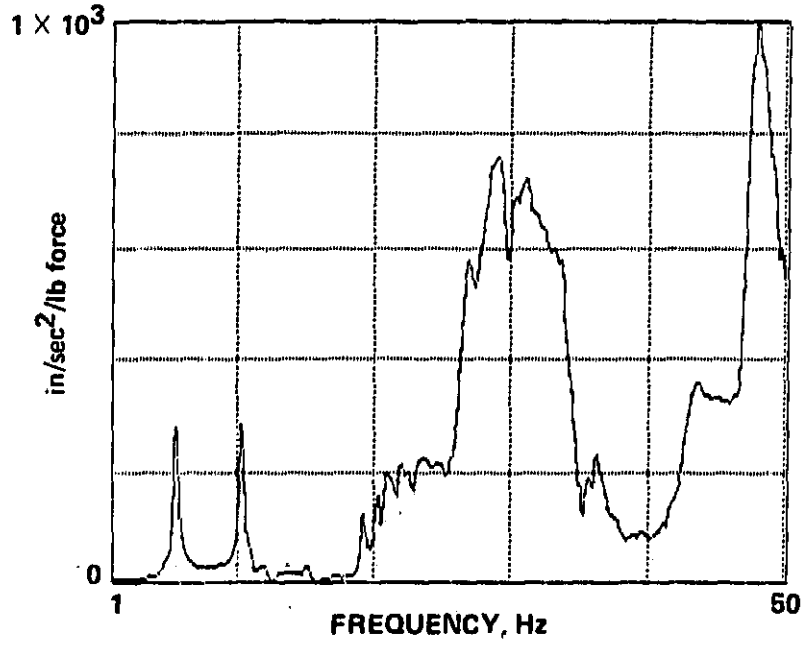

Figure C34.- Location 29 lateral frequency response function with the horizontal stabilizer in the deep stall position.

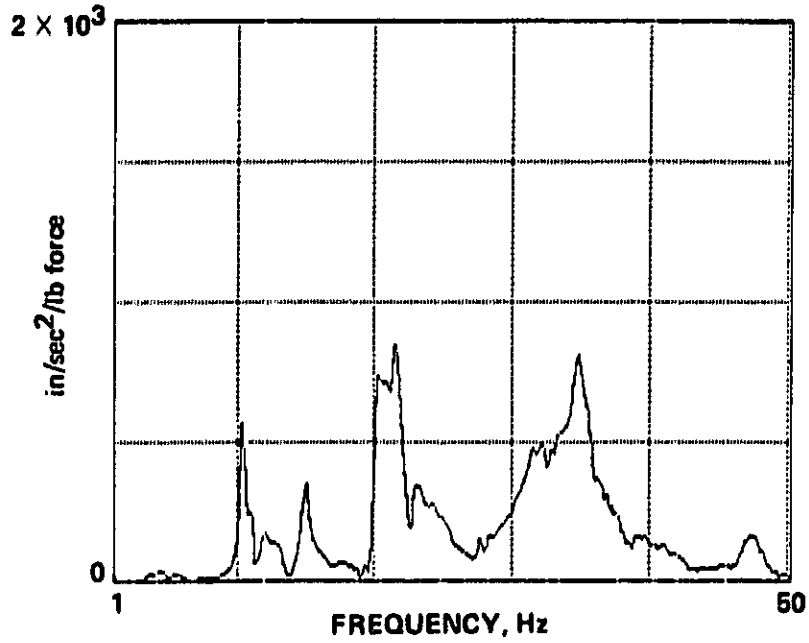

Figure C35.- Location 151 vertical frequency response function with the horizontal stabilizer in the deep stall position.

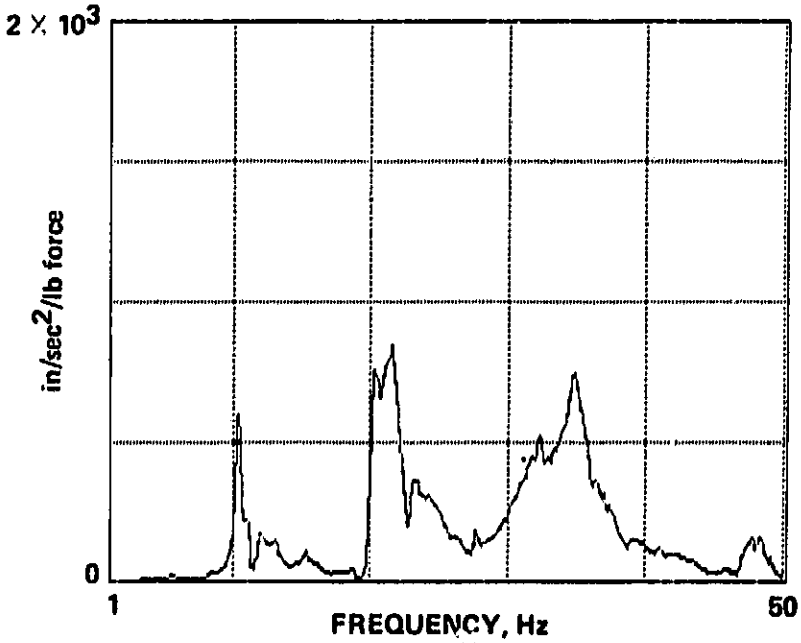

Figure C36.- Location 251 vertical frequency response function with the horizontal stabilizer in the deep stall position.

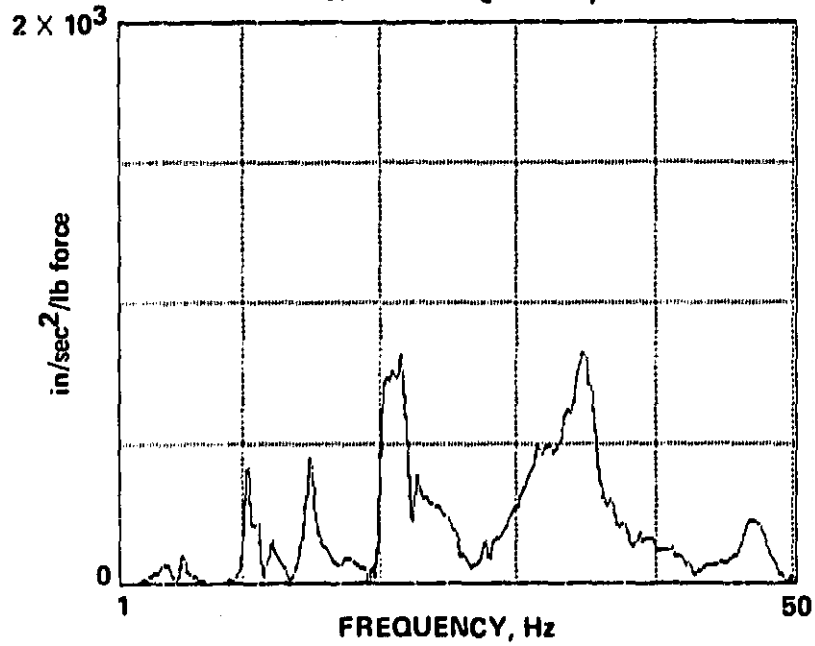

Figure C37.- Location 155 vertical frequency response function with the horizontal stabilizer in the deep stall position.

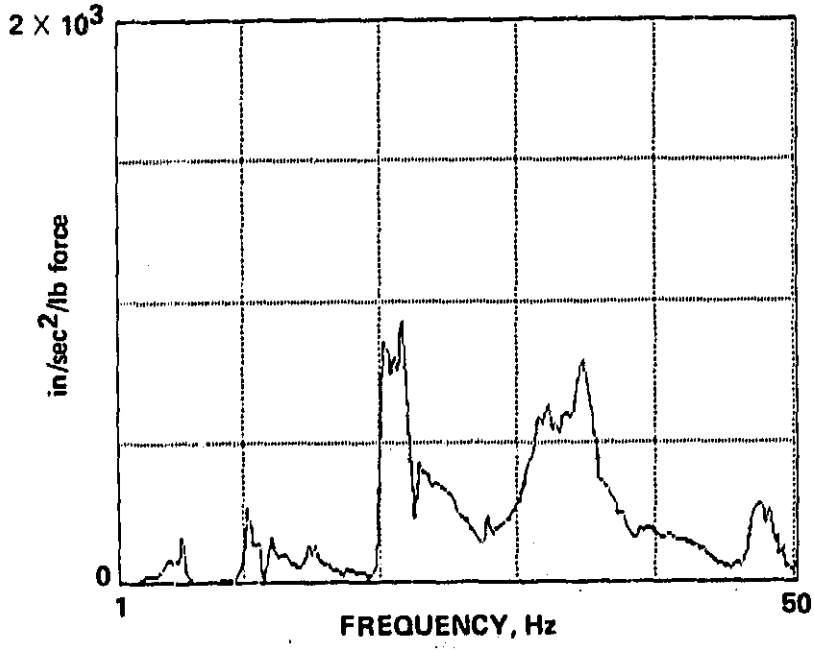

Figure C38.- Location 255 vertical frequency response function with the horizontal stabilizer in the deep stall position.

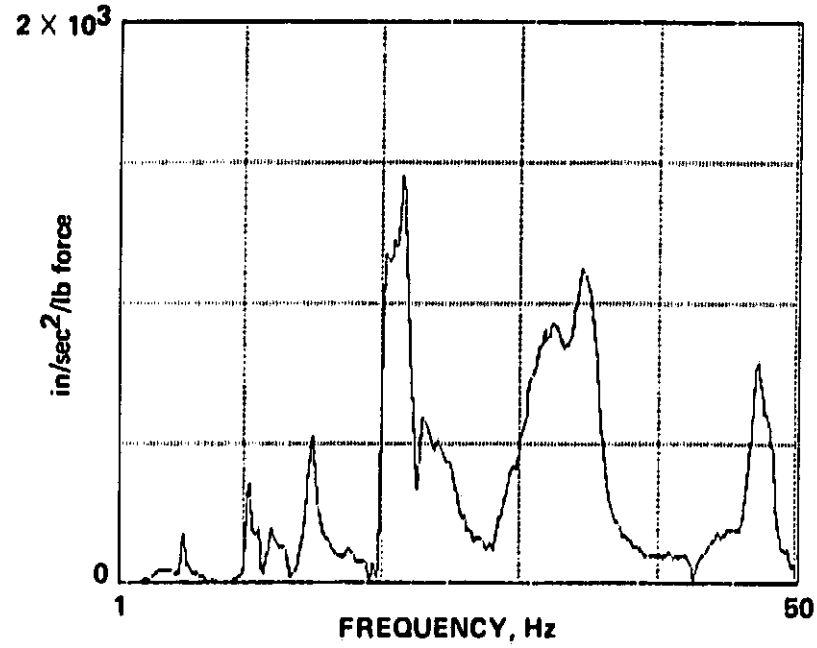

Figure C39.- Location 158 vertical frequency response function with the horizontal stabilizer in the deep stall position.

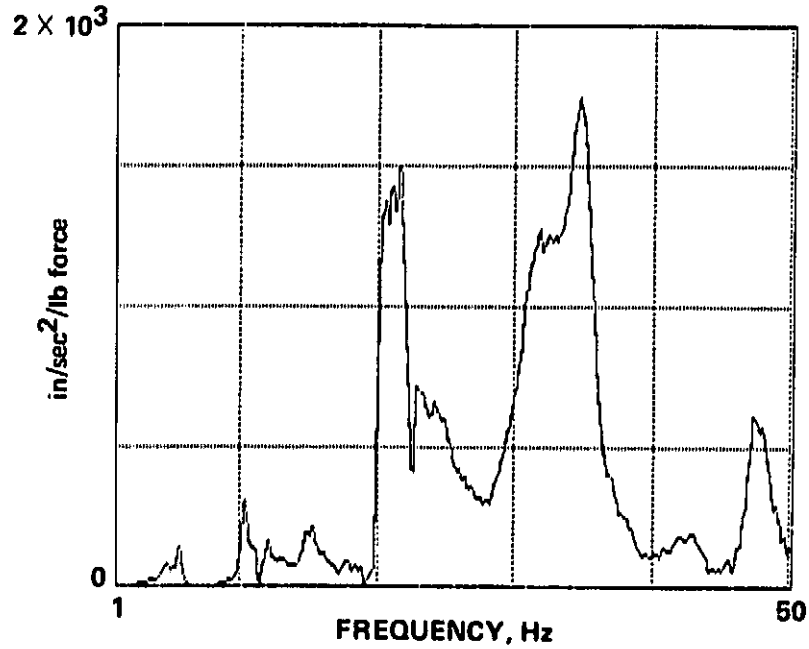

Figure C40.- Location 258 vertical frequency response function with the horizontal stabilizer in the deep stall position.

1. Report No.	2. Government Accession No.	3. Recipient's Catalog No.
NASA TM-85917		

4. Title and Subtitle	5. Report Date
FLUTTER CLEARANCE OF THE SCHWEIZER 1-36 DEEP-STALL SAILPLANE	August 1985
	6. Performing Organization Code
7. Author(s)	8. Performing Organization Report No.
Michael W. Kehoe and Joseph F. Ellison	85136
	10. Work Unit No.
9. Performing Organization Name and Address	
Ames-Dryden Flight Research Facility Edwards, CA 93523	11. Contract or Grant No.
	13. Type of Report and Period Covered
12. Sponsoring Agency Name and Address	Technical Memorandum
National Aeronautics and Space Administration Washington, D.C. 20546	14. Sponsoring Agency Code

15. Supplementary Notes

Point of Contact: Michael Kehoe, Dryden Flight Research Facility, MS D-OFS
Edwards, CA 93523

16. Abstract

A Schweizer 1-36 sailplane was modified for a controlled, deep-stall flight program. This modification allowed the horizontal stabilizer to pivot as much as 70° leading edge down. Ground vibration and flutter testing were accomplished on the sailplane with the horizontal stabilizer in the normal flight and deep-stall flight positions. Test results indicated satisfactory damping levels and trends for the structural modes of the sailplane. The modified sailplane was demonstrated to be free of aeroelastic instabilities to 83 KEAS with the horizontal stabilizer in the normal flight position and to 39 KEAS with the horizontal stabilizer in the deep-stall flight position. This flight envelope was adequate for the controlled, deep-stall flight experiments.

17. Key Words (Suggested by Author(s))	18. Distribution Statement
Ground vibration test Flight flutter test Modal analysis Sailplane	Unlimited Subject Category - 05

19. Security Classif. (of this report)	20. Security Classif. (of this page)	21. No. of Pages	22. Price*
Unclassified	Unclassified	74	A04

*For sale by the National Technical Information Service, Springfield, Virginia 22161